University of Alberta

Synthesis of a phosphotyrosine analog, BrPmp and its incorporation into peptides

by

Naresh S. Tulsi

A thesis submitted to the Faculty of Graduate Studies and Research
in partial fulfillment of the requirements for the degree of

Master of Science

Department of Chemistry

©Naresh S. Tulsi

Spring 2011
Edmonton, Alberta

Permission is hereby granted to the University of Alberta Libraries to reproduce single copies of this thesis and to lend or sell such copies for private, scholarly or scientific research purposes only. Where the thesis is converted to, or otherwise made available in digital form, the University of Alberta will advise potential users of the thesis of these terms.

The author reserves all other publication and other rights in association with the copyright in the thesis and, except as herein before provided, neither the thesis nor any substantial portion thereof may be printed or otherwise reproduced in any material form whatsoever without the author's prior written permission.

Dedicated to My Parents and Brothers

ABSTRACT

Protein tyrosine phosphatases (PTPs) are important therapeutic targets for medicinal chemists and biochemists. General strategies for the development of inhibitors of these enzymes are needed. One known inhibitor of PTPs are analogs containing the α-bromobenzylphosphonate (BBP) motif. We hypothesized that the BBP functional group could be used to develop targeted PTP inhibitors, by incorporation into peptide sequences. Using model compounds, we first tested the stability of the BBP motif to solid phase peptide synthesis (SPPS) conditions. A scaleable synthetic methodology was then developed for generating an amino acid analog that incorporates the BBP functional group. Enzyme inhibition studies with the PTP CD45 demonstrated that the BBP amino acid derivatives were irreversible inhibitors. Using the Fmoc protected BrPmp BBP amino acid, we then incorporated it into longer peptide sequences. We were able to generate a short series of nonapeptides that incorporated BrPmp and identify areas of the chemistry which required improvement.

ACKNOWLEDGEMENTS

I would like to than several people who have provided me with support and guidance in completing this thesis. First off I would like to thank my supervisor Dr Chris Cairo who has provided me with guidance and support throughout my graduate school studies.

I would like to specifically thank Michael Downey for performing all the enzyme assay work undertaken in Chapter 2.

I would also like to thank Ravi Loka, Jonathan Cartmell, Chris Sadek, Mahendra Sandbhor and Mickey Richards for help advice toward my research. I would also like to thank all the Cairo group members for their help during my time here.

Finally I would like to thank my parents, brothers and best friends Mercedes and Ryan for their support.

TABLE OF CONTENTS

Chapter 1: Inhibitors of PTP

1.1 Introduction to PTPs 2

1.2 Catalytic domain and mechanism of activity 3

1.3 CD45 4

1.4 Inhibitors of PTPs 6

  1.4.1 Metal-based inhibitors 7

  1.4.2 Natural products 8

  1.4.3 Reversible nonhydrolyzable pTyr-based inhibitors 10

  1.4.4 Irreversible mechanism based PTP inhibitors 14

    1.4.4.1 Quinone-methide based inhibitors 14

    1.4.4.2 Trans-β-nitrostyrene inhibitors 17

    1.4.4.3 α-Bromo benzylic inhibitors 18

    1.4.4.4 Vinyl sulfone inhibitors 21

    1.4.4.5 Seleninate-based inhibitors 23

1.5 Project objectives 24

1.6 References 25

Chapter 2: Synthesis of a protected BrPmp analog

2.1 Introduction 36

2.2 Synthesis of Zhang's α-bromo phosphonate inhibitor 37

2.3 Design and retrosynthetic analysis of BrPmp 40

2.4□ *α*-Bromobenzylphosphonate (BBP) analogs 41

2.5 Stability of the α-bromo phosphonate to SPPS conditions. 43

2.6 Synthesis of BrPmp from serine 45

2.7 Synthesis of BrPmp from tyrosine 47

2.8 Incorporation of BrPmp into peptide sequences 50

2.9 Inhibition of CD45 51

2.10 Conclusion 54

2.11 Materials and methods 55

    2.11.1 Synthetic methods 55

2. 12 Appendix 75

Chapter 3: Incorporation of BrPmp into peptides

3.1 Introduction 85

3.2 CD45 peptide substrates 86

3.3 Sequence selection 89

3.4 Synthesis of the nona-peptides 93

3.5 Synthesis of penta-peptides incorporating BrPmp 96

3.6 Proposed mechanism of BrPmp degredation during SPPS 99

3.7 Conclusions & future work 101

3.8 Materials and methods 103

    3.8.1 Synthetic methods 103

3.9 Appendix 106

LIST OF TABLES

Table 2.1: Bromination of α-hydroxyphosphonate (2.10) 42

Table 2.2: Results of stability study of 2.10 under various SPPS conditions....... 43

Table 2.3: Results of stability study of 2.12 under various SPPS conditions....... 44

Table 2.4: Carbonylation of iodotyrosine 48

Table 2.5 Inhibition of CD45... 51

Table 3.1 Sequences selected for BrPmp incorporation and their predicted dephosphorylation efficiency... 90

Table 3.2 Expected m/z peaks versus observed m/z peaks for compounds 3.4 - 3.10... 94

Table 3.3 Amidated product observed in attempted synthesis of 3.4 95

Table 3.4 Truncated sequences selected for BrPmp incorporation and their predicted dephosphorylation efficiency.. 97

Table 3.5 Purity of 3.12 and 3.13 by ^{31}P NMR and HPLC.................................. 99

LIST OF FIGURES

Figure 1.1 Conserved catalytic mechanism for the cysteine based PTPs 4

Figure 1.2 Structure of CD45.. 6

Figure 1.3 Common inorganic PTP inhibitors. Structures of vanadate (1.1), disodium aurothiomalate (1.2), and phenyl arsine oxide (1.3) are shown. 8

Figure 1.4 Natural product inhibitors of PTPs. Structures of pulchellalactam (1.4), dihydrocarolic acid (1.5), nornuciferine (1.6), dysidiolude (1.7) and stevasteline A (1.8) are shown.. 10

Figure 1.5 Phosphotyrosine mimetics. Structures of *p*Tyr (1.9), *p*Tyr (S) (1.10), Pmp (1.11) and F_2Pmp (1.12) are shown. 12

Figure 1.6 OMT based phosphotyrosine mimetics. a) Structures of OMT (1.13) and FOMT (1.14) b) A structure of a cyclic peptide incorporating OMT. 13

Figure 1.7 Mechanistic framework of QMG phosphate analogs. a) Quinone methide reactive intermediate b) Mechanism of inactivation of quinone methide generating inhibitors 15

Figure 1.8 QMG based probes 16

Figure 1.9 TBNS as inhibitors of PTPs. a) TBNS inhibitors b) Mechanism of inactivation of TBNS inhibitors... 18

Figure 1.10 α-bromobenzylphosphonate developed by Zhang and colleagues 18

Figure 1.11 Potential mechanism of α-bromobenzylphosphonate inactivation of PTPs 20

Figure 1.12 Vinyl sulfone inhibitors and their mechanism of inhibiton. a) vinyl sulfone inhibitors b) Mechanism of PTP inactivation of vinyl sulfone inhibitors.22

Figure 1.13 Seleninate based PTP inhibitors 23

Figure 2.1: Synthetic tripeptide Asp-BrPmp-Leu 51

Figure 2.2: Kitz-Wilson analysis of compounds 2.31 and 2.32. Compounds (a-b) 2.31 and (c-d) 2.32 were examined using a Kitz-Wilson analysis. 53

Figure 3.1 Peptide substrates of CD45 from Lck and Fyn 88

Figure 3.2 Target peptide sequences with BrPmp incorporation. 91

Figure 3.3 Target peptide sequences with BrPmp incorporation. 92

Figure 3.4: Pentamer sequences selected for BrPmp incorporation 98

Figure 3.5: Proposed mechanism for the formation of Pmp 100

LIST OF SCHEMES

Scheme 2.1 Synthesis of Zhang’s α-bromo phosphonate inhibitor. 38

Scheme 2.2 Retrosynthetic analysis of BrPmp. 40

Scheme 2.3 Synthesis of model α-Bromobenzylphosphonates. 41

Scheme 2.4 Synthesis of Fmoc-L-BrPmp-MeOH 45

Scheme 2.5 Synthesis of benzylic aldehyde 2.24 47

Scheme 2.6 Synthesis of BrPmp. 49

Scheme 3.1 Observed side products in the synthesis of peptides 3.4 – 3.10 96

LIST OF ABREVIATIONS

5-HT1A	5-Hydroxytryptamine 1A
BBP	α-bromobenzylphosphonate
BCR	B cell receptor
BH3-DMS	Borane Dimethyl Sulfide
Boc	Butyloxy carbonyl
BrPmp	Phosphonobromomethylphenylalanine
Cbz	Carboxybenzyl
CD45	Cluster of Differentiation 45
CDC25A	Cell Division Cycle 25A
CDC25B	Cell Division Cycle 25B
CDC25B	Cell Division Cycle 25C
CuAAc	Copper(I) Catalyzed Azide-Alkyne Cycloaddition
Dba	Dibenzylideneacetone
DCM	Dichloromethane
DiFMUP	6,8-difluoro-4-methylumbelliferyl phosphate
DIPEA	Diisopropylethylamine
DMF	Dimethylformamide
Dppf	1,1'-Bis(diphenylphosphino)ferrocene
Dppp	1,3-Bis(diphenylphosphino)propane
DSPs	Dual-Specific Phosphatases
EGF	Epidermal Growth Factor

F2Pmp	α,α-difluorophosphonomethylphenylalanine
Fmoc	Fluorenylmethyloxycarbonyl
FMPP	4-fluoromethyl phenyl
FN	Fibronectin
FOMT	4’-*O*-[2-(2-fluoromalonyl)]-1-tyrosine
HBr	Hydrobromic Acid
HBTU	*O*-benzotriazole-*N*,*N*,*N*’,*N*’-tetramethyl-uronium-hexafluoro-phosphate
HePTP	Hematopoietic Protein Tyrosine Phosphatase
HSQC	Heteronuclear Single Quantum Coherence
IBX	2-Iodoxybenzoic Acid
IC50	Half Maximal Inhibitory Concentration
ITAM	Imunnorecepter Tyrosine-based Activation Motif
KF	Potassium Fluoride
LAH	Lithium Aluminum Hydride
Lmptp	low Mr phosphatase
MeCN	Acetonitrile
MsCl	Mesyl Chloride
NBS	*N*-Bromosuccinimide
NMR	Nuclear Magnetic Resonance
OMT	L-*O*-malonyltyrosine
PBr3	Phosphorous tribromide
PCC	pyridinium chlorochromate

PKs	Protein Kinases
P-loop	Phosphate Binding Loop
Pmp	Phosphonomethyl-phenylalanine
PPh3	Triphenyl Phosphine
PPs	Protein Phosphatases
PTP	Protein Tyrosine Phosphatase
pTyr	Phosphotyrosine
pTyr(S)	Thiopohosphoryl
QMG	Quinone methide generating
SDS-PAGE	Sodium Dodecyl Sulfate Polyacrylamide Gel Electrophoresis
SHP 1	Src Homology Phosphatase-1
SHP 2	Src Homology Phosphatase-2
SKFs	Src family protein tyrosine kinases
SOBr2	Thionyl Bromide
SOCl2	Thionyl Chloride
SPPS	Solid Phase Peptide Synthesis
TBNS	Trans-β-nitrostyrene
TCPTP	T cell protein tyrosine phosphatase
TCR	T cell receptor
TEABr	Triehtylamine Bromide
TFA	Trifluoroacetic Acid
TLC	Thin Layer Chromatography
TMSA	Trifluoro-methane-sulphonic acid

TMSBr	Trimethyl Silane Bromide
TMSI	Trimethyl Silane Iodide
TsCl	Tosyl Chloride
UV-vis	Ultraviolet–visible
VHR	*Vaccinia* H1-Related Phosphatase
Yop51	*Yersinia* Outer Proteins 51
YopH	*Yersinia* Outer Proteins

Chapter 1: Inhibitors of PTPs

1.1 Introduction to PTPs

Phosphorylation and dephosphorylation of proteins in biological systems plays an important role in maintaining homeostasis. The state of phosphorylation is governed by the interplay between protein kinases (PKs) that catalyze phosphorylation and protein phosphatases (PPs) that dephosphorylate serine, threonine, and tyrosine residues. PPs have been classified into two broad categories based on their substrate specificity and structure: protein serine/threonine phosphatases and protein tyrosine phosphatases (PTPs). PTPs are important for the regulation of several signaling pathways, and aberrant PTP function has been associated with several diseases such as cancer and diabetes.[1, 2]

The human genome is currently known to have 107 PTPs that are broadly divided into four families depending on the amino acid sequence present in the catalytic domain. The largest of these families is the Class I cysteine-based PTPs that contain 38 tyrosine specific phosphatases (the classical phosphatases) and 61 dual-specific phosphatases (DSPs).[3] The classical PTPs can be further subdivided into 21 transmembrane receptor-like enzymes (e.g CD45, LAR, PTPσ) and 17 intracellular non-receptor-like PTPs (e.g. PTP1B, SHP1/2, TCPTP).[3] Of the 38 classical PTPs, the 12 receptor PTPs posses two catalytic domains (only one of which is active) while the remaining classical PTPs contain only one catalytic domain. Determining the biological function of this second inactive domain remains elusive, but it may play a role in dimerization,[4] substrate specificity, cytoskeletal interactions,[5] or stability.[3]

DSPs, like classical PTPs, are also capable of dephosphorylating tyrosine residues, and can accommodate phosphorylated serine and threonine residues. DSPs tend to be more structurally diverse than classical PTPs, but contain a smaller conserved catalytic domain.[6]

The second family of PTPs is the Class II cysteine-based PTPs. This family of PTPs is found in both bacterial and mammalian species; however, there is only one known example in the human genome, the low Mr phosphatase (lmptp).[7] A third class of PTPs is the Class III cysteine-based PTPs. These enzymes posses duel specificity and are found in all eukaryotic organisms, with the exception of plants.[8] In humans, this class is comprised of three cell cycle regulators: CDC25A, CDC25B, and CDC25C.[9]

The final class of PTPs in the PTP super-family differs from the previous three based on the presence of an aspartate in place of a cysteine as the active catalytic residue. This class is referred to as the Class IV aspartate-based PTPs. It is comprised of four proteins which play important roles in development (Eya 1-4).[10, 11]

1.2 Catalytic domain and mechanism of activity

The first three classes of PTPs share a signature catalytic domain containing the CX_5R consensus sequence, and share a similar enzymatic mechanism of action.[12] Seven residues of the catalytic consensus sequence form a cup, commonly referred to as the phosphate binding loop (P-loop).[13] The P-loop, and its proposed mechanism of action, are illustrated in **Figure 1.1**. In the first step of the mechanism, the phosphorylated substrate becomes anchored to the P-loop through the three anionic oxygens of the phosphate moiety, stabilized by hydrogen bonding through arginine and aspartic acid residues. The phosphate moiety, now in close proximity to the nucleophilic cysteine residue[14] is attacked, resulting in a phosphocysteine intermediate, which is stabilized through hydrogen bonding via an arginine residue.[15] In the second, rate determining step, the phosphocysteine intermediate is hydrolyzed, liberating an inorganic phosphate which results in the regeneration of the active enzyme.[16] In this step, the aspartate residue acts as a general base by deprotonating an equivalent of water.[17] It is important to note that although PTPs in the first three classes share a similar mechanism of action, their respective rates of turnover vary greatly.[18]

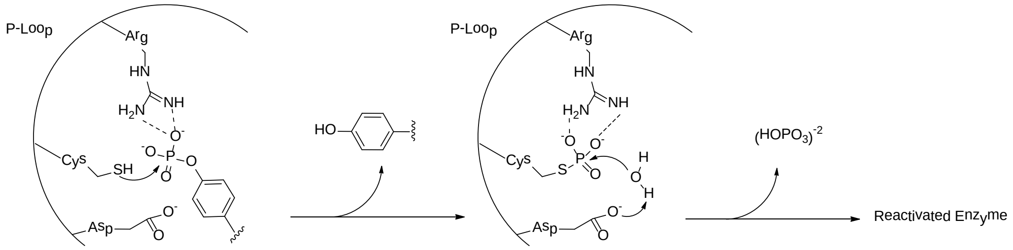

Figure 1.1 Conserved catalytic mechanism for the cysteine based PTPs

1.3 CD45

CD45 is a classical transmembrane PTP that is one of the most ubiquitous cell surface glycoproteins, present on all nucleated hematopoietic cells.[19] It plays an important role in the immune response, and its aberrant function has been linked to several diseases including systemic lupus erythematosus (SLE),[20] Alzheimer's disease,[21] and rheumatoid arthritis.[21] In particular, CD45 plays a critical role in the activation and regulation of B cells and T cells.[22, 23] During T cell maturation the glycan structures attached to CD45 undergo dramatic changes with the loss of sialic acid from core 1 O-glycans.[24] Activation of lymphocytes occurs via the hydrolysis of auto-phosphorylated pTyr sites of primary substrates in CD45, the Src family protein tyrosine kinases: (SFKs).[25] The SFKs are comprised of nine non-receptor kinases Src, Yes, Fyn, Fgr, Lck, Hck, Blk, Lyn, and Frk. Activated SFKs phosphorylate components of either the B cell receptor (BCR) or T-cell receptor (TCR), resulting in further downstream signal transduction events, and eventual leukocyte activation.[25] The SFKs involved in T cell activation are Lck[26] and Fyn;[26] whereas, B cell activation involves Lyn,[27] Fyn,[27] and Blk.[27]

The major structural features of CD45 are illustrated in **Figure 1.2**. CD45 exists in several isoforms due to alternative splicing of three exons which make up the extracellular domain.[28] Each of these isoforms is further differentiated by weight, three dimensional structure, and charge due to O-linked glycosylation encoded in these exons.[4] Two isoforms are illustrated in **Figure 1.2** RABC and RO. The remaining extracellular portion of CD45 is comprised of a region abundant in cysteine residues followed by three fibronectin (FN) type 3 repeats that are also heavily glycosylated with N-linked glycans.[4] A single transmembrane domain connects the extracellular portion of CD45 to its cytoplasmic tail. The cytoplasmic portion of CD45 contains two catalytic domains (D1 and D2), of which only D1 is enzymatically active.

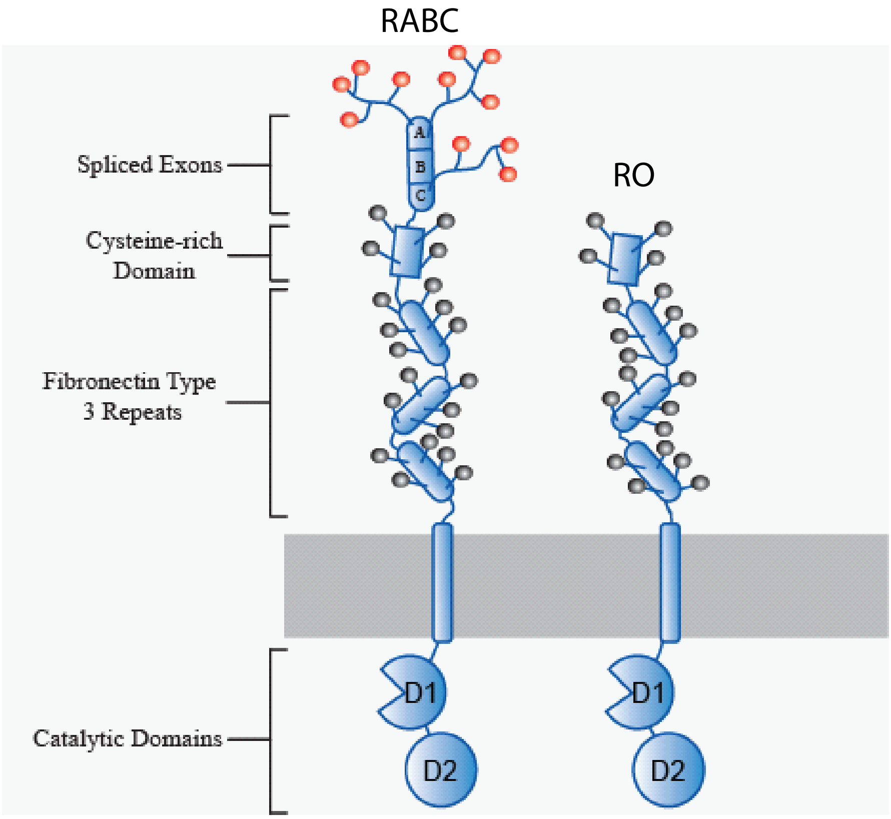
RABC
RO
Spliced Exons
Cysteine-rich Domain
Fibronectin Type 3 Repeats
Catalytic Domains
A
B
C
D1
D2
D1
D2

Figure 1.2 Structure of CD45. CD45 exists in several isoforms due to alternative splicing of the three exons (A, B, and C). Two potential isoforms RABC and RO are illustrated. The remaining extracellular portion of CD45 is comprised of a region abundant in cysteine residues followed by three fibronectin (FN) type 3 repeats and is heavily glycosylated. A single transmembrane domain connects the extracellular portion of CD45 to its cytoplasmic tail that contains two domains, D1 is enzymatically active. Adapted from Hermiston et al.[4]

1.4 Inhibitors of PTPs

Despite the clear importance of PTPs in disease, identifying their respective biological functions remains challenging due to the lack of PTP specific inhibitors. The availability of such inhibitors could not only yield potentially valuable therapeutics for PTP dependent diseases, but could also provide us with chemical tools to elucidate the physiological significance of protein tyrosine phosphorylation in complex signaling pathways. We survey known PTP inhibitors below, beginning with nonspecific metal based inhibitors and natural products before moving on to rationally designed pTyr mimetics.

1.4.1 Metal-based inhibitors

Several metal based complexes and salts have been shown to inhibit a broad range of PTPs (**Figure 1.3**). Perhaps the best known inorganic species is vanadate (**1.1**),[29] which inhibits PTPs by mimicking the phosphate group, binding reversibly at the catalytic site. Other inorganic compounds that have been shown to inhibit PTPs include disodium aurothiomalate (**1.2**),[30] phenyl arsine oxide (**1.3**),[31] and nitric acid.[32] To date no strategies have emerged for the development of specific metal-based PTP inhibitors limiting their usefulness for targeted therapeutics.

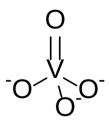

1.1

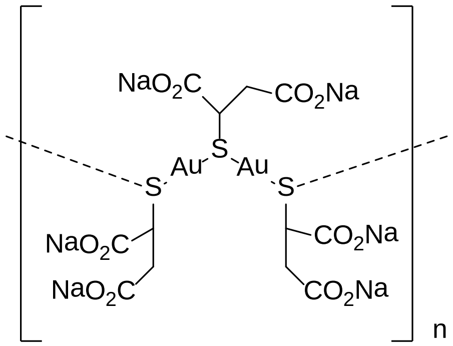

1.2

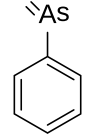

1.3

Figure 1.3 Common inorganic PTP inhibitors. Structures of vanadate (**1.1**), disodium aurothiomalate (**1.2**), and phenyl arsine oxide (**1.3**) are shown.

1.4.2 Natural products

Several natural products have been identified as inhibitors of PTPs (**Figure 1.4**). Moreover, several of these natural products have shown specificity for certain PTPs. Pulchellalactam (**1.4**), a lactam based inhibitor, first isolated from the marine fungus *Corollospora pulchella*, was found to selectively inhibit CD45 (IC_{50} of 0.83 mM) over PTP1B.[33] Preferential inhibition of CD45 over PTP1B has also been observed with α,β-unsaturated lactone-containing inhibitors dihydrocarolic acid (**1.5**) ($IC_{50,CD45}$ = 6.7 μM over $IC_{50,PTP1B}$ = 211.1 μM) and penitricin ($IC_{50,CD45}$ = 12.8 μM over $IC_{50,PTP1B}$ = 87.8 μM) isolated from the black mould *Aspergillus niger*.[34]

The alkaloid nornuciferine (**1.6**) discovered in the screening of *Rollinia ulei* (custard apple) extracts was found to inhibit CD45 (IC_{50} = 5.3 μM) selectively over other non-PTPs, such as PP2B, alkaline phosphatase, and acid phosphatase.[35] Nornuciferine is also thought to posses anti-depressant properties through its ability to bind to 5-HT1A receptors,[36] and is biologically active against the parasitic disease leishmaniasis.[37]

Another promising natural product PTP inhibitor is dysidiolide (**1.7**), first isolated from the marine sponge *Dysidea etheria*.[38] Dysidiolide has been identified as an inhibitor of CDC25A (IC_{50} = 9.4 μM) while not inhibiting other phosphatases such as CD45, PP2B and LAR at this concentration.[38] Dysidiolide has also been shown to inhibit the growth of

A459 human lung carcinoma and P388 murine leukemia cells with low micromolar potency.[38]

The stevastelines, a group of depsipeptide natural products, are a have been shown to inhibit PTPs. Stevastelines were first isolated from *Penicillium sp*. and found to be immunosuppressive agents through inhibition of T cell proliferation.[39] Specifically, they inhibit the DSP VHR (*Vaccinia* H1-Related) Phosphatases, arresting cell cycle progression. Among this class of compounds, stevasteline A (**1.8**) is the most potent VHR inhibitor (IC_{50} = 2.7 μM); however, due to the presence of a charged sulphate group on the threonine residue, it is unable to cross the cellular membrane rendering it ineffective in cell based assays.

While the mechanisms of inhibition of these natural products have not been explored, several are Michael acceptors (**1.4**, **1.5**, and **1.7**). As a result Michael addition may play a role in their mechanism of inhibition.

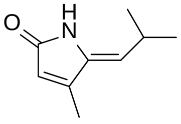

1.4

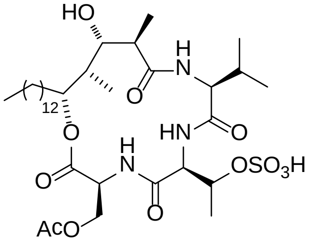

1.8

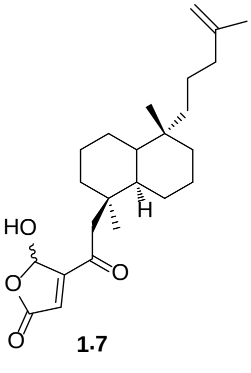

1.7

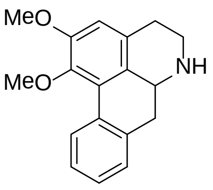

1.6

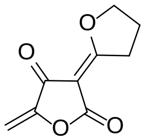

1.5

Figure 1.4 Natural product inhibitors of PTPs. Structures of pulchellalactam (**1.4**), dihydrocarolic acid (**1.5**), nornuciferine (**1.6**), dysidiolude (**1.7**) and stevasteline A (**1.8**) are shown.

1.4.3 Reversible nonhydrolyzable pTyr-based inhibitors

Although there is a rich pool of natural products for medicinal chemists to draw inspiration from in the design of PTP inhibitors, a variety of rational approaches have been employed to identify new inhibitors (**Figure 1.5**). The earliest, and perhaps most elegant, example has been the replacement of the phosphorylated tyrosine with a non-hydrolyzable pTyr mimetic functional group. This replacement may either retard or inhibit the catalytic cycle of the enzyme, thus acting as a competitive inhibitor. One example of this has been illustrated by the replacement of the pTyr moiety (**1.9**) with a thiopohosphoryl (pTyr(S)) functional group (**1.10**). The pTyr(S) residue mimics the phosphate functional group, showing high affinity for PTPs, yet these analogs are poor substrates of the enzymes due to either steric (a sulfur atom is larger than oxygen) and electronic (relatively lower electrophilicity of the central phosphorus atom) properties, which impede the formation of the thiophosphate intermediate required for PTP hydrolysis.[40]

Another example of a nonhydrolyzable phosphotyrosyl mimetic has exploited the replacement of the phosphate group with a phosphonate first developed by Roques and colleagues in the late 80s.[53] They replaced the benzylic oxygen atom of the pTyr with a methylene group, resulting in a phosphonomethyl-phenylalanine (Pmp) derivative (**1.11**). It has been shown that the replacement of the pTyr with the Pmp residue in decamer peptides resulted in competitive inhibitors with IC_{50} values ranging between 10 – 30 μM against PTP1B.[41]

The Pmp derivative developed by Roques and colleagues was further improved upon by Burke et al.[55] in 1992 through the synthesis of the α,α-difluorophosphonomethylphenylalanine (F_2Pmp) pTyr analog (**1.12**). Burke's rationale behind the introduction of the two fluorine atoms at the α-methylene position was based on the observation that the presence of fluorine atoms adjacent to a phosphonate improved the efficacy of pTyr mimetics in aliphatic systems presumably due to electronic effects.[42, 43] This rationale was validated when F_2Pmp was incorporated into a hexameric EGF receptor peptide and found to be 1000 fold more active (IC_{50} = 200 nM) than the Pmp analog (IC_{50} = 200 μM) against PTP1B.[44] Protein crystal structures have suggested that this increase in potency may be attributed to hydrogen bonding interactions between the protein and one of the fluorine atoms.[45] [what about electronics? Wouldn't this mimic the role of the benzylic oxygen?] Supporting this hypothesis, model studies of enantiopure aryl monofluoromethylphosphonic acids have shown to have a 10-fold affinity difference between the *R* and *S* isomers of the α-methylene fluorine.[46]

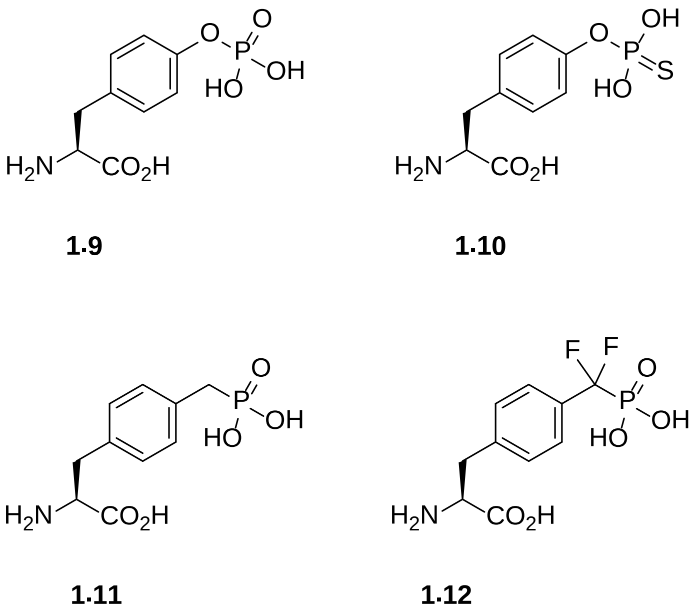

1.9 1.10 1.11 1.12

Figure 1.5 Phosphotyrosine mimetics. Structures of *p*Tyr (**1.9**), *p*Tyr (S) (**1.10**), Pmp (**1.11**) and F_2Pmp (**1.12**) are shown.

One problem with pTyr based inhibitors is their reduced bioavailability due to the charged phosphate group. To address this shortcoming, attempts have been made to explore non-phosphorous containing peptide inhibitors. The first of these was reported by Burke et al. through the introduction of a L-*O*-malonyltyrosine (OMT) containing peptide (**Figure 1.6, 1.13**). Based on chemistry developed by Miller and colleagues,[47] OMT peptide analogs were known to mimic pTyr functionality by utilizing carboxcylic acid groups. Incorporation of the OMT peptide analog into the hexameric EGF receptor peptide showed a 20-fold increase in activity (IC_{50} = 10 μM) against PTP1B when compared to the hexameric peptide containing the Pmp analog (IC_{50} = 200 μM).[48] The activity was further improved by the introduction of a fluorine atom into the OMT function group resulting in 4’-*O*-[2-(2-fluoromalonyl)]-*L*-tyrosine (FOMT, **1.14**). There was a 10-fold increase in potency between the EGF receptor peptide containing fluorinated OMT (IC_{50} = 1 μM) and non-fluorinated OMT analog.[49]

Cyclic OMT (**Figure 1.6b**) peptides are another class of peptide inhibitors that have been explored for the inhibition of PTPs. The cyclic nature of these peptides is thought to restrict the conformational flexibility of the OMT group,[50] thus increasing their affinity for PTPs. Such an observation was made against PTP1B for a linear OMT containing peptide (K_i = 13.0 μM) and a cyclic OMT containing peptide (K_i = 2.6 μM).[50] Another benefit of cyclic peptides is their increased proteolytic stability in comparison to linear peptides containing the OMT analog.

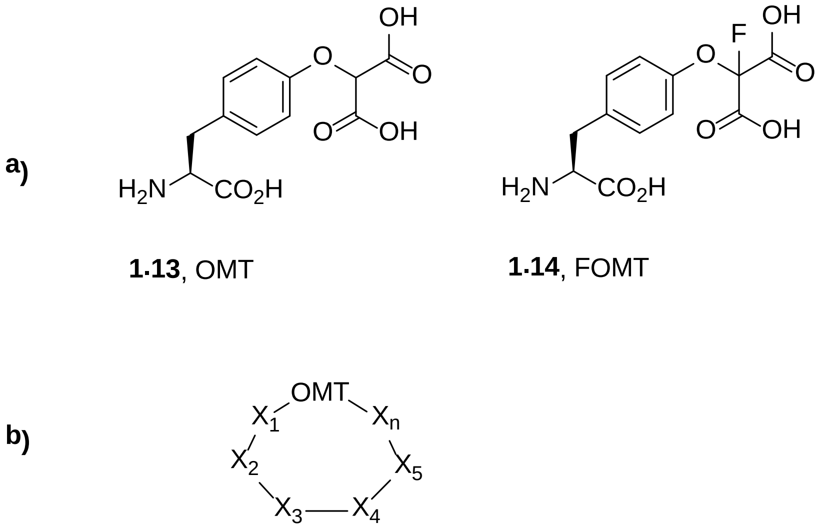

Figure 1.6 OMT based phosphotyrosine mimetics. a) Structures of OMT (**1.13**) and FOMT (**1.14**) b) A structure of a cyclic peptide incorporating OMT.

1.4.4 Irreversible mechanism based PTP inhibitors

In recent years, there has been a growing trend to develop irreversible mechanism based PTP inhibitors. Much of this work has been built on the success of developing similar mechanism-based inhibitors for serine hydrolases and cysteine proteases.[51, 52] Mechanism-based PTP inhibitors typically incorporate a tyrosyl-electrophile that is intended to alkylate the thiolate anion of the nucleophilic cysteine residue present in the catalytic domain of PTP, resulting in irreversible inhibition. Several classes of irreversible PTP inhibitors will be discussed below. The development of more potent and specific inhibitors should provide new insight into the intracellular activity of PTPs.

1.4.4.1 Quinone-methide based inhibitors

Quinone methides (**Figure 1.7a, 1.15**) are common reactive intermediates found in a variety of bioactive compounds.[53] Quinone methide generating (QMG) small molecules were first introduced in 1990 by Danzin and colleagues and were found to inhibit hydrolytic enzymes, such as esterases and glycosidases.[54] Building on this work, Widlanski and colleagues incorporated the QMG motif into several phosphate analogs and found that they inhibited prostatic acid phosphatase.[55] Additionally, Widlanski et al. postulated that these QMG phosphate analogs would also function as PTP inhibitors. This hypothesis was first validated by Withers and colleagues, who developed a mechanistic framework for these QMG phosphate analogs (**Figure 1.7b**).[56] After dephosphorylation of QMG analogs the highly reactive quinone methide species was formed through a 1,6-elimination. The quinone methide is subsequently alkylated by nucleophiles in close proximity, resulting in a covalent adduct.

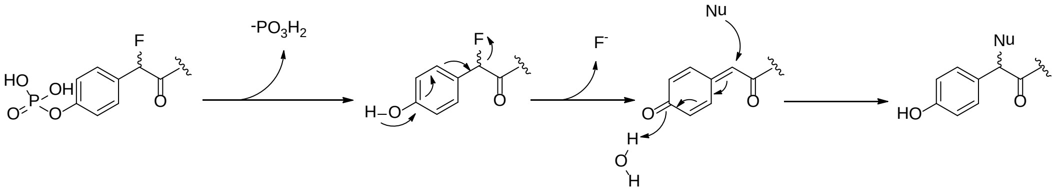

Figure 1.7 Mechanistic framework of QMG phosphate analogs. a) Quinone methide reactive intermediate b) Mechanism of inactivation of quinone methide generating inhibitors**.**[56]

The QMG approach has been recently used by Lo and colleagues in the development of covalent PTP-based probes.[57] These probes consisted of four parts: a phosphate group that served as a recognition element, a latent trapping device derived from mandelic acid, a linker, and a reporting group (biotin or a fluorescent dansyl group) for visualization (**Figure 1.8a**). Incubation of these probes with a cocktail of proteins (trypsin, β-galactosidase, carbonic anhydrase, phosphorylase, PTP1B and albumin) showed the selective formation of a covalent adduct by SDS-PAGE analysis and ^{19}F NMR with PTP1B. However, these probes were not tested against other classes of PTPs and the site of alkylation on PTP1B was not determined. Subsequent mass spectrometry experiments carried out by Lo and colleagues revealed that all six cysteine residues of PTP1B were capable of being modified by the probes, suggesting a lack of specificity for the active site.[58]

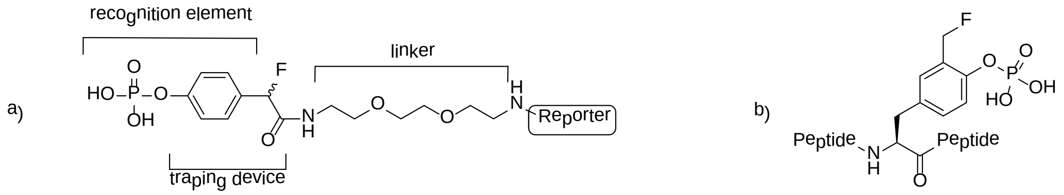

1.16

Figure 1.8 QMG based probes a) Probes incorporating QMG small molecule developed by Lo et al. b) Unatural amino acids containing a 4-fluoromethyl phenyl (FMPP) phosphate motif

Although QM probes have been successfully used to profile and label PTP enzymes, significant limitations remain. For example, the 4-fluoromethylaryl phosphate analogs developed by Widlanksi et al. were not specific for PTPs and were shown to form covalent adducts with other classes of phosphatases, including nonspecific labeling of prostatic acid phosphatase and calcineurin.[55, 56, 59] Furthermore, the reactive intermediate of QMG probes persists long enough to diffuse and react with other species, raising the potential of alkylation of proteins in close proximity to the desired target.

The problems associated with the diffusible nature of QMG probes has been partially solved by the incorporation of the masked quinone methide motif into small peptides. Shao et al.[60] and Lo et al.[61] have independently developed unnatural amino acids containing a 4-fluoromethyl phenyl (FMPP) phosphate motif which were incorporated into tripeptides (**Figure 1.8b, 1.16**). Presumably, the mechanism of these FMPP probes proceeds in a similar fashion to the QMG analogs developed by Widlanksi. Incorporation of the FMPP amino acid into tripeptides increased their specificity between PTP and other phosphatases as well as within the PTP family. Although both Shao et al. and Lo et al. have made significant efforts to overcome the shortcomings of QMG-based inhibitors, the potential for nonspecific labeling by the reactive quinone methide remains a potential problem that will need to be addressed in any therapeutic strategies.

1.4.4.2 Trans-β-nitrostyrene inhibitors

In 2004, Pei et al. first reported the use of trans-β-nitrostyrene (TBNS) as inhibitors of PTPs (**Figure 1.9a**).[62] The mechanism of inactivation was elucidated by HSQC NMR, site directed mutagenesis and UV-vis absorption spectroscopy experiments.[62] Initially, TBNS binds to the PTP active site in a non-covalent fashion (**Figure 1.9b**). Subsequent attack of the nucleophilic cysteine residue in the PTP active site on the nitro group of the TBNS forms a covalent adduct. It is important to note that the double bond alpha to the nitro group was vital for inhibition even though it is not attacked by the cysteine residue in the active site.[62] Pei and colleagues postulated that the double bond is required to maintain a rigid planar geometry critical for binding and orientation of the nitro group for nucleophilic attack.[62] TBNS derivatives were found to inhibit the PTPs PTP1B, SHP-1, and Yop. Overall TBNS represents a promising new class of covalent PTP inhibitors. One significant benefit is its overall electronic neutrality which may allow for increased membrane permeability. However further studies are required to determine its stability to thiols and cross reactivity to other non-PTPs.

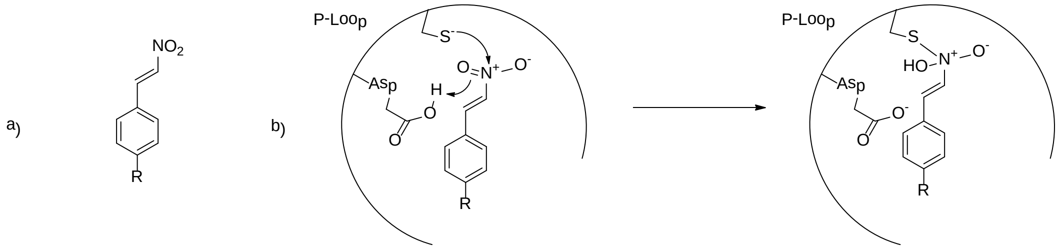

Figure 1.9 TBNS as inhibitors of PTPs. a) TBNS inhibitors b) Mechanism of inactivation of TBNS inhibitors

1.4.4.3 α-Bromo benzylic inhibitors

Novel PTP inhibitors based on an α-bromobenzylphosphonate motif were first developed but Widlanksi et al.[63] and have recently been used by Zhang and colleagues as irreversible, covalent inhibitors of PTPs (**Figure 1.10**).[64] These inhibitors closely resemble the PTP native substrate and contain an amine handle to which visualization tags, such as biotin (**1.17 & 1.18**) or rhodamine, have been attached.[64,65] Confirmation that covalent enzyme-inhibtor adducts were formed was provided by mass spectrometry and Western blotting. Enzyme kinetic experiments supported the notion that these inhibitors target the active site.[64, 66] However the mechanism of inactivation of this class of inhibitors remains unclear.

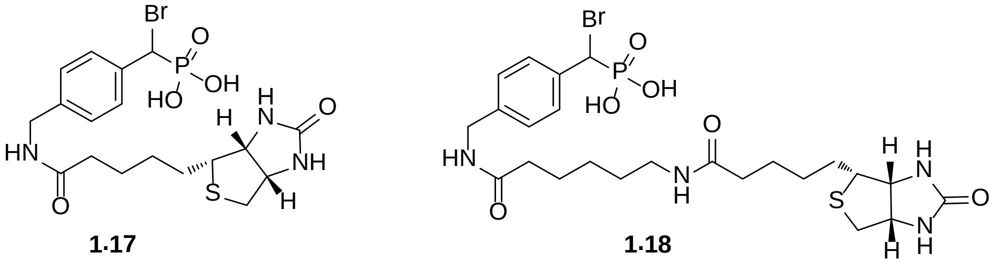
1.17

1.18

Figure 1.10 α-bromobenzylphosphonate developed by Zhang and colleagues

Two potential mechanisms for α-bromobenzylphosphonate inhibition proposed by Zhang are illustrated in **Figure 1.11**.[64] In the first mechanism, the nucleophilic cysteine present in the P-loop attacks the phosphonate group resulting in a phosphocysteine intermediate. The bromide is then expelled by the formation of a phosphono oxirane species which is subsequently opened resulting in the formation of an α-hydroxybenzylphosphonate covalently attached to the cysteine residue. In an alternative proposal the nucleophilic cysteine displaces the bromide at the benzylic position to form a covalent adduct. However, Zhang et al concluded that this second mechanism seems less likely, as crystal structures of PTPs bound to pTyr and its other nonhydrozable derivatives show that the cysteine residue is not close enough to attack the benzylic position.[64] Site directed mutagenesis experiments have excluded the possibility that the aspartic acid residue in the P-loop displaces the bromide.[64]

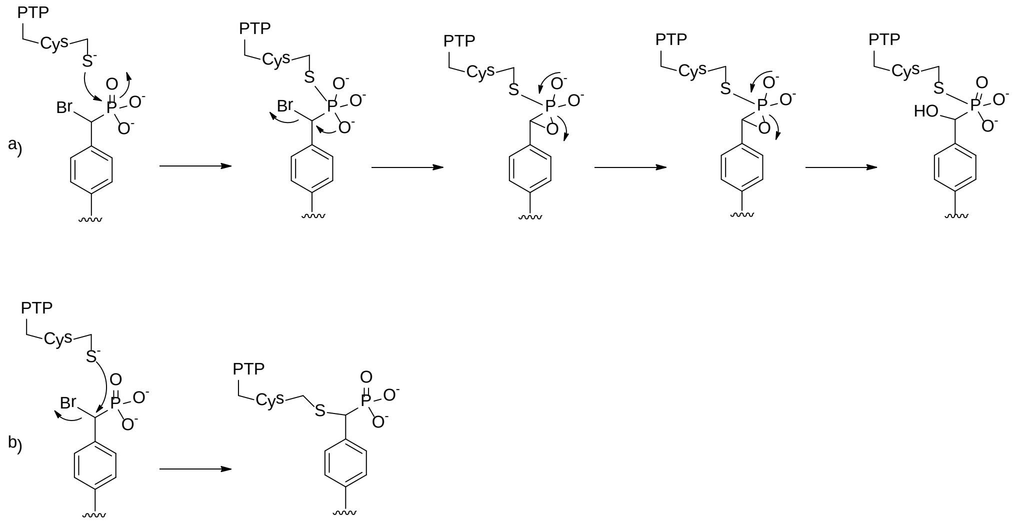

Figure 1.11 Potential mechanism of α-bromobenzylphosphonate inactivation of PTPs a) Nucleophilic cysteine attacks phosphate group resulting in a phosphocysteine intermediate **b)** Nucleophilic cysteine displaces the bromide at the benzylic position resulting in a covalent adduct.

These inhibitors showed high specificity for PTPs and did not show any cross-reactivity to alkaline, potato, prostatic acid, DSP, or λ phosphatases or the entire proteome of *E. coli*.[64] However, these inhibitors were unable to discriminate between members of the PTP family reacting with PTP1B, HePTP, SHP2, LAR, PTPα, PTPH1, VHR, and CDC14.[64]

Zhang and colleagues have gone on to use these inhibitors to investigate the PTP activity in whole cell lysates. Interestingly, cell lysates from different cancer cells lines incubated with α-bromobenzylphosphonate inhibitors displayed very different PTP activities suggesting that these inhibitors may have potential as diagnostics.[65] Zhang and coworkers also used these inhibitors to examine the oxidative regulatory function of H_2O_2 in PTPs.[65]

It is thought that H_2O_2 oxidizes the active site cysteine in PTPs forming cysteinic sulfenic acid (S-OH) rendering it non-nucleophilic, and thus hindering PTP activity.[67-69] Conversely, cysteinic-sulfenic acid can be reduced back to the nucleophilic cysteine residue by various reductants present in the cell, suggesting that H_2O_2 may act as an intracellular messenger.[70] As expected, Zhang and coworkers observed decreased amounts of PTP labeling in the lysates of cells that had been treated with H_2O_2.

Despite their utility for labeling PTPs α-bromobenzylphosphonate inhibitors are not without limitations. The inability to distinguish amongst the PTP family is a significant barrier to the design of specific PTP inhibitors. Other limitations include poor membrane permeability due to the charged nature of the deprotected phosphonate, and potential hydrolysis of the benzylic bromide in basic pH.

1.4.4.4 Vinyl sulfone inhibitors

Building on their previous work on α-bromo benzylic inhibitors, Zhang and colleagues developed a new class of inhibitors based on a vinyl sulfone motif (**Figure 1.12a, 1.19 & 1.20**). Based on kinetics, mass spectrometry and X-ray crystallography experiments, this class of molecules are active site directed, irreversible covalent inhibitors for a wide range of PTPs.[71] The formation of the covalent adduct involves the nucleophilic attack of the cysteine residue (in the active site of the enzyme) on the vinylic position, resulting in the formation of a stable thioether bond via a Michael 1,4-conjugate addition (**Figure 1.12b**).[71]

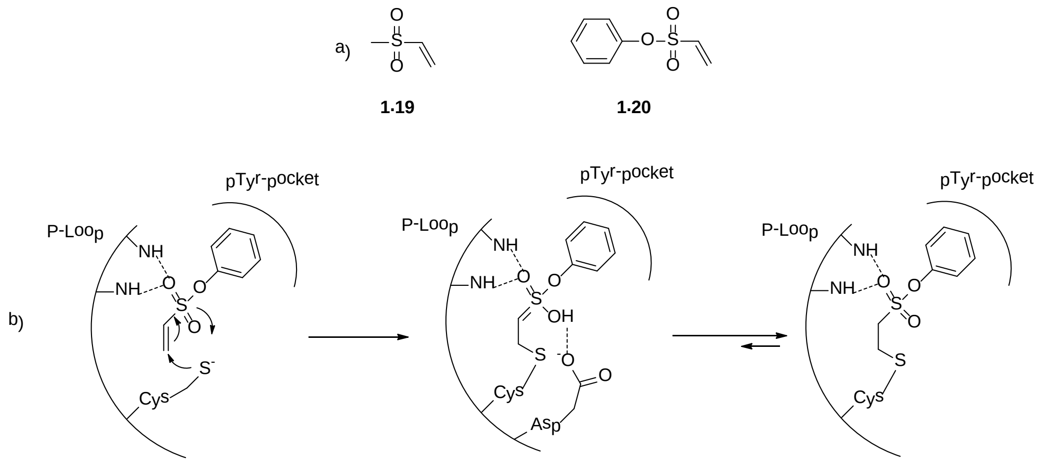

Figure 1.12 Vinyl sulfone inhibitors and their mechanism of inhibiton. a) vinyl sulfone inhibitors b) Mechanism of PTP inactivation of vinyl sulfone inhibitors.

Other conserved structural elements of the PTP catalytic domain assist the binding of vinyl sulfone inhibitors to the PTP active site. The pTyr hydrophobic pocket which stabilizes the phenyl ring[71] plays an important role in binding as methyl vinyl sulfone (**1.19**) had no noticeable effect on inhibition the PTP YopH. Further stabilization is provided by hydrogen bonding interactions between the sulfonyl oxygens and conserved aspartate and arginine resides in the active site.[71]

To explore whether these new inhibitors could show specific labeling of PTPs in a complex proteome, Zhang and colleagues appended an azide tag to the inhibitors and biotin to a small alkyne.[71] The azide labeled inhibitor was then incubated in the cell lysate of a recombinant *E. coli* strain expressing the PTP HePTP.[71] The azide labeled inhibitor (and any covalently attached PTP) was then captured by the biotin labeled alkyne via copper(I) catalyzed azide-alkyne cycloaddition (CuAAc).[72] Western blot analysis showed strong labeling of HePTP with little background labeling from the PTP deficient proteome of *E. coli*.[71] These results suggest that arylvinylsulfone inhibitors are promising inhibitors for PTPs and could provide a useful scaffold for future PTP probe development.

1.4.4.5 Seleninate-based inhibitors

It has been known for several decades that seleninic acids posses the ability to couple to thiols over a wide range of pH to produce a selenosulfide (RSeSR') product (**Figure 1.13**).[73] Armed with this information, Zhang and colleagues have recently replaced the phosphate of pTyr with a seleninic acid motif (-CH_2SeO_2H) creating a new irreversible covalent inhibitor of PTPs.[74] These inhibitors were found to inactivate the bacterial PTP YopH as well as the mammalian PTPs PTP1B, VHR and VHX. Preliminary kinetic, mass spectrometry, and X-ray crystallography experiments suggest that these seleninate based inhibitors are active site directed, irreversible and covalent in nature.[74] These results highlight the potential for seleninate based small molecules to be used as a new class of inhibitors to study the physiological function of PTPs.

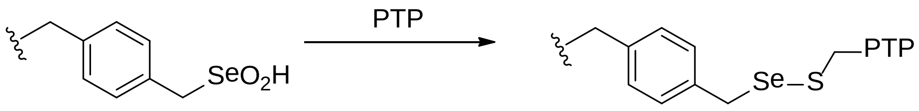

Figure 1.13 Seleninate based PTP inhibitors

1.5 Project objectives

The design of specific PTP inhibitors remains a challenge, and new strategies that provide enhanced activity are of continued interest. Building on the work of Widlanksi et al.,[63] Zhang and colleagues have shown that biotin labelled α-bromobenzylphosphonate analogs **1.17** and **1.18** covalently label a variety of PTPs - albeit without any appreciable specificity.[64] Literature precedent would suggest that PTPs often recognize specific amino acid sequences,[75] and that additional functional groups could impart specificity to the α-bromobenzylphosphonate group (BBP).

We hypothesized that the BBP functional group could be used to develop targeted PTP inhibitors, by incorporation into peptide sequences. This thesis explores our hypothesis by first investigating the synthesis of Widlanski's α-bromobenzylphosphonate analog. Using model compounds, we tested the stability of these compounds to solid phase peptide synthesis (SPPS) conditions. We then developed a synthetic methodology for generating an amino acid analog that incorporates the BBP functional group, and tested its activity against PTP enzymes (Chapter 2). Using this analog, we then attempted to incorporate the BBP group into longer peptide sequences (Chapter 3).

If successful, this methodology will provide a modular strategy for the development of specific PTP inhibitors using automated SPPS.

1.6 References

1. Petrone, A.; Sap, J., Emerging issues in receptor protein tyrosine phosphatase function: Lifting fog or simply shifting? *Journal of Cell Science* **2000**, 113, (13), 2345-2354.

2. Moorhead, G. B. G.; De Wever, V.; Templeton, G.; Kerk, D., Evolution of protein phosphatases in plants and animals. *Biochemical Journal* **2009**, 417, (2), 401-409.

3. Andersen, J. N.; Mortensen, O. H.; Peters, G. H.; Drake, P. G.; Iversen, L. F.; Olsen, O. H.; Jansen, P. G.; Andersen, H. S.; Tonks, N. K.; Moller, N. P. H., Structural and evolutionary relationships among protein tyrosine phosphatase domains. *Molecular and Cellular Biology* **2001**, 21, (21), 7117-7136.

4. Hermiston, M. L.; Xu, Z.; Weiss, A., Cd45: A critical regulator of signaling thresholds in immune cells. *Annual Review of Immunology* **2003**, 21, 107-137.

5. Cairo, C. W.; Das, R.; Albohy, A.; Baca, Q. J.; Pradhan, D.; Morrow, J. S.; Coombs, D.; Golan, D. E., Dynamic regulation of CD45 lateral mobility by the spectrin-ankyrin cytoskeleton of T cells. *Journal of Biological Chemistry* **2010**, 285, (15), 11392-11401.

6. Tonks, N. K., Protein tyrosine phosphatases: From genes, to function, to disease. *Nature Reviews Molecular Cell Biology* **2006**, 7, (11), 833-846.

7. Alonso, A.; Sasin, J.; Bottini, N.; Friedberg, I.; Friedberg, I.; Osterman, A.; Godzik, A.; Hunter, T.; Dixon, J.; Mustelin, T., Protein tyrosine phosphatases in the human genome. *Cell* **2004**, 117, (6), 699-711.

8. Boudolf, V.; Inze, D.; De Veylder, L., What if higher plants lack a CDC25 phosphatase. *Trends in Plant Science* **2006**, 11, (10), 474-479.

9. Honda, R.; Ohba, Y.; Nagata, A.; Okayama, H.; Yasuda, H., Dephosphorylation of human p34(CDC2) kinase on both Thr-14 and Tyr-15 by human CDC25B phosphatase. *Febs Letters* **1993**, 318, (3), 331-334.

10. Tootle, T. L.; Silver, S. J.; Davies, E. L.; Newman, V.; Latek, R. R.; Mills, I. A.; Selengut, J. D.; Parlikar, B. E. W.; Rebay, I., The transcription factor eyes absent is a protein tyrosine phosphatase. *Nature* **2003**, 426, (6964), 299-302.

11. Rayapureddi, J. P.; Kattamuri, C.; Steinmetz, B. D.; Frankfort, B. J.; Ostrin, E. J.; Mardon, G.; Hegde, R. S., Eyes absent represents a class of protein tyrosine phosphatases. *Nature* **2003**, 426, (6964), 295-298.

12. Fauman, E. B.; Saper, M. A., Structure and function of the protein tyrosine phosphatases. *Trends in Biochemical Sciences* **1996**, 21, (11), 413-417.

13. Fauman, E. B.; Yuvaniyama, C.; Schubert, H. L.; Stuckey, J. A.; Saper, M. A., The x-ray crystal structures of *Yersinia* tyrosine phosphatase with bound tungstate and nitrate - mechanistic implications. *Journal of Biological Chemistry* **1996**, 271, (31), 18780-18788.

14. Denu, J. M.; Zhou, G. C.; Guo, Y. P.; Dixon, J. E., The catalytic role of aspartic acid-92 in a human dual-specific protein-tyrosine-phosphatase. *Biochemistry* **1995**, 34, (10), 3396-3403.

15. Guan, K. L.; Dixon, J. E., Evidence for protein-tyrosine-phosphatase catalysis proceeding via a cysteine-phosphate intermediate. *Journal of Biological Chemistry* **1991**, 266, (26), 17026-17030.

16. Zhang, Z. Y.; Vanetten, R. L., Leaving group dependence and proton inventory studies of the phosphorylation of a cytoplasmic phosphotyrosyl protein phosphatase from bovine heart. *Biochemistry* **1991**, 30, (37), 8954-8959.

17. Hengge, A. C.; Denu, J. M.; Dixon, J. E., Transition-state structures for the native dual-specific phosphatase VHR and D92N and S131A mutants, contributions to the driving force for catalysis. *Biochemistry* **1996**, 35, (22), 7084-7092.

18. Chen, L.; Montserat, J.; Lawrence, D. S.; Zhang, Z. Y., VHR and PTP1 protein phosphatases exhibit remarkably different active site specificities toward low molecular weight nonpeptidic substrates. *Biochemistry* **1996**, 35, (29), 9349-9354.

19. Thomas, M. L., The leukocyte common antigen family. *Annual Review of Immunology* **1989**, 7, 339-369.

20. Takeuchi, T.; Pang, M.; Amano, K.; Koide, J.; Abe, T., Reduced protein tyrosine phosphatase (PTPase) activity of CD45 on peripheral blood lymphocytes in patients with systemic lupus erythematosus (SLE). *Clinical and Experimental Immunology* **1997**, 109, (1), 20-26.

21. Penninger, J. M.; Irie-Sasaki, J.; Sasaki, T.; Oliveira-dos-Santos, A. J., CD45: New jobs for an old acquaintance. *Nature Immunology* **2001**, 2, (5), 389-396.

22. Smith-Garvin, J. E.; Koretzky, G. A.; Jordan, M. S., T cell activation. *Annu Rev Immunol* **2009**, 27, 591-619.

23. Harwood, N. E.; Batista, F. D., Early events in b cell activation. *Annu Rev Immunol*, 28, 185-210.

24. Hernandez, J. D.; Klein, J.; Van Dyken, S. J.; Marth, J. D.; Baum, L. G., T-cell activation results in microheterogeneous changes in glycosylation of CD45. *International Immunology* **2007**, 19, (7), 847-856.

25. Ashwell, J. D.; D'oro, U., CD45 and src-family kinases: And now for something completely different. *Immunology Today* **1999**, 20, (9), 412-416.

26. Latour, S.; Veillette, A., Proximal protein tyrosine kinases it immunoreceptor signaling. *Current Opinion in Immunology* **2001**, 13, (3), 299-306.

27. DeFranco, A. L., B-cell activation 2000. *Immunological Reviews* **2000**, 176, 5-9.

28. Fukuhara, K.; Okumura, M.; Shiono, H.; Inoue, M.; Kadota, Y.; Miyoshi, S.; Matsuda, H., A study on CD45 isoform expression during t-cell development and selection events in the human thymus. *Human Immunology* **2002**, 63, (5), 394-404.

29. Rehder, D., The bioinorganic chemistry of vanadium. *Angewandte Chemie-International Edition in English* **1991**, 30, (2), 148-167.

30. Wang, Q. P.; Janzen, N.; Ramachandran, C.; Jirik, F., Mechanism of inhibition of protein-tyrosine phosphatases by disodium aurothiomalate. *Biochemical Pharmacology* **1997**, 54, (6), 703-711.

31. Garciamorales, P.; Minami, Y.; Luong, E.; Klausner, R. D.; Samelson, L. E., Tyrosine phosphorylation in T-cells is regulated by phosphatase-activity - studies with phenylarsine oxide. *Proceedings of the National Academy of Sciences of the United States of America* **1990**, 87, (23), 9255-9259.

32. Caselli, A.; Chiarugi, P.; Camici, G.; Manao, G.; Ramponi, G., In-vivo inactivation of phosphotyrosine protein phosphatases by nitric-oxide. *Febs Letters* **1995**, 374, (2), 249-252.

33. Alvi, K. A.; Casey, A.; Nair, B. G., Pulchellalactam: A CD45 protein tyrosine phosphatase inhibitor from the marine fungus *Corollospora pulchella*. *Journal of Antibiotics* **1998**, 51, (5), 515-517.

34. Alvi, K. A.; Nair, B. G.; Rabenstein, J.; Davis, G.; Baker, D. D., CD45 tyrosine phosphatase inhibitory components from *Aspergillus niger*. *Journal of Antibiotics* **2000**, 53, (2), 110-113.

35. Miski, M.; Shen, X.; Cooper, R.; Gillum, A. M.; Fisher, D. K.; Miller, R. W.; Higgins, T. J., Aporphine alkaloids, CD45 protein-tyrosine-phosphatase inhibitors, from *Rollinia ulei*. *Bioorganic & Medicinal Chemistry Letters* **1995**, 5, (14), 1519-1522.

36. Hasrat, J. A.; DeBruyne, T.; DeBacker, J. P.; Vauquelin, G.; Vlietinck, A. J., Isoquinoline derivatives isolated from the fruit of *Annona muricata* as 5-HTergic 5-HTLA receptor agonists in rats: Unexploited antidepressive (lead) products. *Journal of Pharmacy and Pharmacology* **1997**, 49, (11), 1145-1149.

37. Montenegro, H.; Guterrez, M.; Romero, L. I.; Ortega-Barria, E.; Capson, T. L.; Rios, L. C., Aporphine alkaloids from *Guatteria* spp. With leischmanicidal activity. *Planta Medica* **2003**, 69, (7), 677-679.

38. Gunasekera, S. P.; McCarthy, P. J.; KellyBorges, M.; Lobkovsky, E.; Clardy, J., Dysidiolide: A novel protein phosphatase inhibitor from the caribbean sponge *Dysidea etheria de Laubenfels*. *Journal of the American Chemical Society* **1996**, 118, (36), 8759-8760.

39. Morino, T.; Masuda, A.; Yamada, M.; Nishimoto, M.; Nishikiori, T.; Saito, S.; Shimada, N., Stevastelins, novel immunosuppressants produced by *Penicillium*. *Journal of Antibiotics* **1994**, 47, (11), 1341-1343.

40. Zhao, Z. H., Thiophosphate derivatives as inhibitors of tyrosine phosphatases. *Biochemical and Biophysical Research Communications* **1996**, 218, (2), 480-484.

41. Zhang, Z. Y.; Maclean, D.; Mcnamara, D. J.; Sawyer, T. K.; Dixon, J. E., Protein-tyrosine-phosphatase substrate-specificity - size and phosphotyrosine positioning requirements in peptide-substrates. *Biochemistry* **1994**, 33, (8), 2285-2290.

42. Blackburn, G. M., Phosphonates as analogs of biological phosphates. *Chemistry & Industry* **1981**, (5), 134-138.

43. Blackburn, G. M.; Parratt, M. J., The synthesis of alpha-fluoroalkylphosphonates. *Journal of the Chemical Society-Chemical Communications* **1983**, (16), 886-888.

44. Burke, T. R.; Kole, H. K.; Roller, P. P., Potent inhibition of insulin-receptor dephosphorylation by a hexamer peptide-containing the phosphotyrosyl mimetic F(2)Pmp. *Biochemical and Biophysical Research Communications* **1994**, 204, (1), 129-134.

45. Burke, T. R.; Ye, B.; Yan, X. J.; Wang, S. M.; Jia, Z. C.; Chen, L.; Zhang, Z. Y.; Barford, D., Small molecule interactions with protein-tyrosine phosphatase PTP1B and their use in inhibitor design. *Biochemistry* **1996**, 35, (50), 15989-15996.

46. Kotoris, C. C.; Wen, W.; Lough, A.; Taylor, S. D., Preparation of chiral alpha-monofluoroalkylphosphonic acids and their evaluation as inhibitors of protein tyrosine phosphatase 1B. *Journal of the Chemical Society-Perkin Transactions 1* **2000**, (8), 1271-1281.

47. Miller, M. J.; Braccolino, D. S.; Cleary, D. G.; Ream, J. E.; Walker, M. C.; Sikorski, J. A., Epsp synthase inhibitor design .4. New aromatic substrate-analogs and

symmetrical inhibitors containing novel 3-phosphate mimics. *Bioorganic & Medicinal Chemistry Letters* **1994**, 4, (21), 2605-2608.

48. Kole, H. K.; Akamatsu, M.; Ye, B.; Yan, X. J.; Barford, D.; Roller, P. P.; Burke, T. R., Protein-tyrosine-phosphatase inhibition by a peptide-containing the phosphotyrosyl mimetic, L-*O*-malonyltyrosine. *Biochemical and Biophysical Research Communications* **1995**, 209, (3), 817-822.

49. Burke, T. R.; Ye, B.; Akamatsu, M.; Ford, H.; Yan, X. J.; Kole, H. K.; Wolf, G.; Shoelson, S. E.; Roller, P. P., 4'-*O*-[2-(2-fluoromalonyl)]-L-tyrosine: A phosphotyrosyl mimic for the preparation of signal transduction inhibitory peptides. *Journal of Medicinal Chemistry* **1996**, 39, (5), 1021-1027.

50. Akamatsu, M.; Roller, P. P.; Chen, L.; Zhang, Z. Y.; Ye, B.; Burke, T. R., Potent inhibition of protein-tyrosine phosphatase by phosphotyrosine-mimic containing cyclic peptides. *Bioorganic & Medicinal Chemistry* **1997**, 5, (1), 157-163.

51. Cravatt, B. F.; Wright, A. T.; Kozarich, J. W., Activity-based protein profiling: From enzyme chemistry. *Annual Review of Biochemistry* **2008**, 77, 383-414.

52. Fonovic, M.; Bogyo, M., Activity based probes for proteases: Applications to biomarker discovery, molecular imaging and drug screening. *Current Pharmaceutical Design* **2007**, 13, (3), 253-261.

53. Peter, M. G., Chemical modifications of bio-polymers by quinones and quinone methides. *Angewandte Chemie-International Edition in English* **1989**, 28, (5), 555-570.

54. Halazy, S.; Berges, V.; Ehrhard, A.; Danzin, C., Ortho-(difluoromethyl)aryl-beta-d-glucosides and para-(difluoromethyl)aryl-beta-D-glucosides - a new class of enzyme-

activated irreversible inhibitors of beta-glucosidases. *Bioorganic Chemistry* **1990**, 18, (3), 330-344.

55. Myers, J. K.; Widlanski, T. S., Mechanism-based inactivation of prostatic acid-phosphatase. *Science* **1993**, 262, (5138), 1451-1453.

56. Wang, Q. P.; Dechert, U.; Jirik, F.; Withers, S. G., Suicide inactivation of human prostatic acid-phosphatase and a phosphotyrosine phosphatase. *Biochemical and Biophysical Research Communications* **1994**, 200, (1), 577-583.

57. Lo, L. C.; Pang, T. L.; Kuo, C. H.; Chiang, Y. L.; Wang, H. Y.; Lin, J. J., Design and synthesis of class-selective activity probes for protein tyrosine phosphatases. *Journal of Proteome Research* **2002**, 1, (1), 35-40.

58. Lo, L. C.; Chiang, Y. L.; Kuo, C. H.; Liao, H. K.; Chen, Y. J.; Lin, J. J., Study of the preferred modification sites of the quinone methide intermediate resulting from the latent trapping device of the activity probes for hydrolases. *Biochemical and Biophysical Research Communications* **2005**, 326, (1), 30-35.

59. Born, T. L.; Myers, J. K.; Widlanski, T. S.; Rusnak, F., 4-(fluoromethyl)phenyl phosphate acts as a mechanism-based inhibitor of calcineurin. *Journal of Biological Chemistry* **1995**, 270, (43), 25651-25655.

60. Kalesh, K. A.; Tan, L. P.; Lu, K.; Gao, L. Q.; Wang, J. G.; Yao, S. Q., Peptide-based activity-based probes (ABPS) for target-specific profiling of protein tyrosine phosphatases (PTPs). *Chemical Communications* **2010**, 46, (4), 589-591.

61. Huang, Y. Y.; Kuo, C. C.; Chu, C. Y.; Huang, Y. H.; Hu, Y. L.; Lin, J. J.; Lo, L. C., Development of activity-based probes with tunable specificity for protein tyrosine phosphatase subfamilies. *Tetrahedron* **2010**, 66, (25), 4521-4529.

62. Park, J.; Pei, D. H., Trans-beta-nitrostyrene derivatives as slow-binding inhibitors of protein tyrosine phosphatases. *Biochemistry* **2004**, 43, (47), 15014-15021.

63. Taylor, W. P.; Zhang, Z. Y.; Widlanski, T. S., Quiescent affinity inactivators of protein tyrosine phosphatases. *Bioorganic & Medicinal Chemistry* **1996**, 4, (9), 1515-1520.

64. Kumar, S.; Zhou, B.; Liang, F. B.; Wang, W. Q.; Huang, Z. H.; Zhang, Z. Y., Activity-based probes for protein tyrosine phosphatases. *Proceedings of the National Academy of Sciences of the United States of America* **2004**, 101, (21), 7943-7948.

65. Kumar, S.; Zhou, B.; Liang, F.; Yang, H. Y.; Wang, W. Q.; Zhang, Z. Y., Global analysis of protein tyrosine phosphatase activity with ultra-sensitive fluorescent probes. *Journal of Proteome Research* **2006**, 5, (8), 1898-1905.

66. Sun, J. P.; Wu, L.; Fedorov, A. A.; Almo, S. C.; Zhang, Z. Y., Crystal structure of the *Yersinia* protein-tyrosine phosphatase YopH complexed with a specific small molecule inhibitor. *Journal of Biological Chemistry* **2003**, 278, (35), 33392-33399.

67. Denu, J. M.; Tanner, K. G., Specific and reversible inactivation of protein tyrosine phosphatases by hydrogen peroxide: Evidence for a sulfenic acid intermediate and implications for redox regulation. *Biochemistry* **1998**, 37, (16), 5633-5642.

68. Reddie, K. G.; Carroll, K. S., Expanding the functional diversity of proteins through cysteine oxidation. *Current Opinion in Chemical Biology* **2008**, 12, (6), 746-754.

69. Reddie, K. G.; Seo, Y. H.; Muse, W. B.; Leonard, S. E.; Carroll, K. S., A chemical approach for detecting sulfenic acid-modified proteins in living cells. *Molecular Biosystems* **2008**, 4, (6), 521-531.

70. Barrett, W. C.; DeGnore, J. P.; Keng, Y. F.; Zhang, Z. Y.; Yim, M. B.; Chock, P. B., Roles of superoxide radical anion in signal transduction mediated by reversible regulation of protein-tyrosine phosphatase 1b. *Journal of Biological Chemistry* **1999**, 274, (49), 34543-34546.

71. Liu, S. J.; Zhou, B.; Yang, H. Y.; He, Y. T.; Jiang, Z. X.; Kumar, S.; Wu, L.; Zhang, Z. Y., Aryl vinyl sulfonates and sulfones as active site-directed and mechanism-based probes for protein tyrosine phosphatases. *Journal of the American Chemical Society* **2008**, 130, (26), 8251-8260.

72. Rostovtsev, V. V.; Green, L. G.; Fokin, V. V.; Sharpless, K. B., A stepwise huisgen cycloaddition process: Copper(I)-catalyzed regioselective "Ligation" of azides and terminal alkynes. *Angewandte Chemie-International Edition* **2002**, 41, (14), 2596-+.

73. Kice, J. L.; Lee, T. W. S., Oxidation-reduction reactions of organoselenium compounds. 1. Mechanism of reaction between seleninic acids and thiols. *Journal of the American Chemical Society* **1978**, 100, (16), 5094-5102.

74. Abdo, M.; Liu, S.; Zhou, B.; Walls, C. D.; Wu, L.; Knapp, S.; Zhang, Z. Y., Seleninate in place of phosphate: Irreversible inhibition of protein tyrosine phosphatases. *Journal of the American Chemical Society* **2008**, 130, (40), 13196-13197.

75. Barr, A. J.; Ugochukwu, E.; Lee, W. H.; King, O. N. F.; Filippakopoulos, P.; Alfano, I.; Savitsky, P.; Burgess-Brown, N. A.; Muller, S.; Knapp, S., Large-scale structural analysis of the classical human protein tyrosine phosphatome. *Cell* **2009**, 136, (2), 352-363.

Chapter 2: Synthesis of a Fmoc protected BrPmp analog

2.1 Introduction[1]

Protein tyrosine phosphatases (PTPs) are important targets for medicinal chemists and biochemists. General strategies for the development of inhibitors of these enzymes are needed. Several modular strategies which rely on phosphotyrosine mimics are known for PTP inhibitors. Previous strategies include phosphonomethylphenylalanine (Pmp) derivatives which act as competitive inhibitors. In recent years there has been renewed interest in identifying covalent inhibitors of PTPs. Known covalent inhibitors for PTPs include quinone methides,[1] aryl vinyl sulfonates,[2] nitrostyrene,[3] and □-bromobenzylphosphonate (BBP) derivatives.[4] Widlanski et al. were the first to test the activity of BBP analogs as inhibitors of PTPs using biotin labeled derivative **2**.[5] These derivatives were found to form covalent adducts with PTPs, forming the basis of proteomic strategies for PTP identification. We considered that PTPs often recognize specific amino acid sequences,[6] and that additional functional groups could potentially impart specificity to the α-bromophosphonate group. Building on the work of Widlanski, Zhang and colleagues we have attempted to incorporate their BBP derivatives into peptides via solid phase peptide synthesis (SPPS). We have also developed a convenient route to a phosphonobromomethylphenylalanine (BrPmp, **2.31**), and derivatives appropriately protected for SPPS (Fmoc-L-BrPmp(Me_2)-OH, **2.30**) for more efficient incorporation into peptides.[7] It is hoped that the inclusion of BrPmp and the BBP derivatives into an appropriate peptide sequence not only improves their potency, but allows us to engineering inhibitors and labels for specific for particular PTPs.

---

[1] Portions of the work described in this chapter have been published in N.S. Tulsi, A.M. Downey, and C.W. Cairo, *Bioorganic & Medicinal Chemistry* **2010**, 18, (24), 8679-8686. Enzyme data (Table 2.5, Figure 2.6, Figures A1 – A5) was acquired by A.M. Downey (University of Alberta).

2.2 Synthesis of Zhang's α-bromo phosphonate inhibitor

We initially evaluated the synthesis of a known PTP inhibitor, as reported by Zhang et.al.,[8] and illustrated in **Scheme 2.1**. The starting material, 4-cyanobenzyl bromide, compound **2.1** was hydrolyzed to yield 4-cyanobenzyl alcohol, **2.2**. The cyano group was then reduced by lithium aluminum hydride (LAH), and upon acidic back extraction provided the 4-hydroxymethyl-benzyl-ammonium chloride, **2.3**. A butyloxy carbonyl (Boc) protecting group was then introduced to block the amine functionality, yielding carbamate **2.4**. The hydroxyl group of **2.4** was then oxidized via Corey oxidation with pyridinium chlorochromate (PCC) to obtain aldehyde **2.5**. Condensation of **2.5** and diethyl-phosphite in triethylamine, rendered a racemic mixture of the diethyl ester protected phosphonate, **2.6**. The secondary hydroxyl group was then brominated in the presence of dibromotriphenyl phosphorane, yielding the amino protected α-bromo inhibitor target **2.7**.

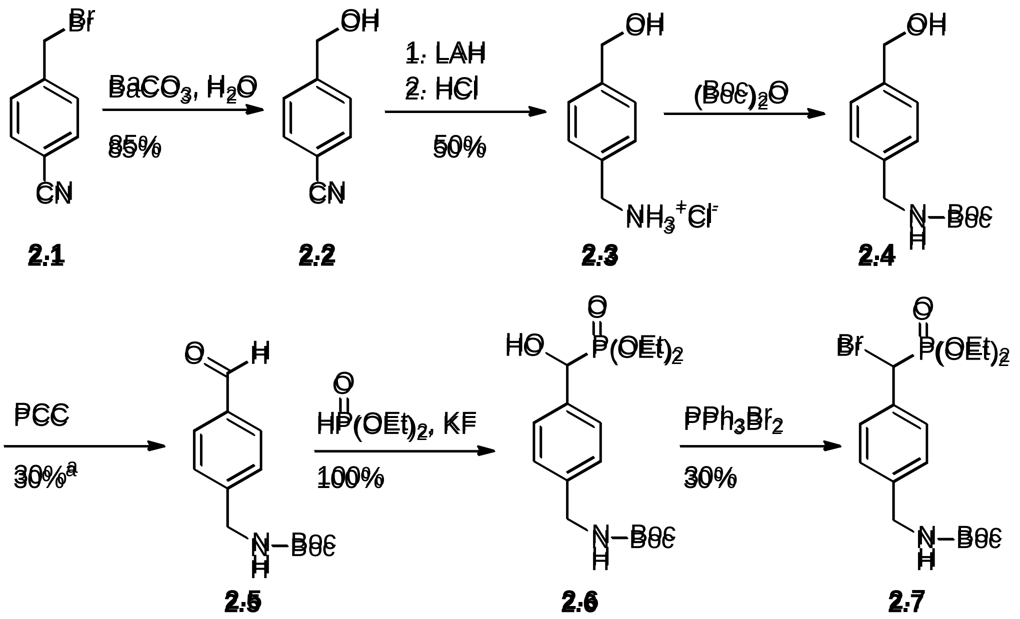

Scheme 2.1 Synthesis of Zhang's α-bromo phosphonate inhibitor. Experimental yield 6% a) Yields over two steps.

Zhang et al. reported an overall yield of 10% for the conversion of **2.1** to **2.7**.[8] Repetition of this reported procedure over six steps in our hands resulted in an overall yield of 6%. The low yielding steps of the route included the reduction of the cyano group with LAH and the bromination of the α-hydroxy phosphonate. In particular, significantly reduced yields were observed (<20%) when the LAH reduction was carried out at scales greater than 2 mmol of **2.2.** One improvement was made to Zhang's synthetic route and involved the condensation of the aldehyde with the reagent diethyl phosphite. A 50 h reflux of **2.5** with diethyl phosphite and triethyl amine was replaced with a solvent free potassium fluoride (KF) catalyzed condensation.[9] The KF catalyzed reaction improved the yield of the α-hydroxy phosphonate, and reaction times were significantly reduced (5 – 10 min). The work-up of the reaction consisted of a simple filtration step with no further purification of the product required.

Even with these improvements, the low overall yield achieved in the synthesis of Zhang's α-bromo phosphonate inhibitors, and the scalability issues with the route made this strategy unattractive for SPPS. Although SPPS has many advantages, one significant drawback is the large excess of reagent required to achieve efficient coupling yields. Significant improvements would have to be made in overall yield and scalability in the synthesis of Zhang's probe to provide a viable strategy. In light of these findings, we decided to focus our efforts on developing a route to an unnatural amino acid which incorporated the α-bromo phosphonate group.

2.3 Design and retrosynthetic analysis of BrPmp

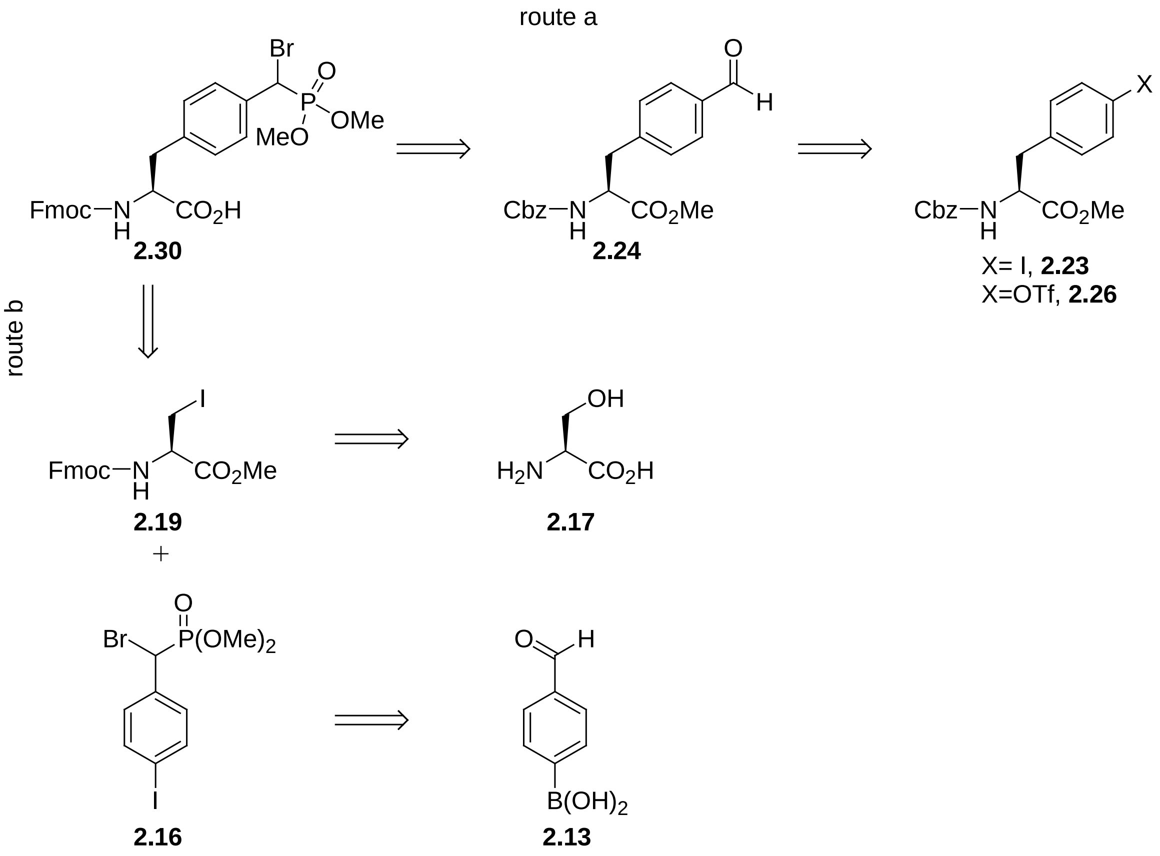
route a
route b
Br
O
P
OMe
MeO
Fmoc—N
H
CO2H
2.30
O
H
Cbz—N
H
CO2Me
2.24
X
Cbz—N
H
CO2Me
X= I, 2.23
X=OTf, 2.26
I
Fmoc—N
H
CO2Me
2.19
+
OH
H2N
CO2H
2.17
O
Br
P(OMe)2
I
2.16
O
H
B(OH)2
2.13

Scheme 2.2 Retrosynthetic analysis of BrPmp.

A retrosynthetic analysis of BrPmp is illustrated **Scheme 2.2**. We envisioned that the protected form of BrPmp, **2.30** could be derived from the formylphenylalanine analog **2.24** in three steps (Scheme 2.2, route a). Disconnection at the benzylic bond adjacent to the aldehyde can yield either the iodotyrosine derivative **2.23**[10] or triflyl-tyrosine amino acid precursor **2.26**.[11] Alternatively, disconnection can initially take place on the other side of the phenyl ring (Scheme 2.2, route b) producing the iodoserine derivative **2.19** and an aryl halide **2.16**.[12] In turn, these precursors can de derived from commercially available reagents serine (**2.17**) and 4-formyl boronic acid (**2.13**).

2.4 α-Bromobenzylphosphonate (BBP) analogs

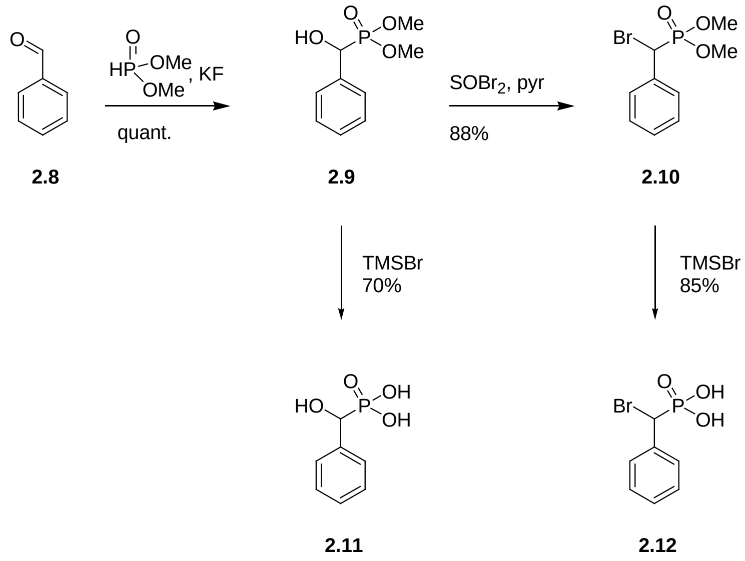

Scheme 2.3 Synthesis of model α-bromobenzylphosphonates.

Before attempting the synthesis of the desired amino acid targets, we first undertook the synthesis of model BBP analogs based on benzaldehyde (**Scheme 2.3**). Condensation of benzaldehyde with dimethyl phosphite gave the desired hydroxy(phenyl)dimethyl phosphonate, **2.9,** in quantitative yield. We chose to employ a dimethylphosphonate due to its stability under acidic conditions. Initial attempts to convert **2.10** to the corresponding bromide were unsuccessful using triphenylphospine dibromide.[8] We then explored a variety of reported bromination conditions for related substrates. Among the conditions tested were $PBr_{3,}$[13] PPh_3/NBS,[5] and MsCl[14] followed by treatment with a bromide nucleophile (triethylammonium bromide or sodium bromide) (**Table 2.1**). We only observed significant formation of product **2.10** after treatment with thionyl bromide and pyridine.[15] The reduced reactivity of the substrate may be due to the sterically congested environment of the hydroxyl. After optimization of the thionyl bromide conditions, we were able to achieve excellent yields for bromination of **2.10** (88%). With access to **2.10**, we then confirmed that deprotection of the dimethoxyphosphonate proceeded in good yield with the use of trimethylsilylbromide, for both the hydroxy and bromo derivatives to give the model hydroxy(phenyl)dimethyl, **2.11**, or bromo(phenyl)dimethyl, **2.12**, respectively. Based on these results, we proceeded to develop a method for generating the desired phenylalanine targets.

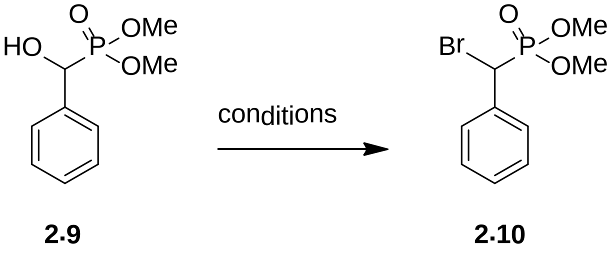

entry	*Conditions*	*solvent*	*time (h)*	*temp (°C)*	*observed product* [a]
1	PBr_3	DCM	12	0 to R.T.	No
2	PBr_3, pyridine	DCM	12	0 to R.T.	No
3	1. MsCl, 2. TEABr	MeCN	24	R.T.	No
4	1. MsCl, 2. NaBr	DMF	12	R.T.	No
5	PH_3, NBS	DCM	12	R.T.	No
6	$SOBr_2$, pyridine	DCM	12	0 to R.T.	Yes

a. As determined by TLC.

Table 2.1: Bromination of α-hydroxyphosphonate (2.10)

2.5 Stability of the α-bromo phosphonate to SPPS conditions.

The ultimate goal of this project was to incorporate the α-bromo phosphonate motif into small peptides, thus the stability of this functional group to common SPPS conditions needed to be established. The BBP analogs **2.10** and **2.12** were incubated with piperidine, trifluoroacetic acid (TFA), and a standard peptide coupling cocktail containing *O*-benzotriazole-*N*,*N*,*N'*,*N'*-tetramethyl-uronium-hexafluoro-phosphate (HBTU), the amino acid glycine and diisopropylethylamine (DIPEA) in dimethylformamide (DMF). The stability of these model compounds were monitored over time utilizing ^{31}P NMR and the results are illustrated in **Tables 2.2** and **2.3**.

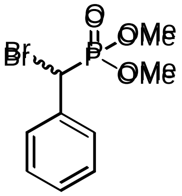

2.10

Number of ^{31}P signals		***Conditions***		
		20% piperidine in DMF	***90% TFA in Water***	***Coupling Conditions^{a}***
Time (min)	*30*	1 (18.9)	1 (20.2)	1 (18.8)
	175	1 (18.9)	1 (20.2)	1 (18.8)
	340	1 (18.9)	1 (20.2)	1 (18.8)
	450	1 (18.9)	1 (20.2)	1 (18.8)

Table 2.2: Results of stability study of 2.10 under various SPPS conditions. a. 5 eq. glycine, 5 eq. HBTU and 10 eq. DIPEA. The number in parenthesis refers to ^{31}P chemical shift in ppm.

The data in **Table 2.2** support that the diethyl protected BBP is stable to the tested SPPS conditions for a prolonged period of time. Unfortunately, this was not the case for the deprotected phosphonate. Noticeable degradation was observed 30 min into incubation with piperidine and continued to accelerate after 175 min. Similar degradation was observed in the standard peptide coupling cocktail, suggesting that incorporation of the α-bromo phosphonate motif into small peptides should be attempted only with a protected form of BrPmp.

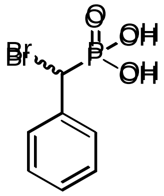

2.12

Number of ^{31}P signals		Conditions			
		1M NaOH	20% piperidine in DMF	90% TFA in water	Coupling Conditions[a]
Time (min)	30	2 (4.5:1)	2 (20:1)	1	1
	175	2 (2:1)	3 (6.25:1:1)	1	5 (50:13.5:1:1:1)
	340	2 (1:1)	5	1	7
	450	2 (1:2.29)	5	1	7

Table 2.3: Results of stability study of 2.12 under various SPPS conditions. a. 5 eq. glycine, 5 eq. HBTU and 10 eq. DIPEA. The ratio in brackets refers to the ratio of integration between observed ^{31}P signals.

2.6 Synthesis of BrPmp from serine

Negishi cross coupling of serine-derived iodo-zinc reagents with aryl halides via Pd catalysis is a useful strategy of enantiomerically pure protected amino acids.[12] Using this strategy, we set out to synthesize the building blocks required for the synthesis of the protected form of BrPmp, **2.21**. The two building blocks required were a suitably protected iodoserine derivative (**2.19**) and an aryl halide containing the α-bromo phosphonate motif (**2.16**). The protecting groups selected for the iodoserine derivative were Fmoc for the α-amino group to ensure compatibility of the final product with automated SPPS. The acid functionality was protected as a methyl ester during the route, but would be removed prior to SPPS.

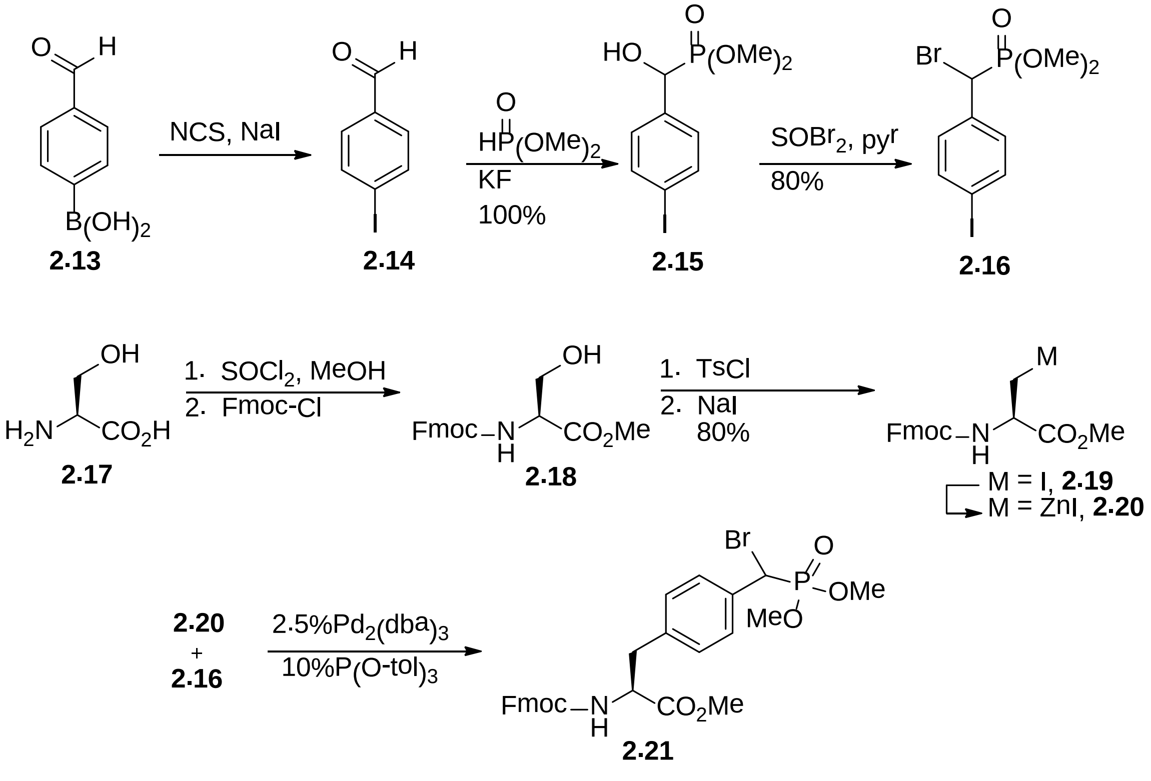
2.13
NCS, NaI
2.14
HP(OMe)2
KF
100%
2.15
SOBr2, pyr
80%
2.16
2.17
1. SOCl2, MeOH
2. Fmoc-Cl
2.18
1. TsCl
2. NaI
80%
M = I, 2.19
M = ZnI, 2.20
2.20
+
2.16
2.5%Pd2(dba)3
10%P(O-tol)3
2.21

Scheme 2.4 Synthesis of Fmoc-L-BrPmp-MeOH

Starting from unprotected serine, the Fmoc and methyl ester protecting groups were installed using standard protocols to give **2.18**.[16] The hydroxyl group of **2.18** was then tosylated and subsequently displaced with an iodide, resulting in **2.19** in good yield.[17] With the iodoserine derivative in hand, our attention turned to the synthesis of the aryl halide building block. Starting from **2.13**, the aryl-boronic acid derivative was converted to the corresponding aryl-iodo derivative via in situ generation of iodosuccinimide. The aldehyde, **2.14**, was then used immediately in a condensation with dimethyl phosphate, using the same chemistry developed in the synthesis of the BBP analogs. The α-hydroxy phosphonate was then brominated using thionyl bromide with pyridine conditions described in **Table 2.1** to yield **2.16**.

The next step of the synthesis required formation of the iodo-zinc reagent, **2.20** in preparation for Negishi coupling.[12] Several reported conditions for the generation of the iodo-zinc reagent were attempted, but all proved to be ineffective in our hands. Among the conditions tried were I_2/Zn,[17] dibromoethane/Zn[17] and Li/$ZnCl_{2.}$[18] The attempted conversions of **2.19** to the iodo-zinc reagent **2.20** were monitored by thin layer chromatography (TLC) and even after several days showed only the presence of starting material and no formation of the product **2.20**. Unable to synthesize **2.20**, this route was abandoned and we focused our efforts on developing BrPmp precursors by modification of tyrosine.

2.7 Synthesis of BrPmp from tyrosine

We first considered a common strategy for modification of phenylalanine via iodotyrosine[19] (**Scheme 2.5**), which could be a good substrate for carbonylation to the corresponding aldehyde,[10] **2.24**. Due to the basic conditions necessary to install the phosphonate later in the route, we selected Cbz as the □-amino protecting group for the first part of the synthesis.

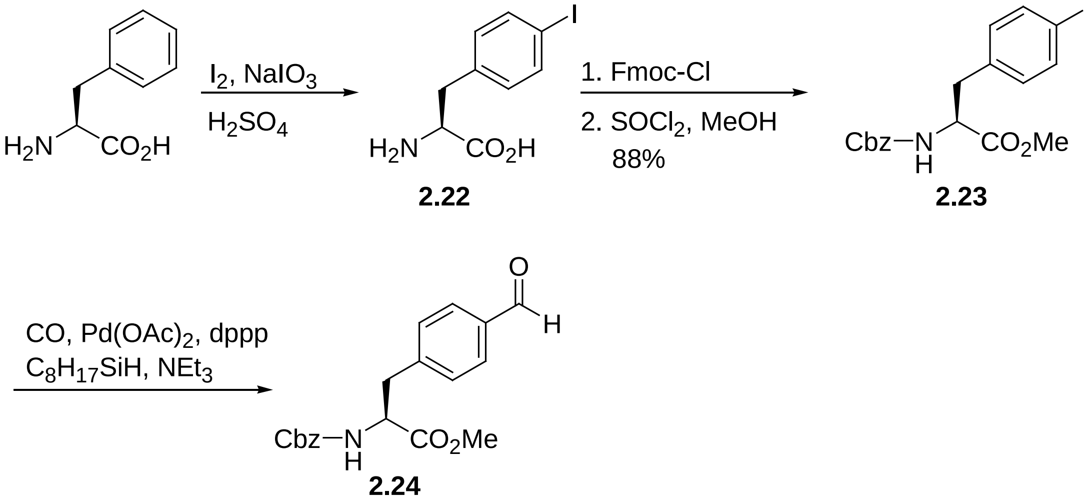
I
H_2N
CO_2H
I_2, $NaIO_3$
H_2SO_4
I
H_2N
CO_2H
2.22
1. Fmoc-Cl
2. $SOCl_2$, MeOH
88%
I
Cbz—N
H
CO_2Me
2.23
CO, $Pd(OAc)_2$, dppp
$C_8H_{17}SiH$, NEt_3
O
H
Cbz—N
H
CO_2Me
2.24

Scheme 2.5 Synthesis of benzylic aldehyde 2.24

The protected phenylalanine was converted to iodotyrosine, **2.22** in good yield (88%) and subsequently protected as a methyl ester after activation with thionyl chloride and □-amino protection as the carboxybenzyl (Cbz) protected amino acid (**2.23**) as previously reported.[20] We attempted conversion of **2.23** to the protected aldehyde **2.24**. However, this strategy gave unreliable results in our hands (**Table 2.3**).[10] Although we could achieve moderate yields, we found that the reaction was not scalable, with decreasing yields at larger scale. We achieved an optimal yield of 60% at the 1 mmol scale of starting material **2.23**. Reactions performed at larger scales than this resulted in significantly decreased yield (<30%) of **2.24**. We were therefore forced to choose an alternative route.

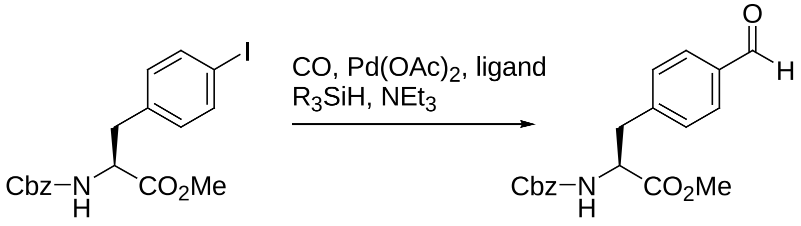

2.23 **2.24**

Entry	*Ligand*	*R_3SiH*	*Time (h)*	*Ttemp (°C)*	*Yield* [a]
1	Dppp	C_8H_{17}	8	70	60%
2	Dppp	C_2H_5	8	70	40%
3	Dppp	C_8H_{17}	8	80	40%
4	Dppp	C_2H_5	8	80	35%
5	Dppf	C_8H_{17}	4	70	30%
6	Dppf	C_2H_5	4	70	20%
7 [b]	Dppf	C_8H_{17}	4	70	30%
8 [b]	Dppf	C_2H_5	4	70	20%

a. Isolated yields are reported at 1 mM scale
b. Added over 4 h.

Table 2.4: Carbonylation of iodotyrosine

We considered an alternative route to the benzylic aldehyde through the conversion of the protected tyrosine **2.25** to the triflate followed by carbonylation (**Scheme 2.6**). Compound **2.25** was converted to triflate **2.26** using *N*-phenyl-bis-trifluoromethane sulfonamide in quantitative yield.[21] The triflate was converted to the carboxylic acid using $Pd(OAc)_2$.[22, 23] The crude acid was then reduced to the benzyl alcohol (**2.27**) with a BH_3-DMS complex.[24] Oxidation of the purified benzyl alcohol to the aldehyde using IBX was performed using standard conditions.[25] We observed that prolonged storage of the intermediate aldehyde, even at –20 °C, resulted in partial conversion to the hydrate. To avoid this issue, the aldehyde was used immediately in the subsequent cesium fluoride catalyzed condensation reaction with dimethyl phosphite to generate compound **2.28**.[9] To make a protected amino acid derivative suitable for automated SPPS, we chose to replace the Cbz group with Fmoc using standard conditions, to obtain compound **2.29**.

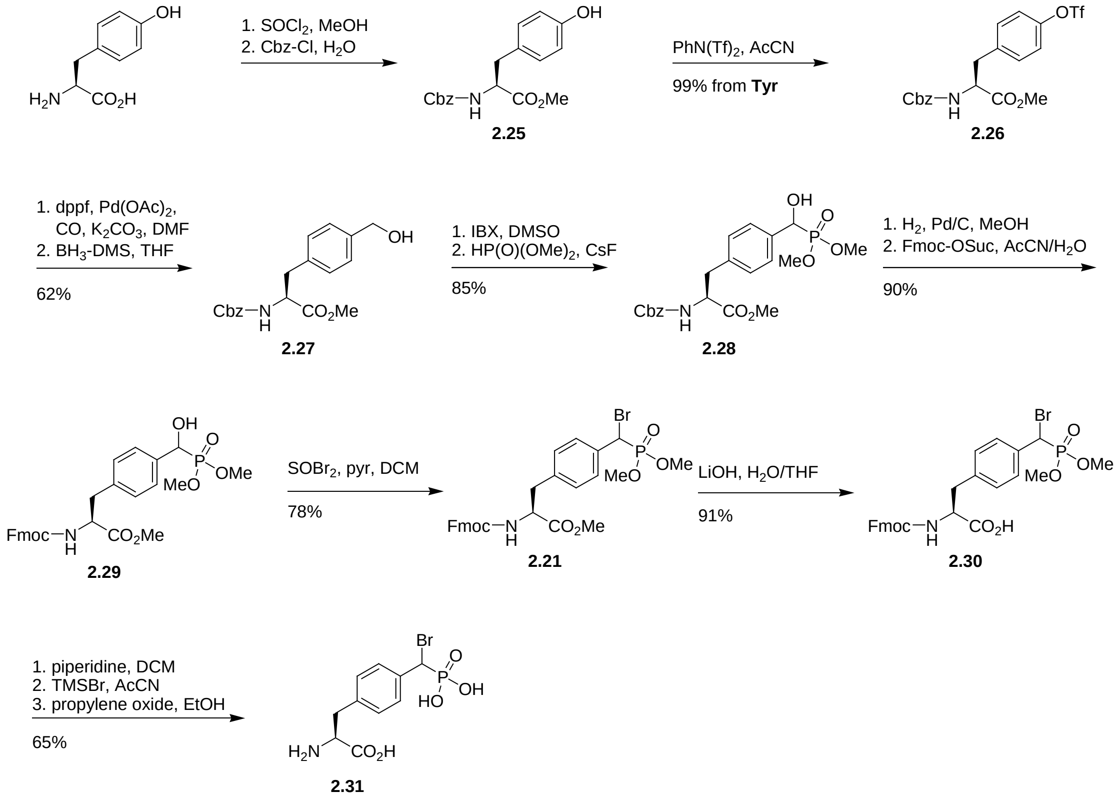

1. SOCl2, MeOH
2. Cbz-Cl, H2O
2.25
PhN(Tf)2, AcCN
99% from Tyr
2.26
1. dppf, Pd(OAc)2, CO, K2CO3, DMF
2. BH3-DMS, THF
62%
2.27
1. IBX, DMSO
2. HP(O)(OMe)2, CsF
85%
2.28
1. H2, Pd/C, MeOH
2. Fmoc-OSuc, AcCN/H2O
90%
2.29
SOBr2, pyr, DCM
78%
2.21
LiOH, H2O/THF
91%
2.30
1. piperidine, DCM
2. TMSBr, AcCN
3. propylene oxide, EtOH
65%
2.31

Scheme 2.6 Synthesis of BrPmp.

The key bromination step followed the conditions tested in our model studies shown in **Table 2.1**. Treatment of **2.29** with thionyl bromide in the presence of pyridine converted the α-hydroxyphosphonate to the fully protected bromide, **2.21**. Subsequent cleavage of the methyl ester with lithium hydroxide provided compound **2.30** in good yield. The overall yield from tyrosine to **2.30** was 30% in 11 steps, with only five chromatographic purification steps. Compound **2.30** was deprotected for use in enzyme assays by treatment with 20% piperidine in DMF to remove Fmoc, followed by cleavage of the phosphonomethyl groups with TMSBr.[26] Propylene oxide was added to remove residual HBr, allowing isolation of compound **2.31** as the free amine in 65% yield. It has not escaped our attention that the final compound is isolated as a mixture of diastereomers at the α-bromo-phosphonate, and that there may be potential differences in activity between the two isomers. However, we chose to first focus on determining the activity of **2.31** when incorporated into a peptide sequence.

2.8 Incorporation of BrPmp into peptide sequences

To test the compatibility of compound **2.30** with SPPS, we chose to synthesize a short peptide sequence, Asp-BrPmp-Leu (**2.32**). The peptide was generated using standard solid phase methods, based on the Fmoc protecting group strategy. For reactions using compound **2.30** we employed HBTU as a coupling agent with DIPEA as a base. Couplings were performed with a 2:1:1 molar ratio of **2.30**:HBTU:DIPEA, in two cycles. To cleave the peptide from resin, dry resin was treated with 95% TFA and 5% water for 1 h, followed by treatment with TMSI for 1.7 h.[26] The phosphonomethyl protecting groups were cleaved with TMSI (instead of TMSBr) due to the long clevage times required for TMSBr (12 to 16 h) which may have resulted in the hydrolysis of the peptidyl amide bonds. Chromatograms of the cleavage products suggested that the coupling reactions were efficient (see Appendix, Figure B1 and B2). The isolated peptides were confirmed by HR-MS and ^{31}P NMR. Attempts to separate the tripeptide into its two diastereoisomers by HPLC on a non-chiral C18 column were unsuccessful.

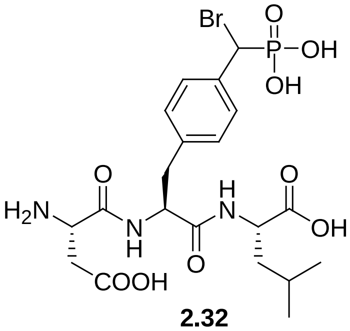

2.32

Figure 2.1: Synthetic tripeptide Asp-BrPmp-Leu

2.9 Inhibition of CD45

To examine the ability of the BrPmp derivatives to act as inhibitors of a PTP, we tested compounds **2.31**, **2.12**, and **2.32** against CD45. Assays were conducted with the fluorogenic substrate, 6,8-difluoro-4-methylumbelliferyl phosphate (DiFMUP), and are summarized in **Table 2.5** (see Appendix, Figures B3 and B4).

Cmpd	*enzyme*	*inhibitor [μM]*	$K_{m, obs}$	*± [μM]* [a]	K_I	*± [μM]* [b]	k_3	*± [min^{-1}]*
-	CD45	0	90	± 20	na		-	
2.12	CD45	1500	99	± 14	na		-	
2.31	CD45	150	141	± 18	40	± 8	0.041	± 0.001
2.32	CD45	35	141	± 34	16	± 4	0.048	± 0.003

Table 2.5 Inhibition of CD45. a. Values were determined by non-linear regression of the observed rate of reaction in the presence of inhibitor using the Michaelis-Menten equation.[27] Error is reported as the relative error from the fit. b. For compounds **2.31** and **2.32**, K_I was determined by Kitz-Wilson analysis. The rate of enzyme inactivation, k_3, was also determined.[28]

The K_m for DiFMUP with CD45 was first determined, and the experiment was then repeated in the presence of compounds **2.12**, **2.31**, and **2.32** to provide an apparent K_m

($K_{m,\ obs}$). We found significant inhibition of CD45 for compounds **2.31** and **2.32** at micromolar concentrations; however, compound **2.12** did not have a significant effect on enzyme kinetics even at millimolar concentration. Previous reports of PTP inhibition using BBP analogs observed irreversible enzyme inhibition.[4] Evaluation of our kinetic data using linear transforms was not consistent with pure competitive inhibition of CD45 by **2.31** or **2.32**; however, this analysis is not conclusive on its own (see Appendix, Figure B5). To provide additional insight into the inhibition of these compounds, we obtained K_I values using a Kitz-Wilson analysis.[27, 28] Compound **2.12** did not give a saturating curve in this analysis, and therefore could not be analyzed by this method, consistent with its failure to alter the rate of reaction (*vide supra*). Compound **2.12** has been previously tested as an inhibitor of the PTP Yop51, and exact kinetic constants were difficult to obtain, and we found similar difficulties for this determination with CD45.[5] Both compound **2.31** and **2.32** gave a saturating curve consistent with K_I values of 40 ± 8 μM and 16 ± 4 μM, respectively (**Figure 2.2**).

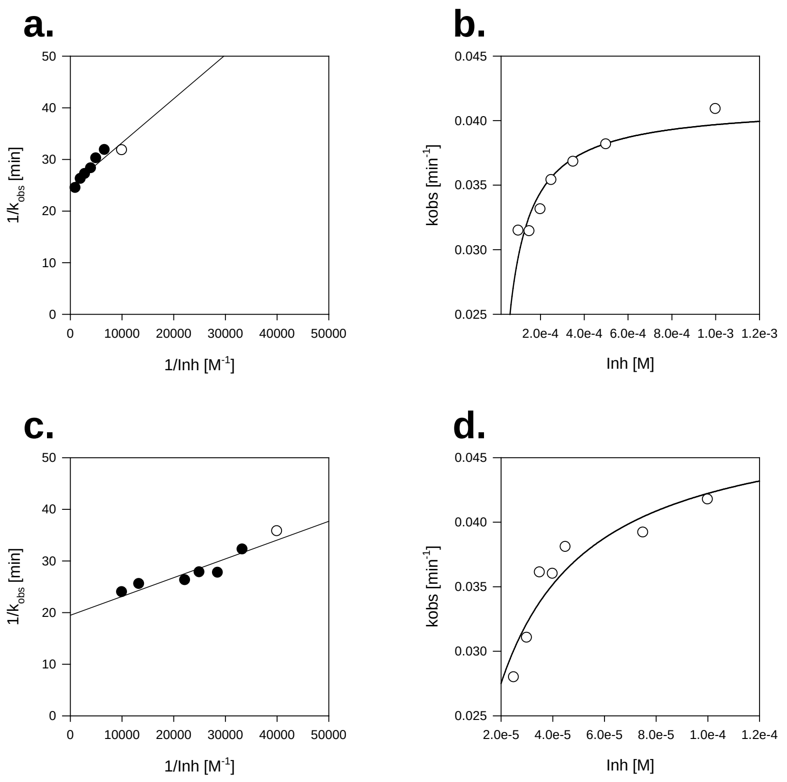

Figure 2.2: Kitz-Wilson analysis of compounds 2.31 and 2.32. Compounds (a-b) 2.31 and (c-d) 2.32 were examined using a Kitz-Wilson analysis.[28] The apparent rate constant (k_{obs}) was determined for a series of concentrations of the inhibitor.[29] The data are plotted as the linear transform (**a**, **c**) or as the non-linear form ($k_{obs} = k_3/(1 + K_I/I)$) (**b**, **d**). Values from the non-linear regression were used for **Table 1**.

These results indicate that the tripeptide was approximately 4-fold more potent than BrPmp alone, suggesting that the adjacent amino acid side chains contribute additional specificity to the inhibitor. The Kitz-Wilson analysis estimated the rate of irreversible inhibition (k_3) of CD45 at 0.05 min^{-1} for both compounds. To provide additional support for the expected mechanism of inhibition, we measured CD45 activity for an enzyme sample which was pre-incubated with the inhibitor and compared it to an enzyme sample that was only incubated with the inhibitor for a short period. We found that pre-incubation of the enzyme reduced activity, and at long incubation times completely inactivated the enzyme (see Appendix, Figure B4), confirming that the inhibitors act irreversibly at long incubation times.

2.10 Conclusion

We have presented an efficient synthetic route for the preparation of BrPmp analogs that can be readily used in automated SPPS. Our method provides the Fmoc-L-BrPmp-OH (**2.31**) derivative in 30% yield over 11 steps from tyrosine, and required only five column separations. These compounds were found to act as irreversible inhibitors of the PTP CD45, but are only weak inhibitors of alkaline phosphatase, supporting the previously observed selectivity of the α-bromobenzylphosphonate functional group.[8] Importantly, the synthetic method reported here is scalable, and the products can be easily modified using standard amino acid chemistry. The observation of improved potency for BrPmp within the context of a peptide sequence suggests that these derivatives could act as specific inhibitors of PTPs. In Chapter 3, we will describe initial studies towards incorporating BrPmp into longer peptide sequences to generate specific PTP inhibitors.

2.11 Materials and methods

Reactions were not conducted under a stream of argon at ambient temperature, unless otherwise noted, and monitored by TLC on silica gel G-25 UV254 (0.25 mm). NMR experiments were conducted on Varian 300, 400, or 500 MHz instruments. Chemical shifts are reported relative to the deuterated solvent peak and are in parts per million (ppm). Phosphoric acid was used as an external standard for ^{31}P NMR. ESI-MS spectra were carried out on samples suspended in solvent with added NaCl.

2.11.1 Synthetic methods

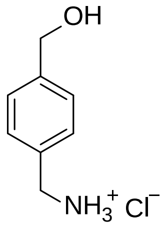

Synthesis of 4-hydroxymethyl-benzyl-ammonium chloride (2.3): Compound **2.1** (4.00 g, 20.5 mmol) and barium carbonate (8.00 g, 45 mmol, 10 equiv) were added to water (120 ml) ad refluxed for 2 hr. The mixture was then filtered and extracted with DCM (3 x 100 ml). The combined organic fractions were then dried over Na_2SO_4, filtered and the solvent removed. The crude product **2.2** was used without further purification. In a three-neck flask under an argon atmosphere was added an ice-cooled solution of compound **2.2** (0.5 g, 2.88 mmol) in anhydrous diethyl ether (5 ml). To this was added, in drops, lithium aluminum hydride solution (15 ml of 1M solution in anhydrous ether) over 45 minutes with constant stirring. The resulting mixture was then removed from an ice bath and refluxed in an oil bath for 3 h. The reaction was quenched by the slow addition of cold water (30 ml) into the ice-cooled reaction flask. After removing the ether by rotary evaporation, the aqueous layer was extracted with □ 4 25 ml of DCM. The combined organic layers were then back-extracted into 3 □ 25 ml of 0.1 M hydrochloric acid. The aqueous layer was freeze-dried to yield **2.3** (0.323 g, 50%) as a white solid. ^{1}H NMR (300 MHz, DMSO) δ 8.33 (s), 7.42 (d, *J* = 8.1 Hz, 2H), 7.34 (d, *J* = 8.1 Hz, 2H), 4.50 (s, 2H), 3.99 (d, *J* = 5.3 Hz, 2H).

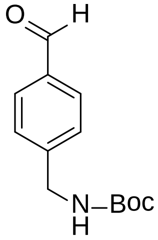

Synthesis of (4-formyl-benzyl)-carbamic acid tert-butyl ester (2.5): Compound **2.3** (0.100 g, 0.600 mmol) was dissolved in THF (4 ml) and water (1 ml) containing potassium hydroxide (0.042 g, 0.75 mmol). Di-tert-butyl dicarbonate (0.200 g, 0.90, 1.5 equiv) was then added and the reaction was stirred for 45 min. Water (13 ml) was then added and the crude product was extracted with DCM (2 x 21 ml), dried with Na_2SO_4, filtered and the solvent removed. The crude product **2.4** was used in the next step without further purification. **2.4** (1.30 g, 5.50 mmol) was dissolved in DCM (19 ml) and PCC (0.93 g, 4.32 mmol) and sodium acetate (90 mg, 1.1 mmol) and the mixture for was stirred for 17 h in the dark. The reaction was then triturated with ether (100 ml) and then filtered through celite. The organic later was washed with water (100 ml), dried over Na_2SO_4 and the solvent removed. The crude product was filtered and purified on silica (30% ethyl acetate and 5% triethylamine in hexanes) to yield **2.5** as an oil (0.39 g, 30%).

^{1}H NMR (300 MHz, $CDCl_3$) δ 10.00 (s), 7.85 (d, *J* = 8.2 Hz, 2H), 7.45 (d, *J* = 8.1 Hz, 2H), 4.40 (d, *J* = 4.4 Hz, 3H), 1.47 (s, 9H).

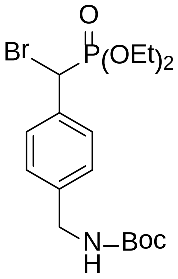

Synthesis of bromo-[4-(tert-butoxycarbonylamino-methyl)-phenyl]-methyl}-phosphonic acid diethyl ester (2.7): Compound **2.5** (1.00 g, 4.40 mmol) was dissolved in diethyl phoshpite (0.567 ml 4.40 mmol, 1 equiv). Potassium fluoride (1.28 g, 22.0 mmol, 5 equiv) was then added and the reaction was vigorously stirred. Once the reaction and come to room temperature DCM (10 ml) was added and the reaction was filtered, and the solvent removed. The crude product **2.6** was used without further purification. **2.6** (1.0 g, 2.75 mmol) was dissolved in AcCN (6 ml), dibromotriphenyl phosphorane (1.55 g, 3.65 mmol) was added and the reaction was stirred on rice for 1.5 h, followed by 2 h at room temperature. The solvent was rotary-evaporated, and the crude was dried on a pump overnight. The crude was then triturated with ethyl acetate and hexane mixture (7:3), and the white cake was filtered off on a sintered funnel. The cake was washed twice with 5 ml of solvent, and the filtrate was concentrated by flushing air before loading on the column. The crude compound was purified on silica (70% ethyl acetate and 30% hexanes) to yield **2.7** as an oil (0.356 g, 30%). ^{1}H NMR (300 MHz, $CDCl_3$) δ 7.55 – 7.51 (m, 2H), 7.27 (d, *J* = 7.9 Hz, 2H), 4.85 (d, *J* = 13.0 Hz, 1H), 4.31 (s, 2H), 4.22 (m, *J* = 7.4, 4.2 Hz, 2H), 4.12 – 4.01 (m, 1H), 3.97 – 3.82 (m, 1H), 1.46 (s, 9H), 1.32 (t, *J* = 7 Hz, 3H), 1.17 (t, *J* = 7.2 Hz, 3H).

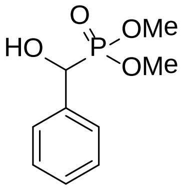

Synthesis of dimethyl [hydroxy(phenyl)methyl]phosphonate (2.9): Dimethyl phosphite (1.86 mL, 20.3 mmol, 1.03 equiv) was added to benzaldehyde, **2.8**, (2 mL, 19.8 mmol, 1 equiv) and stirred for 5 min. KF (5.75 g, 99.0 mmol, 5 equiv) was then added and the reaction mixture was stirred until it solidified (~ 20 min). The crude product was then dissolved in DCM, filtered, and the solvent evaporated yielding **2.9** as a white powder (4.38 g, 100%). The product was dried under high vacuum over P_2O_5. No further purification was required. ^{1}H NMR (400 MHz, $CDCl_3$) δ 7.53 – 7.45 (m, 2H), 7.43 – 7.23 (m, 3H), 5.05 (d, *J* = 11.1 Hz, 1H), 3.69 (d, *J* = 10.4 Hz, 3H), 3.65 (d, *J* = 10.4 Hz, 3H). ^{13}C NMR (101 MHz, $CDCl_3$) δ 136.7, 128.6, 128.5, 127.3 (d, $J_{C\text{-}P}$ = 5.7 Hz), 70.9 (d, $J_{C\text{-}P}$ = 159.6 Hz), 54.3 (d, $J_{C\text{-}P}$ = 7.0 Hz), 53.7 (d, $J_{C\text{-}P}$ = 7.0 Hz). ^{31}P NMR (162 MHz, $CDCl_3$) δ 24.71. ESIMS calculated for $C_9H_{13}O_4PNa$ $[M+Na]^+$ 239.0443, found: 239.0441; mp 85-86 ºC.

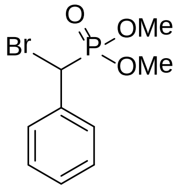

Synthesis of dimethyl [bromo(phenyl)methyl]phosphonate (2.10): In a round bottom flask **2.9** (1 g, 4.63 mmol, 1 equiv) was dissolved in dry DCM (10 mL) and dry pyridine (0.47 mL, 5.78 mmol, 1.25 equiv) was added. Thionyl bromide (0.45 mL, 5.78 mmol, 1.25 equiv) was then added to the round bottom flask under inert atmosphere. The round bottom flask was sealed with a septum, cooled in an ice bath and slowly allowed to come to room temperature overnight. The solvent was then evaporated and the crude product was dissolved in ethyl acetate. The organic layer was washed with 1M HCl, saturated $NaHCO_3$, water, brine, then dried over Na_2SO_4 and filtered. The solvent was evaporated and the crude product was purified on a silica plug 1:4 (hexanes:ethyl acetate) followed by 3:7 (hexanes: ethyl acetate) to give **2.10** as a viscous oil (1.14 g, 88%). The product was dried under high vacuum over P_2O_5. ^{1}H NMR (400 MHz, $CDCl_3$) δ 7.56 (d, *J* = 7.8 Hz, 2H), 7.34 (d, *J* = 7.5 Hz, 2H), 7.26 (1H), 4.88 (d, *J* = 13.1 Hz, 1H), 3.85 (d, *J* = 10.8 Hz, 3H), 3.60 (d, *J* = 10.7 Hz, 3H). ^{13}C NMR (101 MHz, $CDCl_3$) δ 134.6 (d, J_{C-P} = 3.3 Hz), 129.7 (d, J_{C-P} = 6.7 Hz), 129.4 (d, J_{C-P} = 2.2 Hz), 129.0 (d, J_{C-P} = 1.3 Hz), 55.1 (d, J_{C-P} = 7.0 Hz), 54.7 (d, J_{C-P} = 7.0 Hz), 41.1 (d, J_{C-P} = 159.9 Hz). ^{31}P NMR (162 MHz, $CDCl_3$) δ 20.65. ESIMS calculated for $C_9H_{12}BrO_3PNa$ $[M+Na]^+$ 300.9600, found: 300.9596.

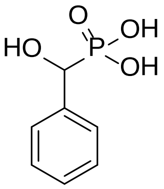

Synthesis of [hydroxy(phenyl)methyl]phosphonic acid (2.11): Compound **2.9** (0.15 g, 0.69 mmol, 1 equiv) was dissolved in dry DCM (5 mL). TMSBr (0.77 mL, 5.52 mmol, 8 equiv) was added to the solution under an inert atmosphere. The reaction was stirred for 20 h at room temperature. The solvent was then evaporated, and MeOH (5 mL) was added to the reaction mixture and stirred for 1 h. The solvent was evaporated and the crude product was dissolved in water (5 mL), filtered and freeze dried, yielding **2.11** as a white powder (130 mg, 70%). ^{1}H NMR (400 MHz, D_2O) δ 7.52 – 7.31 (m, 5H), 4.99 (d, *J* = 12.3 Hz, 1H). ^{13}C NMR (101 MHz, D_2O) δ 137.4, 128.8 (d, J_{C-P} = 2.3 Hz), 128.5 (d, J_{C-}

$_P$ = 2.9 Hz), 127.4 (d, J_{C-P} = 5.7 Hz), 71.0 (d, J_{C-P} = 158.3 Hz). ^{31}P NMR (162 MHz, D_2O) δ 20.98. ESIMS calculated for $C_7H_9O_4PNa$ $[M-H]^-$ 187.0166, found: 187.0162; mp 160-162 ºC.

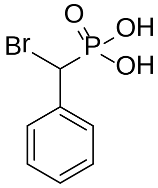

Synthesis of [bromo(phenyl)methyl]phosphonic acid (2.12): Compound **2.10** (0.3 g, 1.08 mmol, 1 equiv) was dissolved in dry DCM (5 mL). TMSBr (1.2 mL, 8.64 mmol, 8 equiv) was added under an inert atmosphere. The reaction was stirred for 20 h at room temperature. The solvent was then evaporated, and MeOH (5 mL) was added to the reaction mixture and stirred for 1 h. The solvent was evaporated and the crude product was dissolved in water (5 mL), filtered and freeze dried yielding **2.12** as a white powder (229 mg, 85%). ^{1}H NMR (400 MHz, D_2O) δ 7.61 – 7.52 (m, 2H), 7.44 – 7.33 (m, 3H), 5.10 – 5.02 (m, 1H). ^{13}C NMR (101 MHz, D_2O) δ 136.5 (d, J_{C-P} = 3.3 Hz), 129.4 (d, J_{C-P} = 6.0 Hz), 129.1, 43.54. ^{31}P NMR (162 MHz, D_2O) δ 15.44. ESIMS calculated for C-$_7H_7BrO_3P$ $[M-H]^-$ 248.9322, found: 248.9317 mp 158-60 ºC.

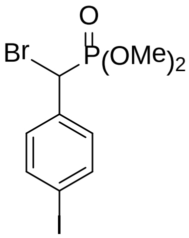

Synthesis of bromo-(4-iodo-phenyl]-methyl)-phosphonic acid diethyl ester (2.16): **2.13** (1.00 g , 6.71 mmol) was added to a mixture of NIS (1.88 g, 8.39 mmol, 1.25 equiv) and anhydrous AcCN (10 ml). The mixture was refluxed for 14 hr under argon in the dark. The crude product was extracted into hexanes (3 x 10 ml) and washed with 1M

$NaHSO_3$, 1M $NaHCO_3$ and dried over Na_2SO_4. The solvent was evaporated and the crude product was used without further purification. **2.14** (718 mg, 3.10 mmol) was dissolved in dimethyl phosphate (0.3 ml, 3.4 mmol, 1.1 equiv), and KF (900 mg, 15.5 mmol, 5 equiv) was added and the reaction was stirred vigorously. The mixture was dissolved in DCM, filtered and the solvent removed. The crude product was used without further purification. **2.15** (0.5 g, 1.5 mmol) was dissolved in DCM (5 ml) and cooled on ice. Dry pyridine (0.18ml, 2.25 mmol, 1.5 equiv) and $SOBr_2$ (0.17 ml, 2.25 mmol, 1.5 equiv) were added under an inert atmosphere and the reaction was allowed to come to room temperature overnight. The solvent was then evaporated and the crude product was dissolved in ethyl acetate. The organic layer was washed with 1M HCl, saturated $NaHCO_3$, water, and brine, dried over Na_2SO_4 and filtered. The solvent was evaporated and the crude product was purified on a silica (diethylether, followed by 10:1 DCM:MeOH) to give **2.16** as a white solid (0.47 g, 80%). ^{1}H NMR (400 MHz, $CDCl_3$) δ 7.72 (d, *J* = 8.2 Hz, 2H), 7.33 (dd, *J* = 8.5, 1.8 Hz, 2H), 4.83 (d, *J* = 13.3 Hz, 1H), 3.89 (d, *J* = 10.8 Hz, 3H), 3.68 (d, *J* = 10.7 Hz, 3H). ^{31}P NMR (162 MHz, $CDCL_3$) δ 19.94 (s).

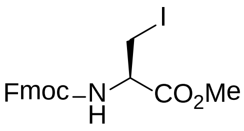

Synthesis of (2R)-(N-Fluorenylmethoxycarbonylamino)-3-iodopropionic acid methyl ester (2.19): Thionyl chloride (4.6 mL, 63.33 mmol, 2 equiv) was added dropwise to dry MeOH (65 mL) at 0 ºC and stirred for 5 min. L-Serine (3.31 g, 31.5 mmol, 1 equiv) was then added and the reaction vessel was fitted with a drying tube filled with drierite and slowly allowed to come to room temperature over 21 h. The solvent was then evaporated and crude product dried over high vacuum for 8 h. To the crude product was added Fmoc-chloride (8.56 g, 33.1 mmol, 1.05 equiv) and $NaHCO_3$ (10.6 g, 126 mmol, 4 equiv) in acetonitrile and water (1:1, 200 mL) and the mixture was stirred at room temperature overnight. The acetonitrile was evaporated under reduced pressure and the crude product was extracted with ethyl acetate (3 x 100 ml). The organic layer was dried over Na_2SO_4 and the crude product **2.18** was used in the next step without purification. **2.18** (2.00 g, 5.86 mmol) was dissolved in pyridine (25 ml) and cool to 5 ºC and TsCl (2.23 g, 11.72 mmol, 2 equiv) was added and the reaction was left to stir overnight. The mixture was poured onto ice water (25 ml) and extracted with ethyl acetate (3 x 50 ml). The organic layer was washed with 1M citric acid (3 x 50 ml), sat. $NaHCO_3$ (2 x 20 ml) and brine (20 ml). The organic layer was dried over Na_2SO_4 and evaporated. The crude product was dissolved in ether, chilled and filtered. The crude product was used without further purification. A solution of NaI (3.52 g, 23.48 mmol, 4 equiv) in dry acetone (20 ml) was added dropwise to tosylate (2.91 g, 5.87 mmol) in dry acetone (30 ml). The mixture was stirred overnight, filtered and the solvent evaporated. The crude product was dissolved in DCM (50 ml) washed with water (3 x 40 ml), 1M $Na_2S_2O_3$ (2 x 30 ml) and brine (2 x 30 ml), dried over Na_2SO_4 and evaporated. The crude product was recrystallized from ethanol and petroleum ether to yield **2.19** as a white solid (2.13 g, 80%). ^{1}H NMR (400 MHz, $CDCl_3$) δ 7.80 (d, *J* = 7.5 Hz, 2H), 7.64 (d, *J* = 7.4 Hz, 2H), 7.44 (t, *J* = 7.4 Hz, 2H), 7.36 (dt, *J* = 8.4, 4.2 Hz, 2H), 5.69 (d, *J* = 7.1 Hz, 1H), 4.67 – 4.55 (m, 1H), 4.44 (m, 2H), 4.28 (t, *J* = 7.1 Hz, 1H), 3.86 (s, 3H), 3.63 (d, *J* = 3.6 Hz, 2H).

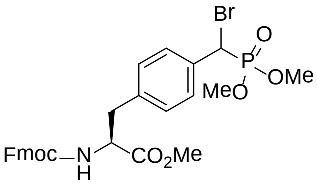

Synthesis of Synthesis of L-Phenylalanine, 4-[(dimethyloxyphosphinyl)bromomethyl]-*N*-[(9*H*-fluoren-9-ylmethoxy)carbonyl]-, methyl ester (2.21): In a round bottom flask **2.29** (2 g, 3.70 mmol, 1 equiv) was dissolved in dry DCM (30 mL) and dry pyridine (0.38 mL, 4.63 mmol, 1.25 equiv) was added. Thionyl bromide (0.36 mL, 4.63 mmol, 1.25 equiv) was then added to the round bottom flask under an inert atmosphere. The round bottom flask was sealed with a septum, cooled in an ice bath and slowly allowed to come to room temperature overnight. The solvent was then evaporated and the crude product was dissolved in ethyl acetate. The organic layer was washed with 1M HCl, saturated $NaHCO_3$, water, and brine, dried over Na_2SO_4 and filtered. The solvent was evaporated and the crude product was purified on a silica plug (diethylether, followed by 10:1 DCM:MeOH) to give **2.29** as a white solid (1.14 g, 78%). Purity (>95%) determined by analytical HPLC, C18, flow: 1 mL min^{-1}, λ: 254 nm, eluent: acetonitrile/0.1% TFA in water 10:90 (2 min) to 50:50 (22 min), retention time: 49.7 min. $[\alpha]_D^{25}$ +34.72° ml dec^{-1} g (*c* 1.02, $CHCl_3$). ^1H NMR (400 MHz, $CDCl_3$) δ 7.77 (d, *J* = 7.5 Hz, 2H), 7.57 (d, *J* = 7.4 Hz, 2H), 7.49 (d, *J* = 7.5 Hz, 2H), 7.41 (t, *J* = 7.4 Hz, 2H), 7.32 (t, *J* = 7.5 Hz, 2H), 7.17 – 6.98 (m, 2H), 5.32 – 5.23 (m, 1H), 4.86 (d, *J* = 13.1 Hz, 1H), 4.66 (dd, *J* = 13.4, 6.1 Hz, 1H), 4.49 – 4.30 (m, 2H), 4.20 (t, *J* = 6.9 Hz, 1H), 3.85 (d, *J* = 10.8 Hz, 3H), 3.72 (s, 3H), 3.59 (dd, *J* = 10.7, 3.8 Hz, 3H), 3.17 – 3.05 (m, 2H). ^{13}C NMR (101 MHz, $CDCl_3$) δ 171.9, 155.7, 144.0 (d, J_{C-P} = 6.5 Hz), 141.6, 137.3, 133.5, 130.0 (d, J_{C-P} = 3.6 Hz), 129.9, 128.0, 127.3, 125.3 (d, J_{C-}

$_{P}$ = 7.6 Hz), 120.3, 67.2 (d, J_{C-P} = 6.2 Hz), 54.9 (m), 52.7, 47.4, 40.8 (d, J_{C-P} = 160.0 Hz), 38.2 (d, J_{C-P} = 7.0 Hz).^{31}P NMR (162 MHz, $CDCl_3$) δ 20.43. ESIMS calculated for $C_{28}H_{29}NO_7BrP$ $[M+Na]^+$ 624.0757, found: 624.0756; mp 68-71 ºC.

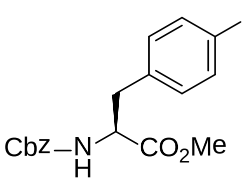

Synthesis of methyl 2-a{[(benzyloxy)carbonyl]amino}-3-(4-iodophenyl)propanoate (2.23): Iodine (5.24 g, 20.64 mmol) and sodium iodate (2.04 g, 10.32 mmol) were added to a solution of phenylalanine (8.52 g, 51.6 mmol) in acetic acid (47 mL) and concentrated sulfuric acid (6.2 mL). The mixture was heated at 70 °C and stirred for 24 h. Sodium periodate (0.4 g) was then added and the reaction mixture was stirred for 30 min. Acetic acid was then evaporated and the crude mixture was diluted with H_2O (80 mL) and washed with Et_2O and DCM. The pH of the aqueous layer was adjusted to pH 5 with concentrated NaOH solution. The precipitate was filtered under vacuum and washed with H_2O (170 mL) and EtOH (65 mL) to afford 13.09 g of the crude product 4-iodophenylalanine. The crude 4-iodophenylalanine product (1.00 g, 3.44 mmol. 1 equiv) was then suspended in water (5 mL), $NaHCO_3$ (0.45 g, 5.35 mmol, 1.5 equiv) was then added and the reaction mixture cooled on ice. Benzyl chloroformate (0.64 mL, 4.52 mmol, 1.3 equiv) in dioxane (5 mL) was added dropwise and the reaction was stirred for 18 h at room temperature. The reaction mixture was then washed with Et_2O, and the pH of the aqueous layer was adjusted to 2 using 1N HCl. The crude product was extracted with ethyl acetate and dried over Na_2SO_4. The solvent was evaporated to give 1.46 g of the crude Cbz protected product as a viscous yellow oil. To dry methanol (8 mL) cooled on ice, was slowly added $SOCl_2$ (0.43 mL, 5.88 mmol, 2.5 equiv). The resulting solution was warmed to room temperature and the crude Cbz protected product (1.00 g, 2.38 mmol, 1 equiv) was added and the mixture was stirred for 18 h at room temperature under argon. The solvent was then evaporated yielding 1.05 g of the methyl ester Cbz crude product as a viscous yellow oil. This product was used in the next step without further purification.

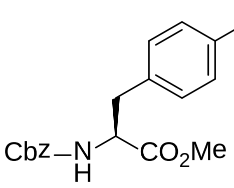

Synthesis of methyl 2-{[(benzyloxy)carbonyl]amino}-3-(4-formylphenyl)propanoate (2.24): A mixture of Cbz-*N*-*L*-4-iodophenylalanine methyl ester **2.23** (439 mg, 1 mmol, 1 equiv), $Pd(OAc)_2$ (11.67 mg, 0.05 mmol, 0.05 equiv), 1,3'-bis(diphenylphosphino)propane (20 mg, 0.05 mmol, 0.05 equiv) and Et_3N (0.35 mL, 2.5 mmol, 2.5 equiv) in dry DMF (5 mL) was purged with CO for 10 min. Trioctylsilane (0.9 mL, 2 mmol, 2 equiv) was added in one portion and the mixture was stirred under a CO balloon for 8 h at 70 ºC. The reaction mixture was then diluted with H_2O (20 mL), extracted with Et_2O, washed with H_2O, saturated $NaHCO_3$, H_2O, dried over Na_2SO_4 and the solvent evaporated. The compound was purified on a silica column (9:1 hexanes:ethyl acetate followed by 4:1 hexanes:ethyl acetate) to give **2.24** (205 mg, 60%) as a colorless oil. ^{1}H NMR (500 MHz, $CDCl_3$) δ 9.98 (1H), 7.78 (d, *J* = 7.6 Hz, 2H), 7.53 – 7.13 (m, 7H), 5.35 – 5.25 (m, 1H), 5.13 – 5.05 (m 2H), 4.75 – 4.67 (m, 1H), 3.73 (3H), 3.28 – 3.10 (m, 2H). ESIMS calculated for $C_{19}H_{19}NO_5$ $[M+Na]^+$ 341.13, found: 341.13.

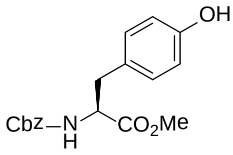

Synthesis of methyl 2-{[(benzyloxy)carbonyl]amino}-3-(4-hydroxyphenyl)propanoate (2.25): Thionyl chloride (4.6 mL, 63.33 mmol, 2 equiv) was added dropwise to dry MeOH (65 mL) at 0 ºC and stirred for 5 min. L-Tyrosine (5.70 g, 31.5 mmol, 1 equiv) was then added and the reaction vessel was fitted with a drying tube filled with drierite and slowly allowed to come to room temperature over 21 h. The solvent was then evaporated and crude product dried over high vacuum for 8 h. The crude product was then dissolved in a 1:1 mixture of acetone (63 mL) and a 7 % solution of Na_2CO_3 in water (63 mL). Benzyl chloroformate (4.7 mL, 34.7 mmol, 1.2 equiv) was then added dropwise and the reaction was stirred for 3 h at room temperature. Ethyl acetate was then added (300 mL), and the organic layer was washed with water (100 mL), brine (100 mL) and dried over Na_2SO_4. The solvent was evaporated to give **2.25** as a viscous yellow oil (10.37 g). The product was used in the next step without purification.

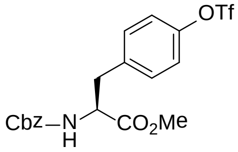

Synthesis of methyl 2-{[(benzyloxy)carbonyl]amino}-3-(4-{[(trifluoromethyl)sulfonyl]oxy}phenyl)propanoate (2.26): Compound **2.25** (10.37 g, 31.5 mmol, 1 equiv) and *N*-phenyl bis-trifluoromethane sulfonamide (12.39 g, 34.65 mmol, 1.1 equiv) were dissolved in acetonitrile (150 mL). Et_3N (5.3 mL, 37.8 mmol, 1.2 equiv) was then added and the reaction was stirred for 3 h. The reaction mixture was then diluted with ethyl acetate (150 mL) and water (100 mL). The organic layer was washed with brine, dried over Na_2SO_4 and the solvent was evaporated. The product was purified on a silica column (3:2 hexane:ethyl acetate followed by 2:3 hexanes:ethyl acetate) to obtain 14.38 g (99% yield) as a white solid. ^{1}H NMR (400 MHz, $CDC1_3$) δ 7.47 – 7.07 (m, 9H), 5.32 – 5.24 (m, 1H), 5.12 – 5.05 (m, 2H), 4.66 (dd, *J* = 13.7, 6.1 Hz, 1H), 3.71 (3H), 3.22 – 3.05 (m, 2H). ESIMS calculated for $C_{19}H_{18}F_3NO_7S$ $[M+Na]^+$ 484.0648, found: 484.0645; mp 70-73 ºC.

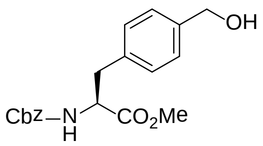

Synthesis of methyl 2-{[(benzyloxy)carbonyl]amino}-3-[4-(hydroxymethyl)phenyl]propanoate (2.27): Compound **11** (7.70 g, 16.70 mmol, 1 equiv), $Pd(OAc)_2$ (378 mg, 1.68 mmol, 0.1 equiv) and 1,1'-Bis(diphenylphosphino)ferrocene (dppf) (1.86 g, 3.34 mmol, 0.2 equiv) were dissolved in dry DMF (40 mL). K_2CO_3 (11.54 g, 83.5 mmol, 5 equiv) was then added to the reaction mixture and CO gas was bubbled through for 15 min. The reaction mixture was then heated at 60 ºC for 8 h under a CO balloon. The reaction mixture was then cooled and partitioned between ethyl acetate and saturated $NaHCO_3$. The aqueous layer was acidified with a 10 % aqueous solution of citric acid and extracted with ethyl acetate (4 × 75 mL). The organic layer was washed with brine, dried over Na_2SO_4 and the solvent was evaporated to give the crude carboxylic acid as a tan colored solid (4.89 g). The acid was dried over P_2O_5 and was used in the next step without purification. The crude acid was dissolved in dry THF (70 mL) and cooled in an ice bath. The reaction was charged with BH_3-DMS complex (10 M, 6.96 mL, 68.47 mmol, 4 equiv) added dropwise. The reaction mixture was warmed to room temperature over 2 h. A solution of saturated $NaHCO_3$ was added dropwise until the bubbling ceased. Ethyl acetate (70 mL) was added and the organic layer was separated and dried over Na_2SO_4 and then reduced. The crude product was purified on a silica column (3:2 hexane:ethyl acetate followed by 2:3 hexanes:ethyl acetate) to give **2.27** (3.56 g, 62%) as a white solid. $[\alpha]_D^{25}$ +50.56° ml dec^{-1} g (*c* 0.99, $CHCl_3$). ^{1}H NMR (500 MHz, $CDCl_3$) δ 7.41 – 7.23 (m, 7H), 7.08 (d, *J* = 8.0 Hz, 2H), 5.23 (d, *J* = 7.8 Hz, 1H), 5.12 – 5.05 (m, 2H), 4.65 (3H), 3.72 (3H), 3.17 – 3.02 (m, 2H), 1.76 (1H). ^{13}C NMR (101 MHz, $CDCl_3$) δ 172.2, 155.9, 140.0, 136.5, 135.3, 129.7, 128.8, 128.4, 128.3, 127.5, 67.2, 65.2, 55.0, 52.6, 38.1. ESIMS calculated for $C_{19}H_{21}NO_5Na$ $[M+Na]^+$ 366.1312, found: 366.1311; mp 74-77 °C.

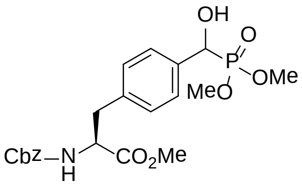

Synthesis of L-Phenylalanine, 4-[(dimethyloxyphosphinyl)hydroxymethyl]-*N*-[(phenylmethoxy)carbonyl]-, methyl ester (2.28): Compound **2.27** (3.56 g, 10.37 mmol, 1 equiv) was dissolved in DMSO (22 mL) and 2-iodoxybenzoic acid (3.77 g, 13.48 mmol, 1.3 equiv) was added and the reaction mixture and stirred for 1 h. The reaction mixture was then diluted with water (60 mL) and diethylether (60 mL) and filtered. The organic layer was separated and washed with water (2 ×50 mL), brine, and dried over Na_2SO_4. The solvent was evaporated and the crude aldehyde was used immediately in the next step without purification. The aldehyde was dissolved in dimethyl phosphite (1.05 mL, 11.41 mmol 1.1 equiv) with mild heating. CsF (9.45 g, 62.22 mmol, 6 equiv) was added and the reaction was stirred until it solidified. The crude product was then dissolved in DCM (40 mL), filtered, and the solvent evaporated. The crude product was purified on a silica plug (first with diethylether, then 1:20 DCM:MeOH) to give **2.28** as a white solid (3.98 g, 85%). $[\alpha]_D^{25}$ +38.08° ml dec^{-1} g (*c* 1.55, $CHCl_3$). ^{1}H NMR (400 MHz, $CDCl_3$) δ 7.40 (dd, *J* = 8.1, 1.9 Hz, 2H), 7.37 – 7.27 (m, 5H), 7.11 (d, *J* = 8.0 Hz, 2H), 5.39 – 5.26 (m, 1H), 5.07 (2H), 5.00 (d, *J* = 11.0 Hz, 1H), 4.63 (d, *J* = 7.6 Hz, 1H), 3.69 (d, *J* = 2.8 Hz, 3H), 3.65 (d, *J* = 4.7 Hz, 3H), 3.62 (3H), 3.16 – 3.04 (m, 2H). ^{13}C NMR (101 MHz, $CDCl_3$) δ 172.1, 155.9, 136.3 (d, $J_{C\text{-}P}$ = 23.9 Hz), 135.5, 129.6 (d, $J_{C\text{-}P}$ = 2.1 Hz), 128.8, 128.4, 128.3, 127.5 (d, $J_{C\text{-}P}$ = 5.8 Hz), 70.6 (d, $J_{C\text{-}P}$ = 159.4 Hz), 67.2, 55.0, 54.1 (d, $J_{C\text{-}P}$ = 7.1 Hz), 53.9 (d, $J_{C\text{-}P}$ = 7.1 Hz), 52.6, 38.2. ^{31}P NMR (162 MHz, $CDCl_3$) δ 24.53 (87P), 11.64 (1P). ESIMS calculated for $C_{21}H_{26}NO_8P$ $[M+Na]^+$ 474.1288, found: 474.1288; mp 68-71 ºC

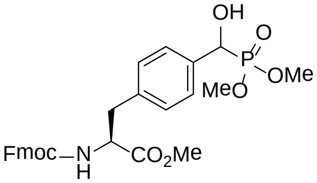

Synthesis of L-Phenylalanine, 4-[(dimethyloxyphosphinyl)bromomethyl]-*N*-[(9*H*-fluoren-9-ylmethoxy)carbonyl]-, methyl ester (2.29): Compound **2.28** (3 g, 6.65 mmol, 1 equiv) was dissolved in dry MeOH and Pd/C (200 mg, 30 mg/mmol) was added. A three way stopcock (connected to an H_2 balloon and vacuum line) was fitted to the reaction vessel. The reaction mixture was then flushed with H_2 (3×) and stirred at room temperature for 6 h. The reaction mixture was filtered through a celite pad and the solvent evaporated. A mixture of the residue, Fmoc-succinimide (2.35 g, 6.98 mmol, 1.05 equiv) and $NaHCO_3$ (2.34 g, 27.92 mmol, 4 equiv) in acetonitrile and water (1:1, 130 mL) was stirred at room temperature overnight. The acetonitrile was evaporated under reduced pressure and the crude product was extracted with ethyl acetate. The organic layer was dried over Na_2SO_4, evaporated under reduced pressure and purified on a silica plug (diethylether, followed by 10:1 DCM:MeOH) to give **2.29** as a white solid (3.59 g, 90%). ^{1}H NMR (400 MHz, $CDCl_3$) δ 7.76 (d, *J* = 8.0 Hz, 2H), 7.64 – 7.48 (m, 2H), 7.48 – 7.35 (m, 4H), 7.34 – 7.28 (m, 2H), 7.1 (d, *J* = 8.0 Hz, 2H), 5.33 (d, *J* = 7.8 Hz, 1H), 5.02 (d, *J* = 11.0 Hz, 1H), 4.70 – 4.60 (m, 1H), 4.45 – 4.29 (m, 2H), 4.21 – 4.18 (m, 1H), 3.70 (d, *J* = 7.0 Hz, 4H), 3.67 – 3.65 (m, 3H), 3.63 – 3.62 (m, 2H), 3.20 – 3.00 (m, 2H). ^{13}C NMR (101 MHz, $CDCl_3$) δ 172.1, 155.8, 144.0 (d, $J_{C\text{-}P}$ = 7.5 Hz), 141.6, 136.2, 135.7 – 134.3 (m), 129.7, 128.0, 127.5 (d, $J_{C\text{-}P}$ = 5.8 Hz), 127.3, 125.3 (d, $J_{C\text{-}P}$ = 6.1 Hz), 120.2, 70.6 (d, $J_{C\text{-}P}$ = 159.5 Hz), 67.2, 55.0, 54.1 (d, $J_{C\text{-}P}$ = 7.1 Hz), 54.0 (d, $J_{C\text{-}P}$ = 7.1 Hz), 52.6, 47.4, 38.2. ^{31}P NMR (162 MHz, $CDCl_3$) δ 24.51. ESIMS calculated for $C_{28}H_{30}NO_8P$ $[M+Na]^+$ 562.1601, found: 562.1595; mp 65-70 ºC

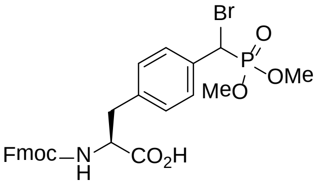

Synthesis of L-Phenylalanine, 4-[(dimethyloxyphosphinyl)bromomethyl]-*N*-[(9*H*-fluoren-9-ylmethoxy)carbonyl]; Fmoc-L-BrPmp(*O*Me$_2$)-OH (2.30): Compound **2.21** (3.00 g, 5.00 mmol, 1 equiv) was dissolved in THF (35 mL) and cooled in an ice bath. LiOH (240 mg, 10.00 mmol, 2 equiv) was dissolved in water (35 mL) and cooled in an ice bath. The lithium hydroxide solution was then added to the reaction mixture and stirred for 30 min. The THF was then evaporated, and the aqueous layer was washed with diethylether (30 mL). The aqueous layer was acidified to pH 2 with concentrated HCl and was extracted with ethyl acetate (4 × 75 ml). The combined organic layers were dried over Na_2SO_4, and concentrated to a white solid (2.67 g, 91% yield). Purity (>95%)

determined by analytical HPLC, C18, flow: 1 mL min^{-1}, λ: 254 nm, eluent: acetonitrile/0.1% TFA in water 10:90 (2 min) to 50:50 (22 min), retention time: 35.9 min. $[\alpha]_D^{25}$ +40.24° ml dec^{-1} g (*c* 1.31, $CHCl_3$). ^{1}H NMR (400 MHz, $CDCl_3$) δ 7.76 (d, *J* = 7.2 Hz, 2H), 7.57 (d, *J* = 6.3 Hz, 2H), 7.48 – 7.35 (m, 4H), 7.30 (t, *J* = 7.2 Hz, 2H), 7.16 (2H), 5.52 (d, *J* = 13.1 Hz, 1H), 4.98 – 4.81 (m, 1H), 4.67 (1H), 4.47 (m, 1H), 4.33 (1H), 4.19 (1H), 3.82 (d, *J* = 10.7 Hz, 3H), 3.54 (t, *J* = 10.4 Hz, 3H), 3.18 (2H). ^{13}C NMR (101 MHz, $CDCl_3$) δ 155.98, 144.0 (d, $J_{C\text{-}P}$ = 10.5 Hz), 141.6, 137.8, 132.7, 130.3, 129.8 (d, $J_{C\text{-}P}$ = 5.5 Hz), 128.0, 127.3, 125.3 (d, $J_{C\text{-}P}$ = 7.5 Hz), 120.2, 77.6, 77.3, 76.9, 67.1, 55.6 – 54.9 (m), 54.8, 47.4, 41.1 (d, $J_{C\text{-}P}$ = 7.6 Hz), 39.5 (d, $J_{C\text{-}P}$ = 7.6 Hz), 37.8. ^{31}P NMR (162 MHz, $CDCl_3$) δ 20.59 (d, *J* = 38.6 Hz). ESIMS calculated for $C_{27}H_{27}NO_7BrP$ $[M+Na]^+$ 610.0601, found: 610.0595; mp 84-88 ºC.

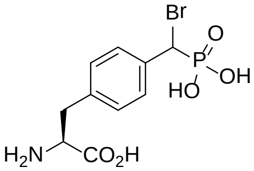

Synthesis of L-BrPmp-OH (2.31): Compound **2.30** (200 mg, 0.34 mmol, 1 equiv) was dissolved in a solution of 20% piperidine in dry DCM (10 mL) and stirred at room temperature for 30 min. The solvent was then evaporated and the residue was dried on high vacuum over P_2O_5 overnight. The residue was then dissolved in dry acetonitrile (10 mL) and TMSBr (0.47 mL, 3.4 mmol, 10 equiv) was added under an inert atmosphere and the reaction mixture was stirred overnight. The organic solvent was evaporated and the crude residue was dissolved in water and the aqueous layer was washed with diethylether (5 mL) and freeze dried. The crude bromide salt was then dissolved in anhydrous EtOH (3 mL), propylene oxide (36 µl, 0.51 mmol, 1.5 equiv) was added and the reaction mixture was stirred overnight resulting in a white precipitate the next day.

Water (5 mL) was added and the EtOH was then removed under reduced pressure. The aqueous layer was filtered and freeze dried. The crude product was dissolved in water (1 mL) and passed through a C18 Sep-pak syringe column. The aqueous fractions were freeze dried yielding **2.31** (94 mg, 65%) as a white solid of the piperidine salt. $[\alpha]_D^{25}$ -16.56º ml dec^{-1} g (*c* 1.36, $CHCl_3$). ^{1}H NMR (400 MHz, D_2O) δ 7.54 (d, *J* = 7.8 Hz, 2H), 7.26 (d, *J* = 7.6 Hz, 2H), 4.95 (d, *J* = 11.6 Hz, 1H), 4.07 – 3.92 (m, 1H), 3.28 (d, *J* = 10.5 Hz, 1H), 3.16 – 3.00 (m, 5H), 1.77 – 1.68 (m, 4H), 1.67 – 1.57 (m, 2H). ^{13}C NMR (101 MHz, D_2O) δ 135.6, 135.6 (d, *J* = 1.1 Hz), 129.9 (d, *J* = 5.8 Hz), 129.8 (d, *J* = 1.4 Hz), 56.0, 46.2, 44.8, 36.2, 22.5, 21.7. ^{31}P NMR (162 MHz, D_2O) δ 13.47. ESIMS calculated for $C_{10}H_{12}NO_5BrP$ $[M-H]^-$ 335.9642, found: 335.9640; decomp. 140 ºC.

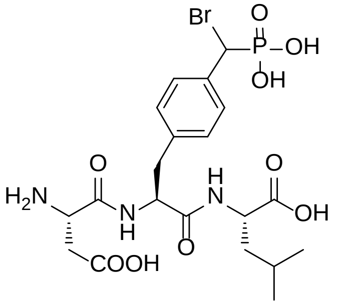

Synthesis of tripeptide Asp-BrPmp-Leu (2.32): The tripeptide was assembled manually on Wang resin (0.6 mmol/g), preloaded with an Fmoc protected Leu residue (Fmoc-L-Leu-OH). Following a standard protocol: Fmoc-L-BrPmp(*O*Me_2)-OH **2.30** (2 equiv) was coupled to the resin using HBTU (1.96 equiv) in the presence of DIPEA (4 equiv) in NMP for 3.5 h. The reaction was monitored by Kaiser test. The coupling was repeated using the same equivalents of Fmoc-L-BrPmp(*O*Me_2)-OH, HBTU and DIPEA in NMP for 3.5 h. Fmoc-Asp(*t*Bu)-OH (5 equiv) was coupled using HBTU (4.9 equiv) in the presence of DIPEA (10 equiv) in NMP for 3.5 h. Fmoc deprotection was achieved with 20% piperidine in NMP. The resin was washed with NMP, AcOH, DCM, and MeOH.

Immediately after washing the resin with CH_3CN, DCM and MeOH, a mixture of TFA/H_2O/TIPS (95:2.5:2.5) was added and the resin was shaken at room temperature for 3 h. The cleaved peptide was precipitated in diethylether, filtered, dissolved in a mixture of H_2O and CH_3CN and lyophilized. The lyophilized peptide was suspended in CH_3CN, and TMSI (20 equiv) was added under an inert atmosphere and the reaction mixture shaken for 100 min at room temperature. The CH_3CN/TMSI solution was evaporated under reduced pressure, and the crude product was dissolved in water and washed with diethylether (3 ×) and the aqueous layer was lyophilized. The peptide was purified by HPLC (C-18 semipreparative column) using a linear gradient (CH_3CN/H_2O mobile phase containing 0.1% TFA). 4 mg of pure compound was recovered from 18 mg crude product (33% of theoretical yield). Purity (>95%) determined by analytical HPLC, C18, flow: 1 mL min^{-1}, λ: 212 nm, eluent: 0.1% TFA in acetonitrile/0.1% TFA in water 10:90 (2 min) to 20:80 (22 min), retention time: 22.4 min. ^1H NMR (500 MHz, D_2O) δ 7.57 (d, J = 6.8 Hz, 2H), 7.30 (dd, J = 7.9, 2.2 Hz, 2H), 5.02 (d, J = 11.7 Hz, 1H), 4.75 – 4.69 (m, 1H), 4.43 – 4.32 (m, 1H), 4.32 – 4.22 (m, 1H), 3.23 – 3.06 (m, 2H), 2.99 – 2.84 (m, 2H), 1.67 – 1.59 (m, 2H), 0.92 (dd, J = 19.7, 4.7 Hz, 6H). ^{31}P NMR (162 MHz, D_2O) δ 13.78 (d, J = 4.8 Hz). ESIMS calculated for $C_{20}H_{29}N_3O_9BrP$ $[M-H]^-$ 564.0752, found: 564.0732.

2.10.3 Phosphatase enzyme inhibition Assay

Enzyme assays were conducted using human CD45-cytoplasmic domain (Enzo Life Science; diluted to 4 mU/µL in 50 mM HEPES, pH 7.2, 1 mM EDTA, and 0.1% nonidet P-40), or bovine alkaline phosphatase (New England Bio Labs; diluted to 4 mU/µL in 100 mM NaCl, 50 mM tris-HCl, 10 mM $MgCl_2$ 1 mM dithiothreitol, pH 7.9). Enzyme activity was detected with a fluorogenic substrate (6,8-difluoro-4-methylumbelliferyl phosphate; DiFMUP) (Invitrogen). Assays were performed in black 96-well plates and read in a Spectra Max M2 plate reader (Molecular Devices). For CD45 assays, substrate concentration was between 1 µM to 50 µM, for alkaline phosphatase substrate concentration was between 10 nM to 10 µM. Stock solutions of inhibitors (100 mM of compound **7** in deionized water; and 10 mM of compound **16** in 50% deionized water and 50% DMSO) were prepared and stored at -20 ˚C. Final solutions in microplate wells contained a total volume of 100 µl consisting of 2 µl of diluted enzyme, inhibitor, and DiFMUP substrate diluted to 100 µL in the appropriate buffer. All wells were incubated for 10 min at 37 ˚C in the plate reader prior to the addition of DiFMUP. After incubation, substrate was added and the plate was read at an excitation maximum of 358 nm and an emission maximum of 450 nm every 30 seconds for 125 min (CD45) or 65 min (alkaline phosphatase).

2. 12 Appendix

Figure B1: Crude Analytical HPLC Chromatogram of 2.32

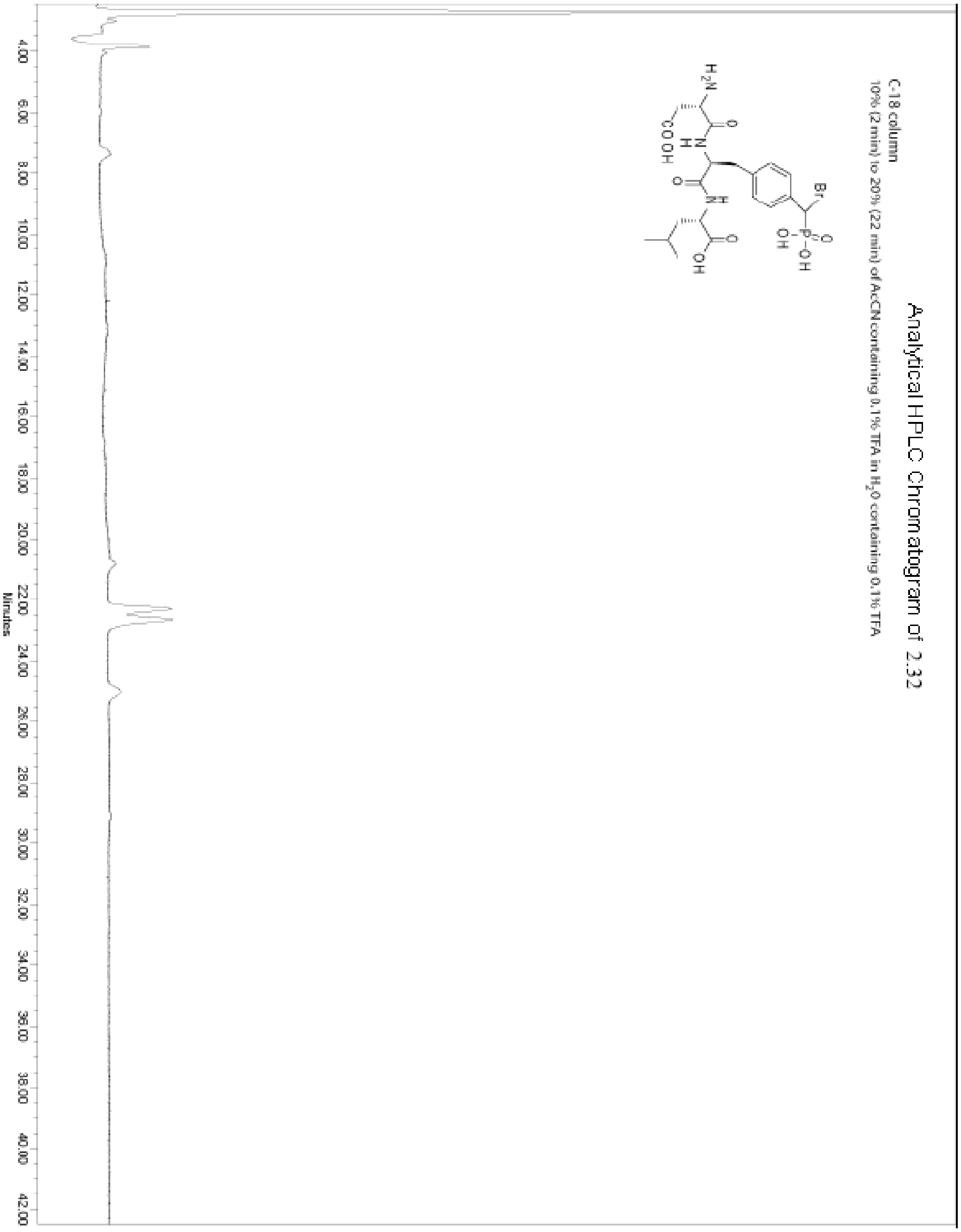

Figure B2: Purified Analytical HPLC Chromatogram of 2.32

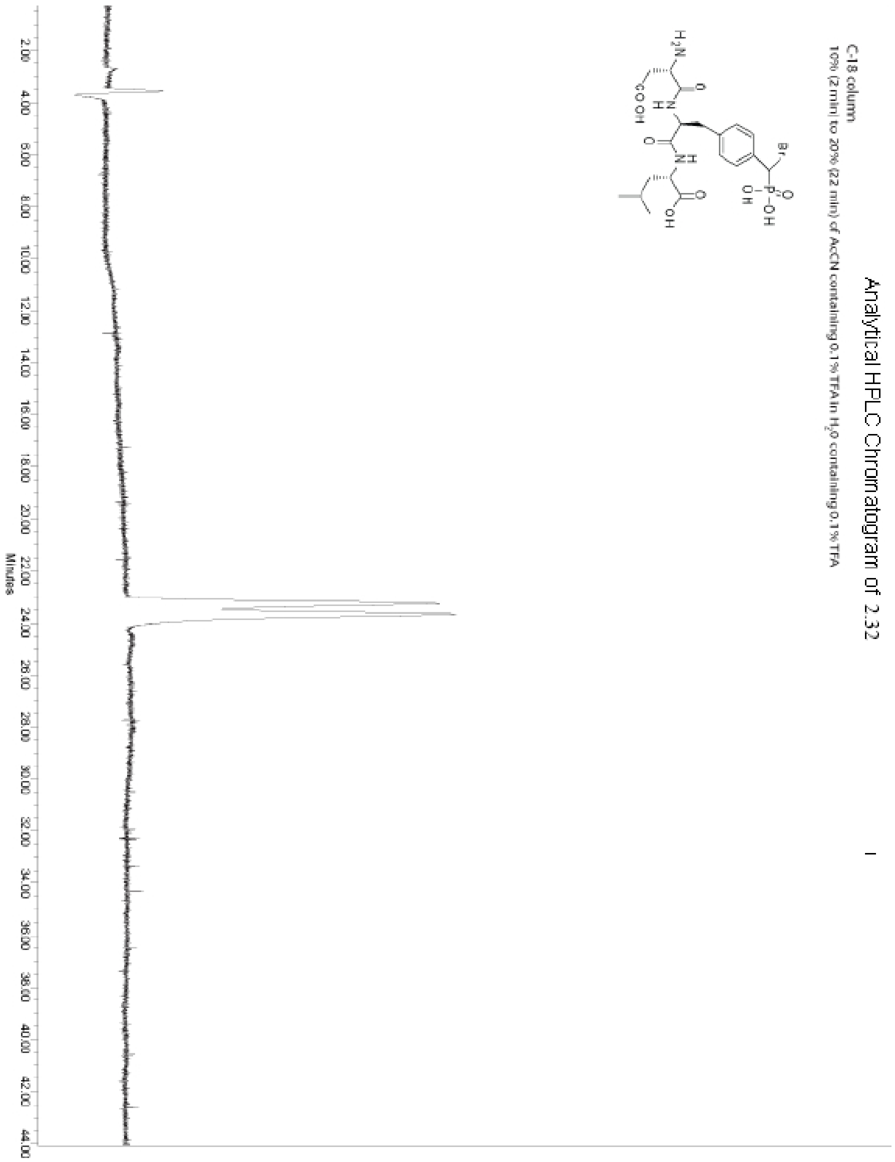

Figure B3: CD45 inhibition by compounds 2.31, 2.32, and 2.12.

Kinetic plots of CD45 hydrolysis of DiFMUP (a.) alone, and in the presence of compounds (**b.**) **2.32**, (**c.**) **2.31**, and (**d.**) **2.12**.

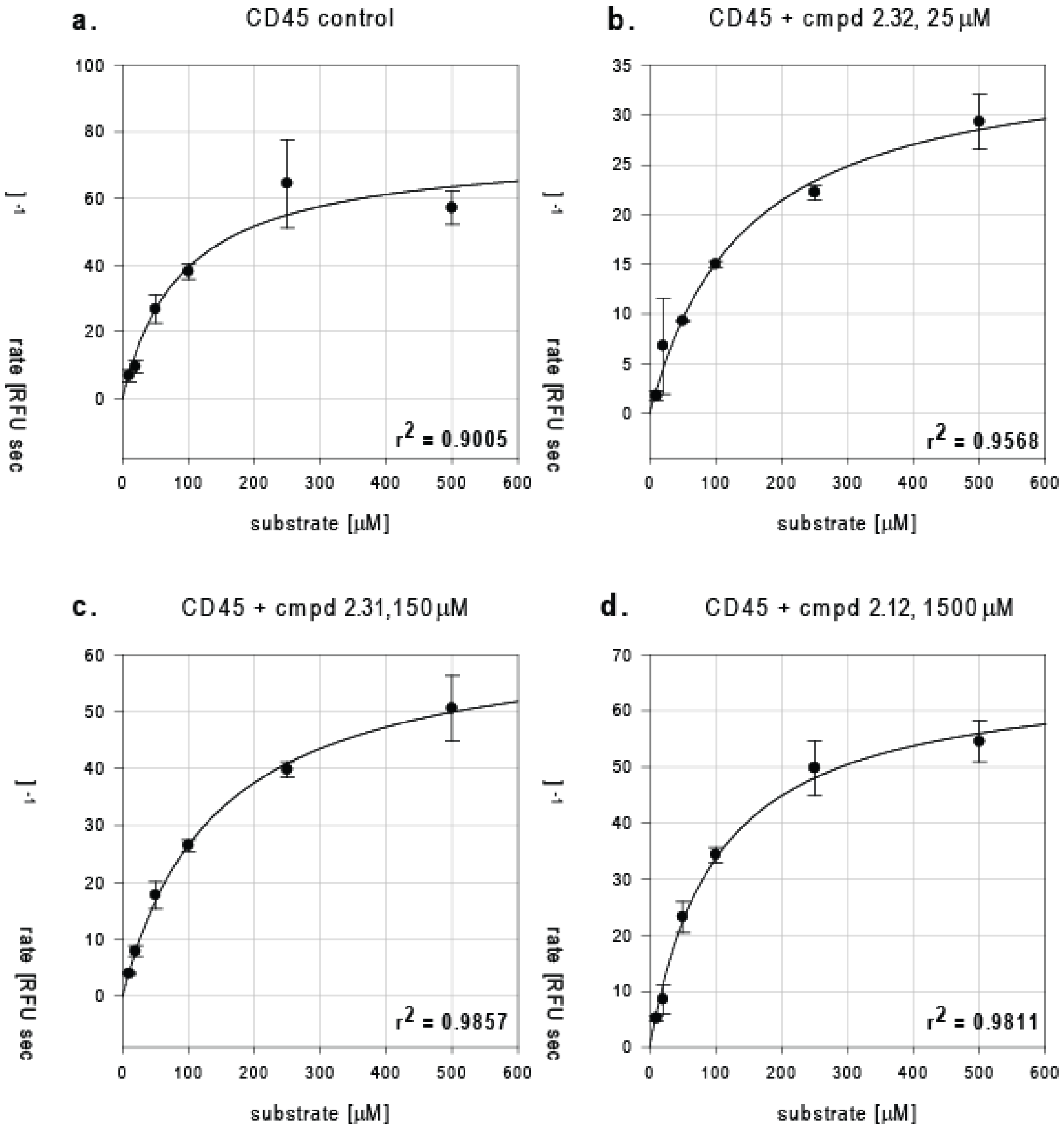

Figure B4: Reciprocal plots of CD45 inhibition.

Lineweaver-Burke reciprocal plots for inhibition of CD45 by compounds (**a.**) **2.31**, (**b.**) **2.32**, and (**c.**) **2.12**. Data is the same shown in Figure A1. The lowest concentration (0.1 μM DiFMUP) was dropped from all curves.

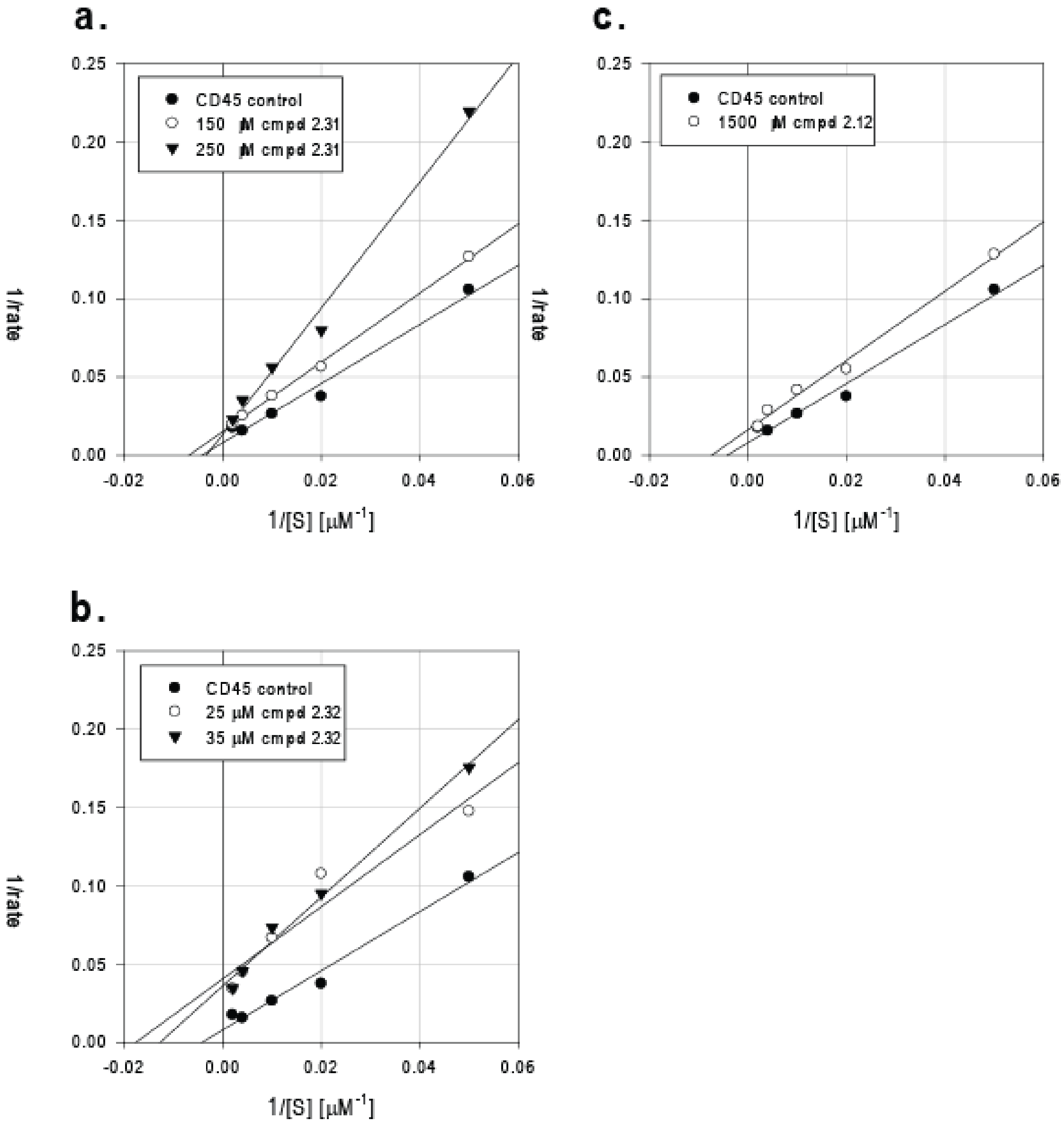

Figure B5: Time dependent inhibition of CD45 by compound 2.31.

To test the mechanism of CD45 inhibition, three solutions of CD45 in assay buffer were prepared, with one containing inhibitor (**2.31**). The solutions were incubated for 13 h at 4 °C. At the end of the incubation period, inhibitor was added to the second enzyme sample, and the third had only buffer added. After 10 min, all three samples were observed for turnover of DiFMUP substrate (100 μM) as above. The sample which was pre-incubated with inhibitor showed dramatically reduced enzyme activity (15 RFU sec^{-1}) relative to the sample which was only briefly exposed to the inhibitor (1520 RFU sec^{-1}). The negative control still showed significant enzyme activity (2100 RFU sec^{-1}). This observation supports an irreversible mechanism of inhibition for CD45 by compound **2.31**. Fit values were determined for the region of the curve between 10 – 30 min.

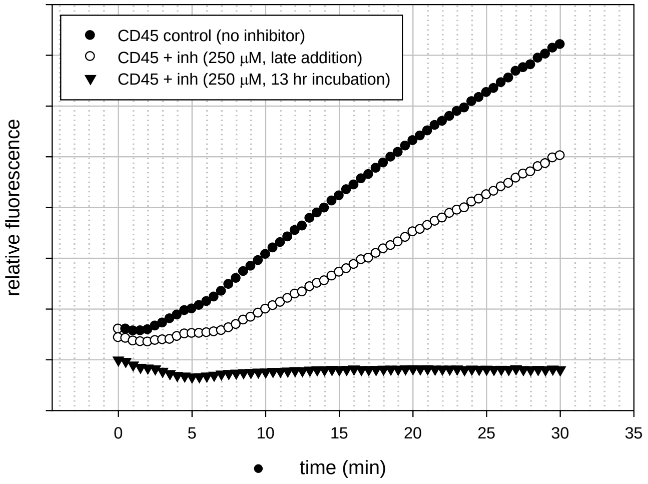

2.13 References

1. Lo, L. C.; Pang, T. L.; Kuo, C. H.; Chiang, Y. L.; Wang, H. Y.; Lin, J. J., Design and synthesis of class-selective activity probes for protein tyrosine phosphatases. *Journal of Proteome Research* **2002**, 1, (1), 35-40.

2. Liu, S.; Zhou, B.; Yang, H.; He, Y.; Jiang, Z. X.; Kumar, S.; Wu, L.; Zhang, Z. Y., Aryl vinyl sulfonates and sulfones as active site-directed and mechanism-based probes for protein tyrosine phosphatases. *Journal of the American Chemical Society* **2008**, 130, (26), 8251-8260.

3. Park, J.; Pei, D., Trans-î²-nitrostyrene derivatives as slow-binding inhibitors of protein tyrosine phosphatases. *Biochemistry* **2004**, 43, (47), 15014-15021.

4. Kumar, S.; Zhou, B.; Liang, F.; Wang, W. Q.; Huang, Z.; Zhang, Z. Y., Activity-based probes for protein tyrosine phosphatases. *Proceedings of the National Academy of Sciences of the United States of America* **2004**, 101, (21), 7943-7948.

5. Taylor, W. P.; Zhang, Z. Y.; Widlanski, T. S., Quiescent affinity inactivators of protein tyrosine phosphatases. *Bioorganic & Medicinal Chemistry* **1996**, 4, (9), 1515-1520.

6. Barr, A. J.; Ugochukwu, E.; Lee, W. H.; King, O. N. F.; Filippakopoulos, P.; Alfano, I.; Savitsky, P.; Burgess-Brown, N. A.; Muller, S.; Knapp, S., Large-scale structural analysis of the classical human protein tyrosine phosphatome. *Cell* **2009**, 136, (2), 352-363.

7. Tulsi, N. S.; Downey, A. M.; Cairo, C. W., A protected l-bromophosphonomethylphenylalanine amino acid derivative (BrPmp) for synthesis of

irreversible protein tyrosine phosphatase inhibitors. *Bioorganic & Medicinal Chemistry* **2010**, 18, (24), 8679-8686.

8. Kumar, S.; Zhou, B.; Liang, F. B.; Wang, W. Q.; Huang, Z. H.; Zhang, Z. Y., Activity-based probes for protein tyrosine phosphatases. *Proceedings of the National Academy of Sciences of the United States of America* **2004**, 101, (21), 7943-7948.

9. Texierboullet, F.; Foucaud, A., A convenient synthesis of dialkyl 1-hydroxyalkanephosphonates using potassium or cesium fluoride without solvent. *Synthesis-Stuttgart* **1982**, (2), 165-165.

10. Morera, E.; Ortar, G.; Varani, A., An improved preparation of 4-hydroxymethyl-l-phenylalanine. *Synthetic Communications* **1998**, 28, (22), 4279-4285.

11. Cacchi, S.; Ciattini, P. G.; Morera, E.; Ortar, G., Palladium-catalyzed carbonylation of aryl triflates - synthesis of arenecarboxylic acid-derivatives from phenols. *Tetrahedron Letters* **1986**, 27, (33), 3931-3934.

12. Rilatt, I.; Caggiano, L.; Jackson, R. F. W., Development and applications of amino acid derived organometallics. *Synlett* **2005**, (18), 2701-2719.

13. Swamy, K. C. K.; Kumar, K. V. P. P.; Suresh, R. R.; Kumar, N. S., Easy and stereoselective synthesis of cyclopropyl-substituted phosphonates via alpha-chlorophosphonates. *Synthesis-Stuttgart* **2007**, (10), 1485-1490.

14. Creary, X.; Underiner, T. L., Stabilization demands of diethyl phosphonate substituted carbocations as revealed by substituent effects. *Journal of Organic Chemistry* **1985**, 50, (12), 2165-2170.

15. Gross, H.; Costisella, B.; Ozegowski, S.; Keitel, I.; Forner, K., Alpha-substituted phosphonates .67. Reaction of salicylaldehyde with triethylphosphite - new c-o

phosphoryl group rearrangement. *Phosphorus Sulfur and Silicon and the Related Elements* **1993**, 84, (1-4), 121-128.

16. Pianowski, Z. L.; Winssinger, N., Fluorescence-based detection of single nucleotide permutation in DNA via catalytically templated reaction. *Chemical Communications* **2007**, (37), 3820-3822.

17. Tabanella, S.; Valancogne, I.; Jackson, R. F. W., Preparation of enantiomerically pure pyridyl amino acids from serine. *Organic & Biomolecular Chemistry* **2003**, 1, (23), 4254-4261.

18. Kruppa, M.; Imperato, G.; Konig, B., Synthesis of chiral amino acids with metal ion chelating side chains from L-serine using negishi cross-coupling reaction. *Tetrahedron* **2006**, 62, (7), 1360-1364.

19. Lei, H. Y.; Stoakes, M. S.; Herath, K. P. B.; Lee, J. H.; Schwabacher, A. W., Efficient synthesis of a phosphinate bis-amino acid and its use in the construction of amphiphilic peptides. *Journal of Organic Chemistry* **1994**, 59, (15), 4206-4210.

20. Lin, S.; Yang, Z. Q.; Kwok, B. H. B.; Koldobskiy, M.; Crews, C. M.; Danishefsky, S. J., Total synthesis of TMC-95A and -B via a new reaction leading to Z-enamides. Some preliminary findings as to SAR. *Journal of the American Chemical Society* **2004**, 126, (20), 6347-6355.

21. Yokomatsu, T.; Yamagishi, T.; Matsumoto, K.; Shibuya, S., Stereocontrolled synthesis of hydroxymethylene phosphonate analogues of phosphorylated tyrosine and their conversion to monofluoromethylene phosphonate analogues. *Tetrahedron* **1996**, 52, (36), 11725-11738.

22. Cacchi, S.; Ciattini, P. G.; Morera, E.; Ortar, G., Palladium-catalyzed carbonylation of aryl triflates. Synthesis of arenecarboxylic acid derivatives from phenols. *Tetrahedron Letters* **1986**, 27, (33), 3931-3934.

23. Cai, C. Z.; Breslin, H. J.; He, W., A convenient, large-scale synthesis of 4 '-carboxamido *N*-boc-2 ',6 '-dimethyl-l-phenylalanines. *Tetrahedron* **2005**, 61, (28), 6836-6838.

24. Klein, L. L.; Li, L. P.; Chen, H. J.; Curty, C. B.; DeGoey, D. A.; Grampovnik, D. J.; Leone, C. L.; Thomas, S. A.; Yeung, C. M.; Funk, K. W.; Kishore, V.; Lundell, E. O.; Wodka, D.; Meulbroek, J. A.; Alder, J. D.; Nilius, A. M.; Lartey, P. A.; Plattner, J. J., Total synthesis and antifungal evaluation of cyclic aminohexapeptides. *Bioorganic & Medicinal Chemistry* **2000**, 8, (7), 1677-1696.

25. Frigerio, M.; Santagostino, M., A mild oxidizing reagent for alcohols and 1,2-diols-*O*-iodoxybenzoic acid (IBX) in DMSO. *Tetrahedron Letters* **1994**, 35, (43), 8019-8022.

26. Larose, L.; Gish, G.; Pawson, T., Construction of an SH2 domain-binding site with mixed specificity. *Journal of Biological Chemistry* **1995**, 270, (8), 3858-3862.

27. Copeland, R. A., *Enzymes: A practical introduction to structure, mechanism, and data analysis*. 2nd ed.; John Wiley & Sons, Inc.: New York, NY, 2000.

28. Kitz, R.; Wilson, I. B., Esters of methanesulfonic acid as irreversible inhibitors of acetylcholinesterase. *Journal of Biological Chemistry* **1962**, 237, (10), 3245-&.

29. Skorey, K.; Ly, H. D.; Kelly, J.; Hammond, M.; Ramachandran, C.; Huang, Z.; Gresser, M. J.; Wang, Q. P., How does alendronate inhibit protein-tyrosine phosphatases? *Journal of Biological Chemistry* **1997**, 272, (36), 22472-22480.

Chapter 3: Incorporation of BrPmp into peptides

3.1 Introduction

Despite our detailed knowledge of the conserved catalytic domain and mechanism shared by most PTPs, relatively little is know about PTP substrate specificity. This is largely due to the fact that only a few physiological substrates have been strongly linked to PTPs.[1] Yet within intracellular environments, PTPs exhibit a high level of substrate specific dephosphorylation essential for homeostasis.[2] It is currently believed that PTP substrate specificity is controlled by two mechanisms. The first mechanism is based on the presence of structural elements, referred to as targeting domains, contained within some PTPs that direct physiological substrates to the catalytic site.[3] The second mechanism is based on the primary sequence of the phosphorylated substrate. This mechanism is supported by studies in which synthetic phosphorylated tyrosine (*p*Tyr) peptides of varying sequence produced kinetic constants (k_{cat}/K_m) which varied by several orders of magnitude for the same PTP.[4-11]

The regulation of PTP specificity by the primary amino acid sequence of the substrate provides an attractive avenue for researchers to explore. Sequence specific data for a particular PTP could aid in the discovery of physiological PTP substrates and will also assist in the development of specific peptide based inhibitors. A number of approaches ranging from kinetic assays of phosophopeptides to combinatorial peptide libraries have been utilized to identify specific substrates for PTPs. Yao et al. have recently identified several new substrates for PTP1B, SHP1/2 and TCPTP by employing a phosphopeptide microarray.[12] Using a phage library, van Huijsuijnen et al. identified distinct consensus substrate motifs for several PTPs including PTP1B, PTP-β.[13] Several primary amino acid substrate sequences for CD45 have been determined by employing kinetic assays of phosphopeptides.[14, 15] We propose that the incorporation of BrPmp into these sequences would allow the development of potent, and specific, CD45 inhibitors. In this chapter we will describe the design and synthesis of peptide based inhibitors.

3.2 CD45 peptide substrates

Previous work by Hegedus et. al. demonstrated that the PTP activity of CD45 is selective, removing phosphate groups from specific *p*Tyr residues based on the primary sequence.[14] Using synthetic phosphopeptides derived from the imunnorecepter tyrosine-based activation motif (ITAM) of the CD3ζ chain in the T cell receptor (TCR) complex (18 amino acids in length); the efficiency of dephosphorylation by CD45 was dependent on the primary sequence of the peptide. In addition, the position of the *p*Tyr residue(s) also affected efficiency of dephosphorylation with *N*-terminal *p*Tyr being poorer substrates than identical peptides containing *C*-terminal *p*Tyr.

Substrate specificity differences between PTPs based solely on the primary amino acid sequence have been reported. Relatively short peptides (tetramers) containing a sulfotyrosyl-motif in place of a *p*Tyr residue can have up to a 24-fold selectively difference between the PTPs PTP1B and CD45.[16] It has also been demonstrated that an *N*-terminal acidic residue directly adjacent to a sulfotyrosyl residue was essential for high affinity binding to PTP1B.

A consensus sequence for CD45 was proposed based on examinination of X-ray crystal structures of the enzyme active site bound to a CD3 ζITAM-1 phosphopeptide.[17] The consensus sequence preferred by CD45 is $X_{-3}X_{-2}X_{-1}$*p*Tyr$X_1X_2X_3$L, where X_{-3} and X_{-2} are either an aspartic(Asp) or glutamic(Glu) acid residue, X_1 & X_2 are a hydrophilic residues, and X_3 is an hydrophobic residue.[17] This consensus sequence is consistent with two well characterized substrates of CD45, the protein tyrosine kinases Lck and Fyn. Both Lck and Fyn have two *p*Tyr sites, one near the *C*-terminus (TEGQ*p*TyrQPQ in Lck, **3.1** and TEPQ*p*TyrQPG in Fyn, **3.2**) and the other contained in their activation loop (DENE*p*TyrTAR in Lck, **3.3** and EDNE*p*TyrTAR in Fyn, **3.4**).[17, 18] All four substrates contain a hydrophobic residue at X_2, hydrophilic residues at X_1 and X_{-1}, and an acidic residue around the X_{-2} position (**Figure 3.1**).

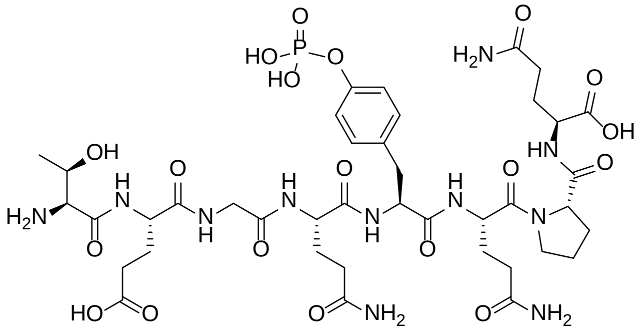

3.1

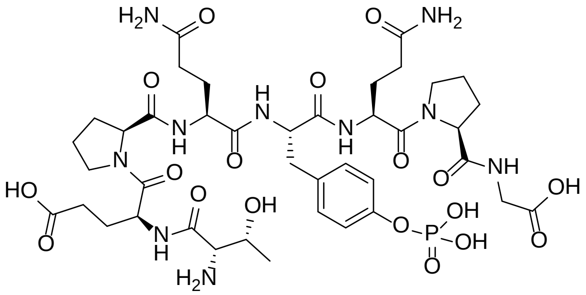

3.2

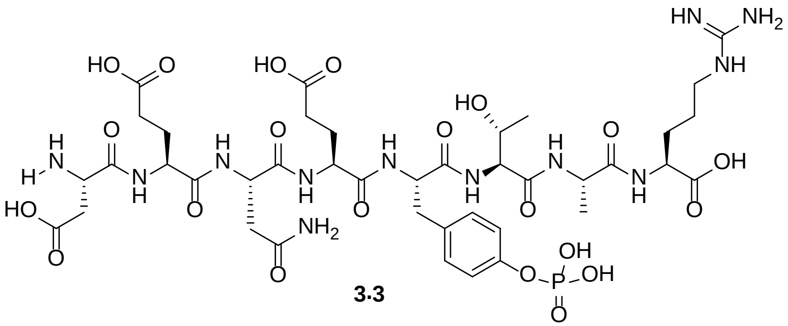

3.3

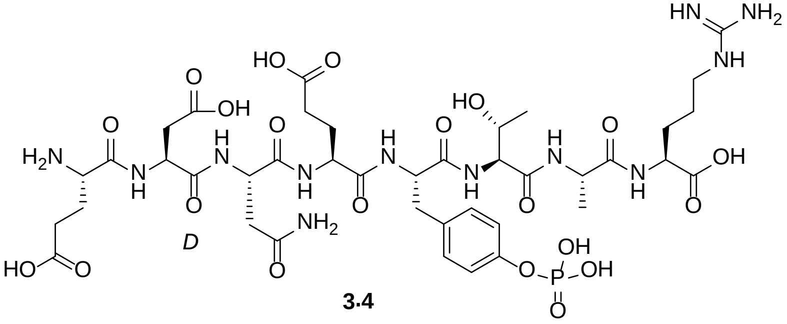

3.4

Figure 3.1 Peptide substrates of CD45 from Lck and Fyn

Perhaps the most comprehensive study to date of PTP substrate selectivity has recently been performed by Barr et al.[15] In this study the authors assayed a panel of diverse phosphopeptides (38 in total) derived from known PTP substrates against 28 highly purified PTPs. CD45 was found to be quite promiscuous, and with a few exceptions, dephosphorylated the majority of assayed substrates with reasonable activity. This finding is surprising since several of the phosphopeptides dephosphorylated fall outside the expected CD45 consensus sequence established by Nam et al.[17] In contrast, the PTP RPTPσ showed a high level of specificity for a phosphopeptide derived from N-cadherin, a recently identified substrate.[19] Overall the 28 PTPs assayed showed a vast difference in dephosphorylation efficiency against the phosphopeptides tested, reinforcing the idea that the substrate primary amino acid sequence plays an important role in PTP specificity.

Armed with the knowledge of PTP substrate specificity, and our previous observation of the improved potency of BrPmp within the context of a tripeptide sequence, we set out to develop specific PTP peptidyl inhibitors that incorporate the BrPmp residue. These peptides could be used to probe PTP substrate specificity, or to develop specific labels for PTPs.

3.3 Sequence selection

We chose to focus on the PTPs CD45, PTP1B and SHP2. These enzymes were selected based on substrate specificity profiles established in previous studies.[14, 15, 18] The peptide sequences selected for BrPmp incorporation in place of the *p*Tyr residue are illustrated in **Table 3.1, Figure 3.2** and **Figure 3.3**.

Label	**Source**	**Sequence**	**CD45**	**PTP1B**	**SHP2**	**Ref.**
3.4	MET-1235	DKEY(BrPmp)SVHN	++	+	-	17
3.5	GHR-487	NIDF(BrPmp)AQVS	-	+	-	18
3.6	TIE2-816	DPTI(BrPmp)PVLD	+	-	+	19
3.7	Lck	EDNE(BrPmp)TARE	++	n.d.	n.d.	14
3.8	Lck	TEGQ(BrPmp)QPQP	+	n.d.	n.d.	14
3.9	CD3ζ	RREE(BrPmp)DVLD	++	n.d.	n.d.	11
3.10	CD3ζ	HDGL(BrPmp)QGLS	-	n.d.	n.d.	11

Table 3.1 Sequences selected for BrPmp incorporation and their predicted dephosphorylation efficiency respective toCD45, PTP1B & SHP2 (++ = strong dephosphorylation activity, + = moderate activity, - = minimal dephosphorylation activity, n.d.= no data on dephosphorylation activity). Substrate specificity was based on the results cited.

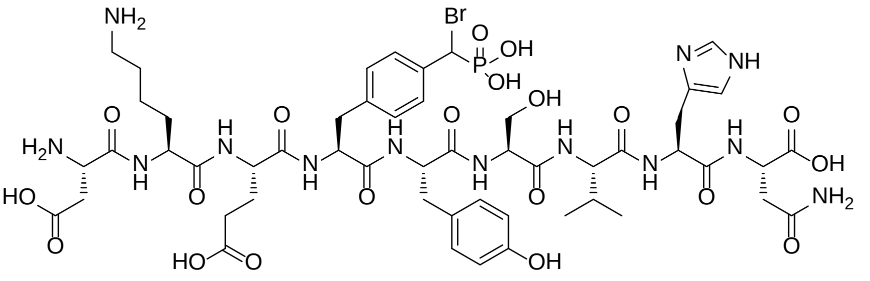

3.4

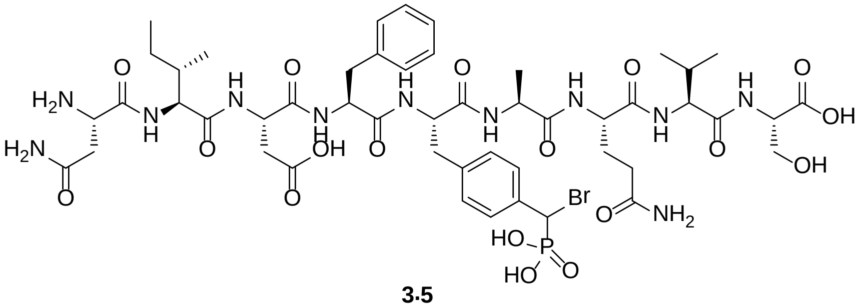

3.5

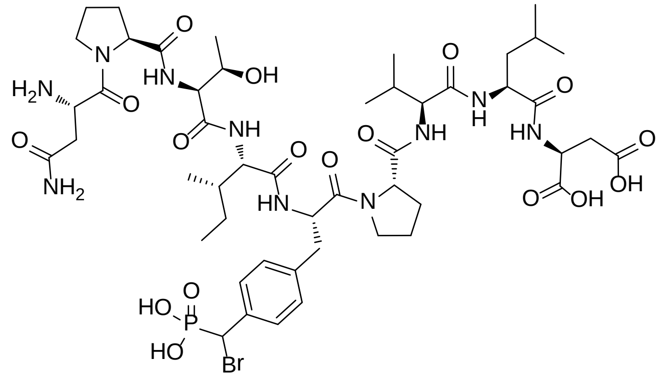

3.6

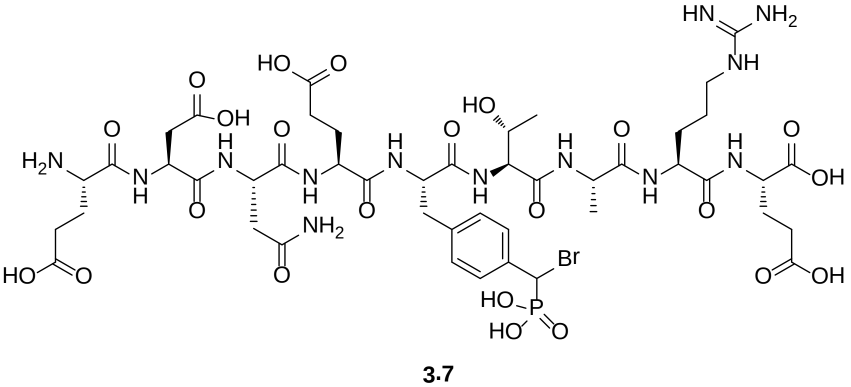

3.7

Figure 3.2 Target peptide sequences with BrPmp incorporation.

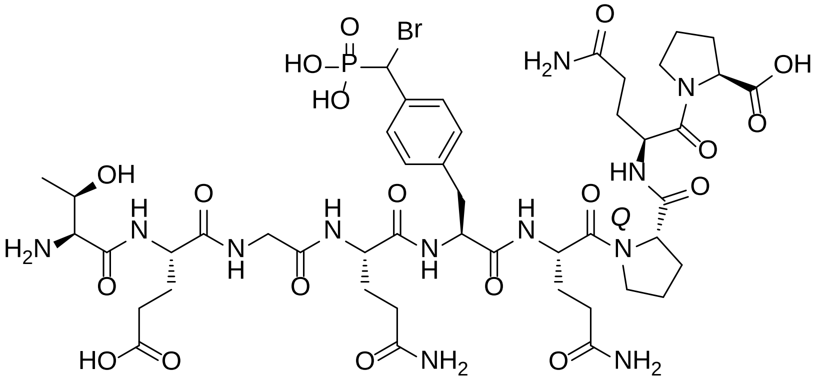

3.8

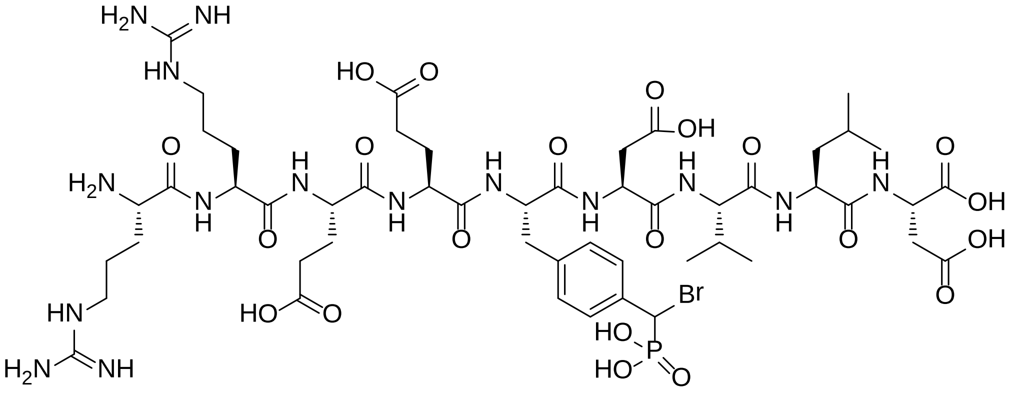

3.9

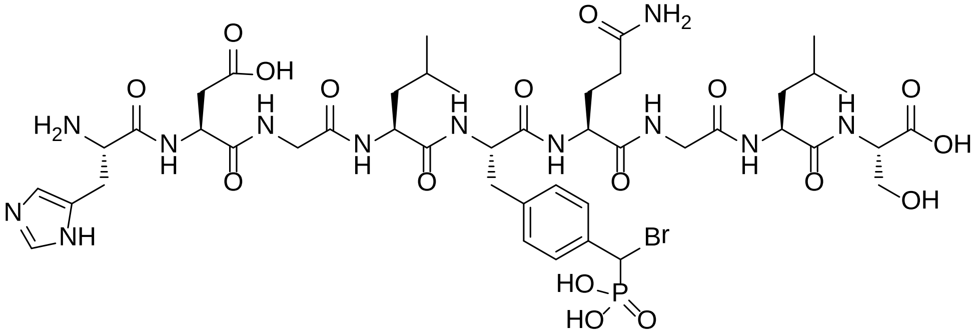

3.10

Figure 3.3 Target peptide sequences with BrPmp incorporation.

The first sequence (**3.4**) was derived from the Met receptor tyrosine kinase (MET-1235) and is a growth factor receptor that when activated induces cellular motility, division and morphogenic changes.[20] Sequence **3.5** was derived from the transmembrane growth hormone receptor. Binding of growth hormone to this receptor activates various signal transduction pathways leading to cellular growth.[21] Sequence **3.6** was sourced from the angiopoietin receptor, which is responsible for the formation of new blood vessels upon binding to the protein growth factor angiopoietin.[22] The last four sequences (**3.7 – 3.10**) were derived from CD45 substrates Lck[18] and the ITAM domain of the CD3ζ chain of the T cell receptor (TCR) complex[14].

The peptides were arbitrarily truncated to 9 residues in length, with four residues on either side of BrPmp residue. The expected dephosphorylation efficiency of each sequence with regard to CD45, PTP1B and SHP2 is also listed in **Table 3.1**. Expected substrate activity is noted from strong (++) to weak(-) based on reported substrate activity.

3.4 Synthesis of the nona-peptides

Peptide residues, with the exception of **2.30**, were incorporated utilizing standard automated solid phase methods, based on the Fmoc protecting group strategy. Compound **2.30** was incorporated manually using HBTU as a coupling agent with DIPEA as a base. Couplings for **2.30** were performed with a 2:1:1 molar ratio of

2.30:HBTU:DIPEA, in two cycles. The peptides were then cleaved from the resin with 95% TFA and 5% water for 4 h. The crude lypholized products were subsequently treated with TMSI for 1.7 h to remove the methyl phosphonate protected groups and purified by HPLC.[23]

Label	Sequence	Exp. m/z Peak	Major Obs m/z Peaks
3.4	DKEY(BrPmp)SVHN	1309.4	1308.5
3.5	NIDF(BrPmp)AQVS	1211.39	1378.7, 1317.5, 1207.6
3.6	DPTI(BrPmp)PVLD	1186.43	1135.6, 1062.4, 1040.4
3.7	EDNE(BrPmp)TARE	1281.36	1483.4, 1445.4,1317.5, 922.0
3.9	RREE(BrPmp)DVLD	1349.47	1317.5, 1207.6, 659.3
3.10	HDGL(BrPmp)QGLS	1144.36	1284.6, 1229.5, 1137.5, 1123.6

Table 3.2 Expected m/z peaks versus observed m/z peaks for compounds 3.4 - 3.10

HR-MS of the purified fractions of compounds **3.4 - 3.10** did not detect any of the desired m/z peaks (**Table 3.2**). Furthermore the typical isotopic pattern of brominated compounds was completely absent in the mass spectra of compounds **3.5 - 3.10**, suggesting that the bromide atom in the BrPmp residue was no longer present. Unfortunately we were unable to assign any of the major peaks in the mass spectra of compounds **3.5 – 3.10** with any certainty as they did not correspond to standard mass losses. A brominated compound was observed in the mass spectrum of **3.4** but was one unit lighter than the expected peak. Subsequent MS/MS analysis of this sample indicated that a hydroxyl functional group on the

C-terminal carboxylic acid of the peptide had been replaced with an amine via an unknown side reaction (**Table 3.3, 3.11)**.

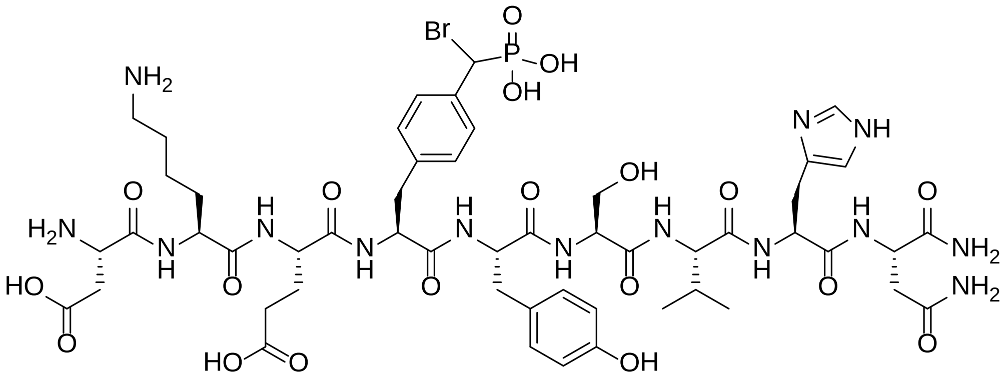

3.11

Label	Sequence	Purity of BrPmp ^{31}P NMR / HPLC	Observed MS
3.11	DKEY(BrPmp)SVHN(NH_2)	100%/100%	1308.5

Table 3.3 Amidated product observed in attempted synthesis of 3.4

To determine if the loss of the bromide occurred during peptide synthesis or under TMSI deprotection, **3.6** was remade and submitted for mass spectral analysis after cleavage from the resin (**Scheme 3.1**). Surprisingly the mono- and not the di-protected phosphonate ester of the BrPmp peptide was detected. This suggests that the methyl ester phosphonate protecting group was not stable to SPPS conditions even though we had previously performed stability studies on model compounds to test for this possibility (see Section 2.3). Treatment of the mono-protected phosphonate **3.6** with TMSI resulted in the complete loss of the bromide as previously detected by mass spectrometry (**Table 3.2**). We concluded that extended exposure of the dimethylphosphonate protected BrPmp to Fmoc deprotection conditions had resulted in mono-deprotection of the phosphotyrosine analog. The resulting methylphosphonate was then susceptible to loss of the bromide, resulting in the generation of the Pmp peptide (see Sec 3.7).

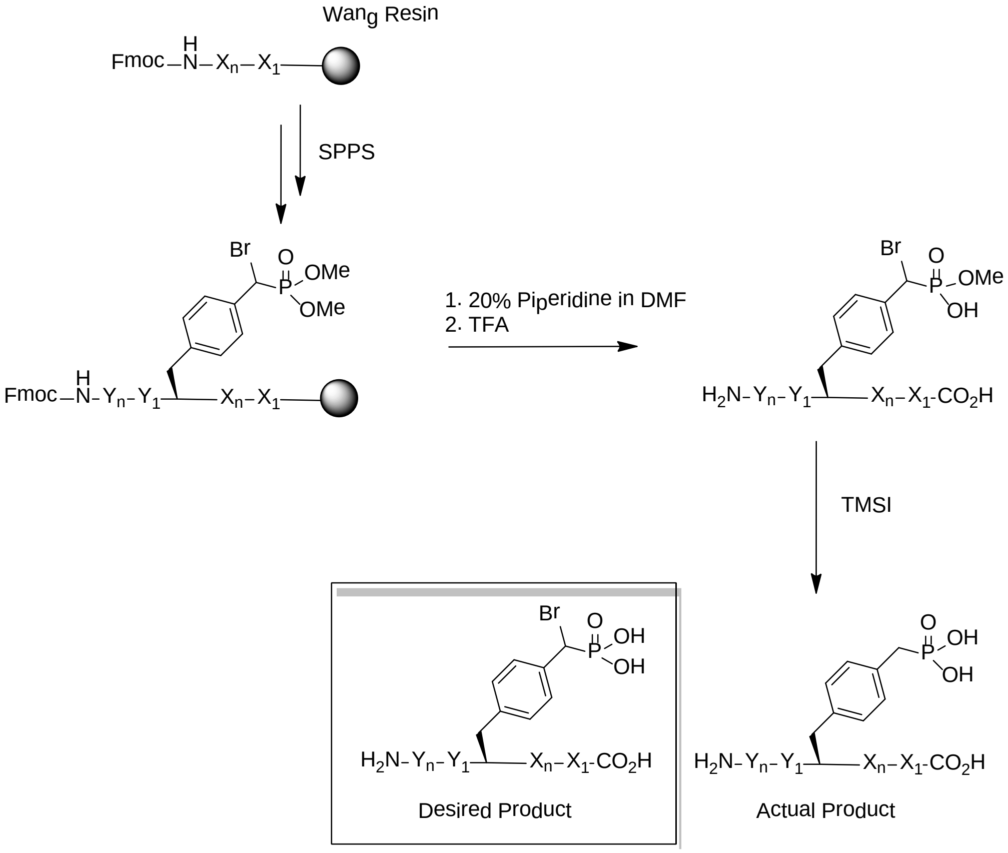

Wang Resin
Fmoc–NH–Xn–X1
SPPS
Br
OMe
OMe
Fmoc–NH-Yn-Y1–Xn–X1
1. 20% Piperidine in DMF
2. TFA
Br
OMe
OH
H2N-Yn-Y1–Xn–X1-CO2H
TMSI
Br
OH
OH
H2N-Yn-Y1–Xn–X1-CO2H
Desired Product
OH
OH
H2N-Yn-Y1–Xn–X1-CO2H
Actual Product

Scheme 3.1 Observed side products in the synthesis of peptides 3.4 – 3.10

3.5 Synthesis of penta-peptides incorporating BrPmp

Unable to synthesize nonamers without loss of the bromide, the sequences were further truncated into pentamers (see **Table 3.3, Figure 3.4**) with three residues on the *C*-terminal side of the BrPmp residue and one residue on the *N*-terminal side. We decided to add only one additional amino acid after the introduction of the BrPmp residue due to the apparent decomposition of the bromide under SPPS conditions. Pentamers **3.11**, **3.12**, and **3.13** were synthesized according to the same method used for compounds **3.4 – 3.10**.

Label	**Source**	**Sequence**	**CD45**	**PTP1B**	**SHP2**
3.12	GHR-487	F(BrPmp)AQVS	-	+	-
3.13	TIE2-816	I(BrPmp)PVLD	+	-	+
3.14	CD3ζ	L(BrPmp)QGLS	n.d.	n.d.	n.d.

Table 3.4 Truncated sequences selected for BrPmp incorporation and their predicted dephosphorylation efficiency respective to CD45, PTP1B & SHP2 (+, moderate activity, -, minimal dephosphorylation activity, n.d., no data on dephosphorylation activity). Substrate specificity was based on the results cited in Table 3.1.

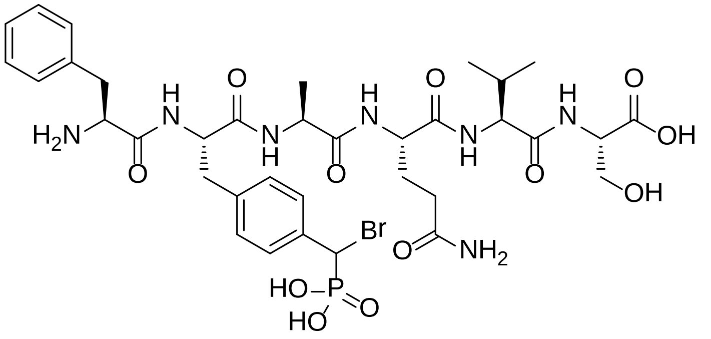

3.12

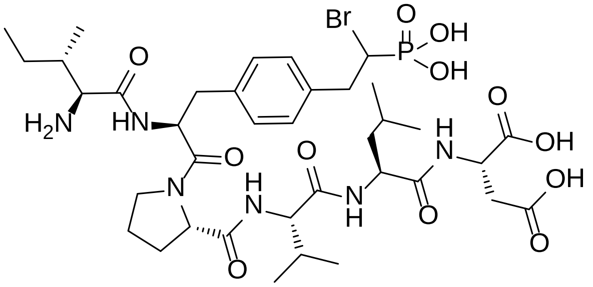

3.13

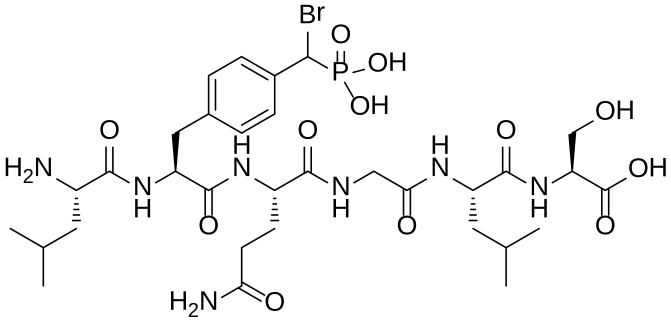

3.14

Figure 3.4: Pentamer sequences selected for BrPmp incorporation

Compounds **3.12** and **3.13** were purified by HPLC. Chromatograms of compound **3.14** showed side products with a similar retention to the desired product and proved too difficult to separate by HPLC (Appendix Figures C1 – C3). Incorporation of the BrPmp residue into crude peptides **3.12** and **3.13** was initially confirmed by HR-MS. However, ^{31}P NMR of the purified fractions of **3.12** and **3.13** showed two distinct phosphorous signals; one at 12.3 ppm (corresponding to BrPmp containing peptide) and another signal at 22.5 ppm (corresponding to the Pmp residue in place of BrPmp). Given the greater than 92% purity observed in both the chromatograms for **3.12** and **3.13** this suggests that the replacement of BrPmp with a Pmp residue in an otherwise identical peptide results in a very similar retention time. HR-MS of the purified fractions of **3.12** and **3.13** also confirmed the presence of BrPmp and Pmp containing peptides (**Table 3.4**). The purity of the BrPmp containing peptides in the isolated fractions, as determined by ^{31}P NMR integrations and HPLC for compounds, **3.12** and **3.13** are illustrated in **Table 3.4**.

Label	**Sequence**	**Purity of BrPmp** **^{31}P NMR / HPLC**	**Observed MS**
3.12	F(BrPmp)AQVS	77%/>92%	868.23, 756.33
3.13	I(BrPmp)PVLD	67%/>92%	873.28, 795.37

Table 3.5 Purity of 3.12 and 3.13 by ^{31}P NMR and HPLC

3.6 Proposed mechanism of BrPmp degredation during SPPS

The most puzzling question is the mechanism of Pmp formation from BrPmp. There is no obvious hydride source in either the SPPS or the TMSI deprotection conditions. As noted above, we observed the complete loss of the characteristic mass spectral isotopic pattern of brominated compounds once **3.6** was subjected to TMSI, suggesting that this reagent may play a role in generating the Pmp residue. A potential mechanism involving TMSI, is illustrated in **Figure 3.5.**

Cleavage of the iodo-silyl bond, followed by attack at the benzylic bromide, would generate an iodo-bromide species and a silyl cation. Concommittant attack by the stabilized phosphonate anion would result in a benzylic silane. The resulting intermediate, **3.16,** could then undergo a Brook-like rearrangement, exchanging the phosphonate H atom with the oxaphilic-silyl group to form 3.17. .[24] Finally, silyl ester 3.18 is quenched with water resulting in the formation of the Pmp derivative. This mechanism provides a potential explanation for our observations, as partial phosphonate deprotection during synthesis would be necessary for the Brook rearrangement. We propose that protecting groups which are more stable to extended SPPS conditions could avoid this problem.

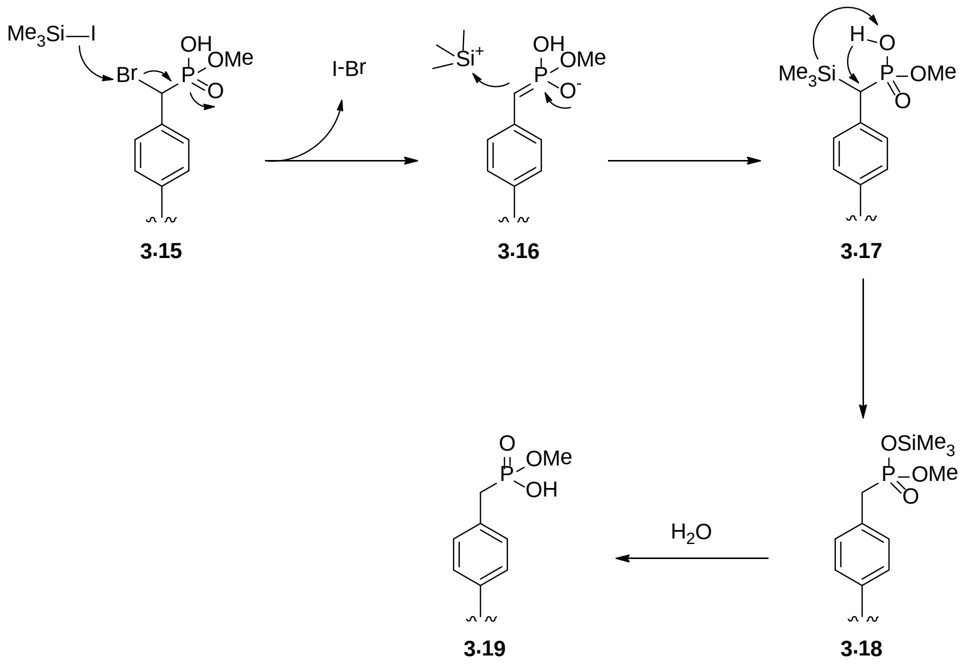

Figure 3.5: Proposed mechanism for the formation of Pmp

Although this mechanism remains to be tested, we cannot rule out the possibility that an alternative pathway may occur during SPPS contributing to the loss of the bromide. If the proposed mechanism is involved, a potential solution would lie in the investigation of new phosphonate protecting groups that are not only stable to SPPS conditions but posses deprotection conditions that are compatible with BrPmp residue.

3.7 Conclusions & future work

We have attempted to incorporate the BrPmp residue into peptide sequences of 5 to 9 residues. Unfortunately, we observed loss of the key α-bromo phosphonate functionality in all of the attempted conditions. This was a surprising result given our previous success in synthesizing the tripeptide **2.32** using similar SPPS conditions. This problem may be based on the incompatibility of the phosphonate protecting groups with SPPS conditions or the incompatibility of the BrPmp residue with the protecting group removal conditions. One potential solution to this problem may be alternative phosphonate protecting groups that alleviate these twin problems.

One major drawback associated with standard phosphonate protecting groups (methyl, ethyl, benzyl, *t*-butyl) is their limitations, for peptide chemistry. Benzyl protected phosphonate protecting groups succumb to mono-dealkylation after repeated exposure to piperidine during Fmoc deprotection.[25] Efficient removal of ethyl protecting groups requires relatively long exposure to strong acids such as trifluoro-methane-sulphonic acid (TFMSA) or TMSBr.[26] The *t*-butyl group, although easily cleaved by TFA, undergoes autocatalytic degradation and must be used immediately upon synthesis.[26] One alternative phosphonate protecting group that may solve the problems we observe here is the diamidate ($-PO(NMe_2)_2$) protecting group.[27] The diamidate is compatible with standard SPPS coupling and Fmoc deprotection conditions, the phosphodiamidate is cleaved by acid hydrolysis.[27] Another benefit of the phosphodiamidate protecting group is that it will most likely be compatible with the chemistry developed in the synthesis of BrPmp and can be introduced in a similar fashion to the current methyl ester protecting group, once the reagent diamidatephosphite has been prepared.[28]

With a suitably protected BrPmp residue in hand, we can begin to identify specific phosphopeptide analogs which label CD45 and other PTPs. Once we have a series of specific substrates for CD45 we can incorporate lipid tags (for membrane localization), and fluorescent dyes (for visualization) into these peptides to observe the catalytic activity and sub-cellular localization of this enzyme in live cells. These reagents will become useful tools for biochemical and microscopy studies and will provide additional insight into behaviour of phosphatase enzymes.

3.8 Materials and methods

3.8.1 Synthetic methods

General synthesis of peptides (3.4 – 3.14): The peptides were assembled on preloaded Wang resin. Amino residues, with the exception of Fmoc-L-BrPmp(*O*Me$_2$)-OH **2.30**, were incorporated utilizing standard automated Fmoc based solid phase methods. Fmoc-L-BrPmp(*O*Me$_2$)-OH **2.30** (2 equiv) was coupled manually to the resin using HBTU (1.96 equiv) in the presence of DIPEA (4 equiv) in NMP for 3.5 h. The reaction was monitored by the Kaiser test. The coupling was repeated using the same equivalents of Fmoc-L-BrPmp(*O*Me$_2$)-OH, HBTU and DIPEA in NMP for 3.5 h. Fmoc deprotection was achieved with 20% piperidine in NMP. The resin was washed with NMP, AcOH, DCM, and MeOH. Immediately after washing the resin with CH_3CN, DCM and MeOH, a mixture of TFA/H_2O/TIPS (95:2.5:2.5) was added and the resin was shaken at room temperature for 3 h. The cleaved peptide was precipitated in diethylether, filtered, dissolved in a mixture of H_2O and CH_3CN and lyophilized. The lyophilized peptide was suspended in CH_3CN, and TMSI (20 equiv) was added under an inert atmosphere and the reaction mixture shaken for 100 min at room temperature. The CH_3CN/TMSI solution was evaporated under reduced pressure, and the crude product was dissolved in water and washed with diethylether (3 ×) and the aqueous layer was lyophilized. The peptides were purified by HPLC (C-18 semipreparative column) using a linear gradient (CH_3CN/H_2O mobile phase containing 0.1% TFA).

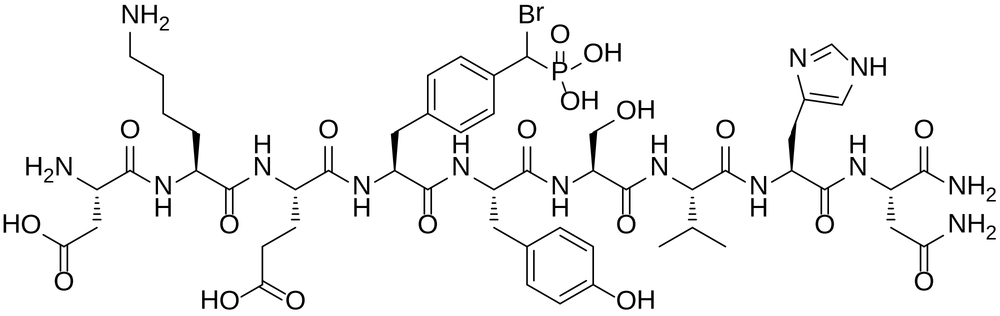

Compound 3.11 ^{31}P NMR (162 MHz, D_2O) δ 12.43. MALDI calculated for $C_{52}H_{75}BrN_{14}O_7P$ $[M+H]^+$ 1038.4248, found: 1038.4242.

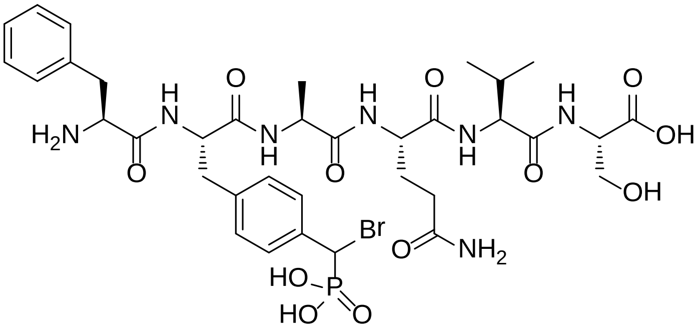

Compound 3.12 ^{1}H NMR (500 MHz, D_2O) δ 7.42 (d, *J* = 7.9 Hz, 2H), 7.28 (d, *J* = 6.0 Hz, 4H), 7.13 (d, *J* = 7.7 Hz, 3H), 7.08 (d, *J* = 8.2 Hz, 1H), 4.86 (d, *J* = 11.6 Hz, 2H), 4.54 (d, *J* = 5.6 Hz, 3H), 4.35 – 4.22 (m, 4H), 4.17 (dd, *J* = 13.9, 6.7 Hz, 2H), 4.14 – 4.02 (m, 4H), 3.77 (t, *J* = 5.0 Hz, 4H), 3.10 (d, *J* = 7.5 Hz, 2H), 3.10 – 2.97 (m, 5H), 2.91 (s, 2H), 2.85 – 2.78 (m, 3H), 2.26 (d, *J* = 8.3 Hz, 4H), 2.07 – 1.94 (m, 4H), 1.95 – 1.81 (m, 3H), 1.28 (dd, *J* = 7.0, 2.4 Hz, 4H), 1.17 (t, *J* = 7.3 Hz, 2H), 0.86 (t, *J* = 6.4 Hz, 8H). ^{31}P NMR (202 MHz, D_2O) δ 20.60 (s, 1P), 12.26 (s, 3.4P). ESIMS calculated for $C_{35}H_{47}BrN_7O_{12}P$ $[M-H]^-$ 868.2287, found: 868.2281

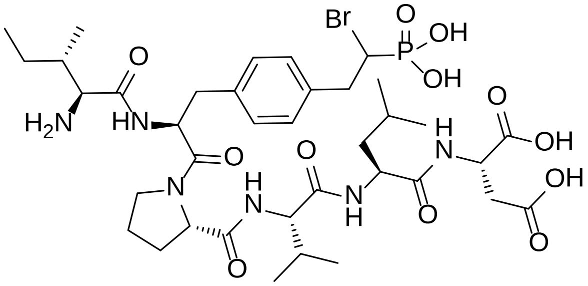

Compound 3.13 ^{1}H NMR (500 MHz, D_2O) δ 7.46 (dd, *J* = 13.9, 8.1 Hz, 2H), 7.24 - 7.14 (m, 4H), 4.93 – 4.86 (m, 2H), 4.66 – 4.19 (m, 7H), 4.00 (d, *J* = 8.0 Hz, 1H), 3.97 – 3.64 (m, 3H), 3.61 (d, *J* = 6.9 Hz, 2H), 3.14 – 3.07 (m, 1H), 2.98 – 2.73 (m, 5H), 2.40 – 2.10 (m, 1H), 2.00 (s, 1H), 1.84 – 1.33 (m, 10H), 1.18 (t, *J* = 7.5 Hz 1H), 1.16 – 1.02 (m, 1H), 0.92 – 0.73 (m, 26H). ^{31}P NMR (202 MHz, D_2O) δ 20.97 (d, *J* = 17.4 Hz, 1P), 12.32 (d, *J* = 5.1 Hz, 2P). ESIMS calculated for $C_{36}H_{54}BrN_6O_{12}P$ [M-H]$^-$ 873.2804, found: 873.2803.

3.9 Appendix

Fiure C1 Analytical HPLC Chromatogram of 3.11

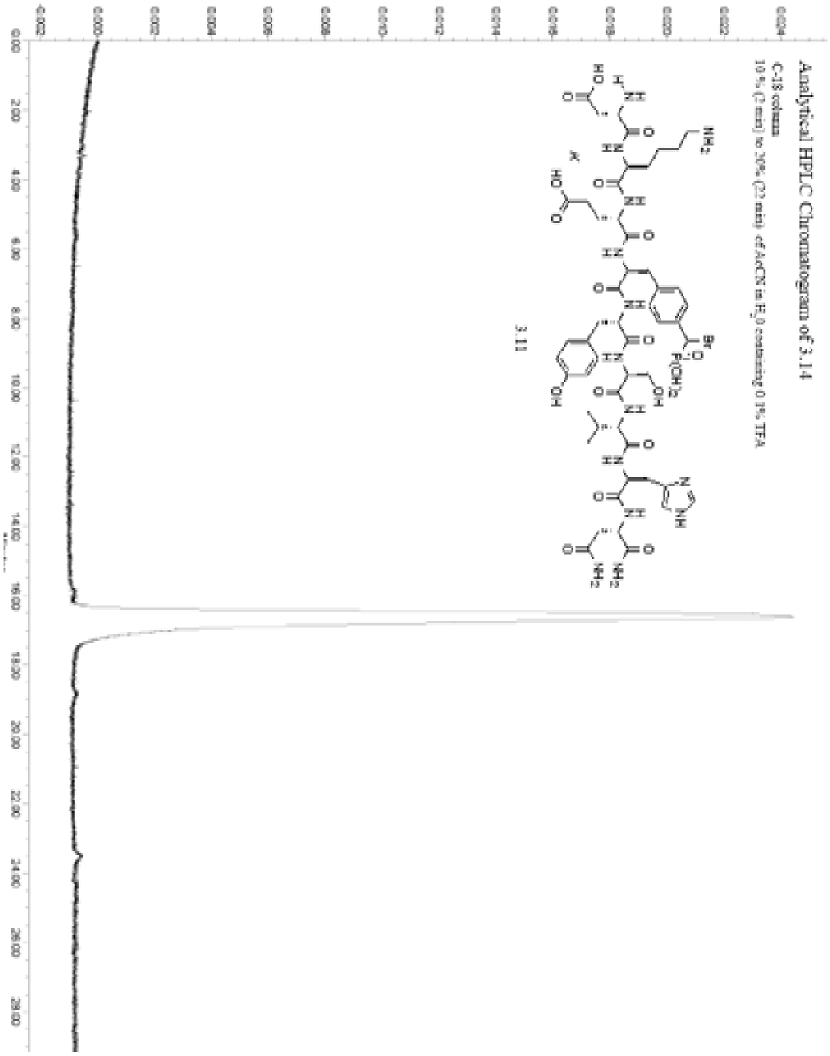

Figure C2 Analytical HPLC Chromatogram of 3.12

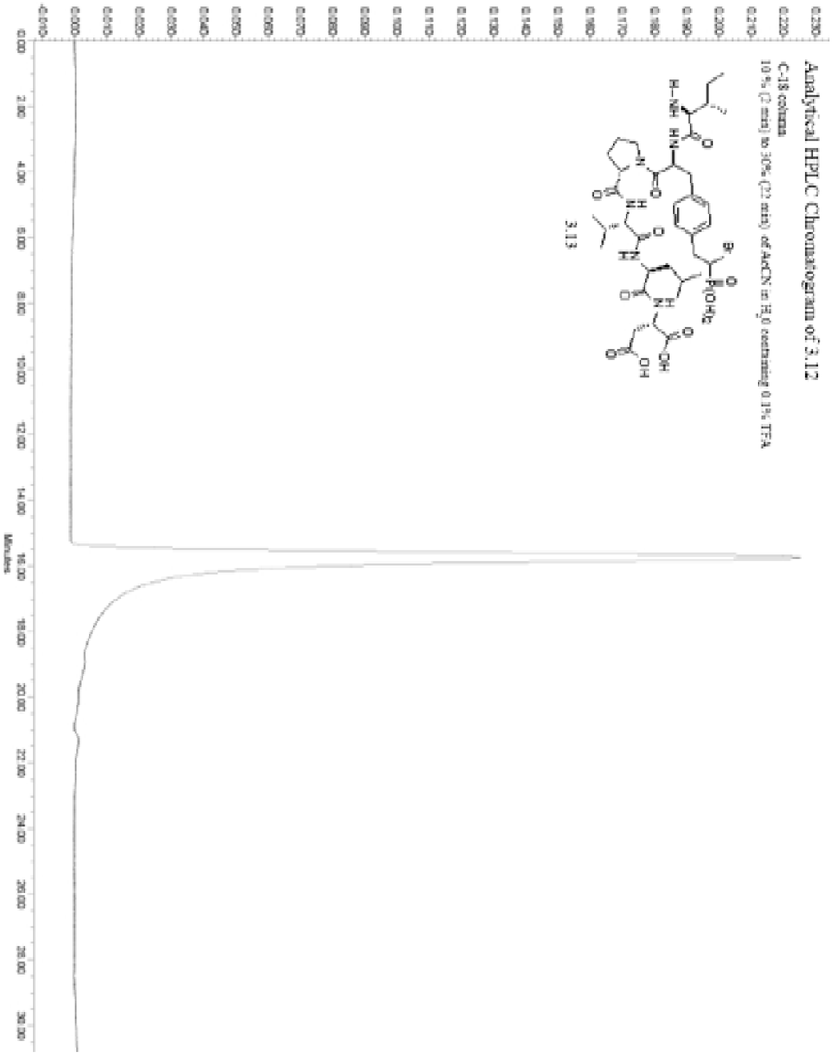

Figure C3: Analytical HPLC Chromatogram of 3.13

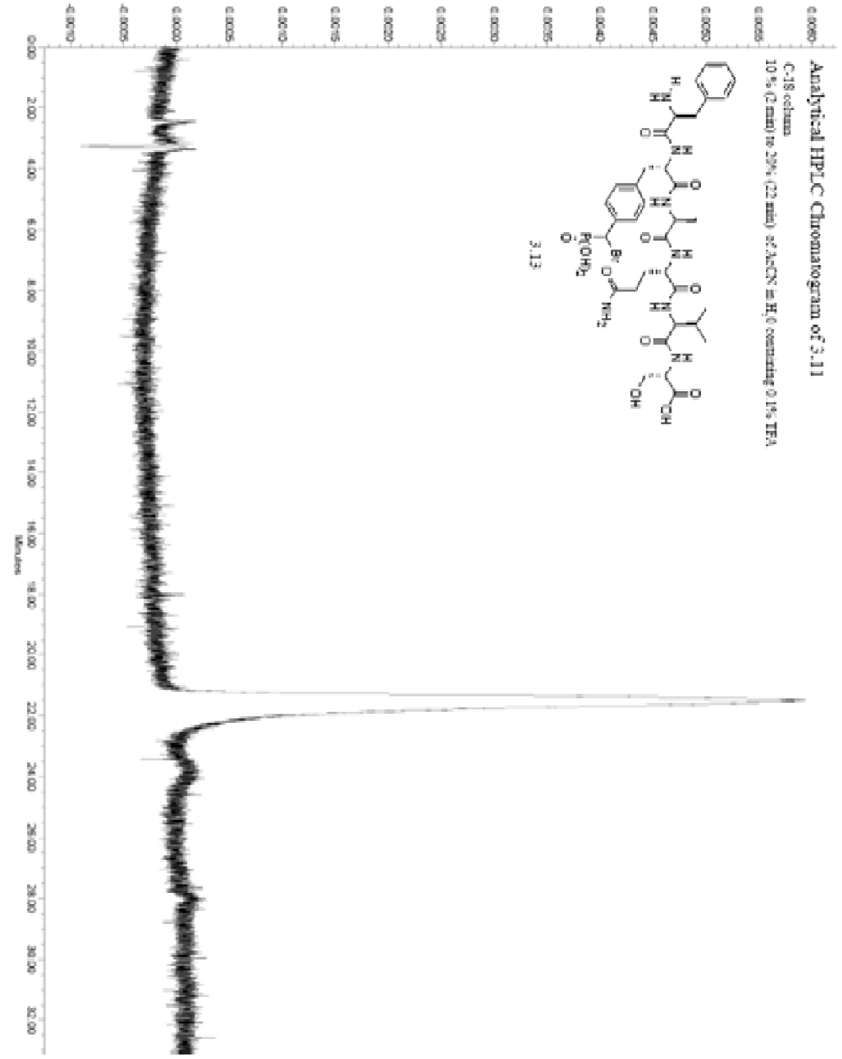

3.10 References

1. van Huijsduijnen, R. H.; Bombrun, A.; Swinnen, D., Selecting protein tyrosine phosphatases as drug targets. *Drug Discovery Today* **2002**, 7, (19), 1013-1019.

2. Tonks, N. K.; Neel, B. G., Combinatorial control of the specificity of protein tyrosine phosphatases. *Current Opinion in Cell Biology* **2001**, 13, (2), 182-195.

3. Hubbard, M. J.; Cohen, P., On target with a new mechanism for the regulation of protein-phosphorylation. *Trends in Biochemical Sciences* **1993**, 18, (5), 172-177.

4. Cho, H. J.; Ramer, S. E.; Itoh, M.; Winkler, D. G.; Kitas, E.; Bannwarth, W.; Burn, P.; Saito, H.; Walsh, C. T., Purification and characterization of a soluble catalytic fragment of the human transmembrane leukocyte antigen related (LAR) protein tyrosine phosphatase from an escherichia-coli expression system. *Biochemistry* **1991**, 30, (25), 6210-6216.

5. Zhang, Z. Y.; Maclean, D.; Mcnamara, D. J.; Sawyer, T. K.; Dixon, J. E., Protein-tyrosine-phosphatase substrate-specificity - size and phosphotyrosine positioning requirements in peptide-substrates. *Biochemistry* **1994**, 33, (8), 2285-2290.

6. Harder, K. W.; Owen, P.; Wong, L. K. H.; Aebersold, R.; Clarklewis, I.; Jirik, F. R., Characterization and kinetic-analysis of the intracellular domain of human-protein-tyrosine-phosphatase-beta (HPTP-beta) using synthetic phosphopeptides. *Biochemical Journal* **1994**, 298, 395-401.

7. Bobko, M.; Wolfe, H. R.; Saha, A.; Dolle, R. E.; Fisher, D. K.; Higgins, T. J., CD45 protein-tyrosine-phosphatase - determination of minimal peptide length for substrate recognition and synthesis of some tyrosine-based electrophiles as potential active-site-directed irreversible inhibitors. *Bioorganic & Medicinal Chemistry Letters* **1995**, 5, (4), 353-356.

8. Zhang, Z. Y.; Thiemesefler, A. M.; Maclean, D.; Mcnamara, D. J.; Dobrusin, E. M.; Sawyer, T. K.; Dixon, J. E., Substrate-specificity of the protein-tyrosine phosphatases. *Proceedings of the National Academy of Sciences of the United States of America* **1993**, 90, (10), 4446-4450.

9. Cho, H. J.; Krishnaraj, R.; Itoh, M.; Kitas, E.; Bannwarth, W.; Saito, H.; Walsh, C. T., Substrate specificities of catalytic fragments of protein-tyrosine phosphatases (HPTP-beta, LAR, and CD45) toward phosphotyrosylpeptide substrates and thiophosphotyrosylated peptides as inhibitors. *Protein Science* **1993**, 2, (6), 977-984.

10. Dechert, U.; Affolter, M.; Harder, K. W.; Matthews, J.; Owen, P.; Clarklewis, I.; Thomas, M. L.; Aebersold, R.; Jirik, F. R., Comparison of the specificity of bacterially expressed cytoplasmic protein-tyrosine phosphatases SHP and SH-PTP2 towards synthetic phosphopeptide substrates. *European Journal of Biochemistry* **1995**, 231, (3), 673-681.

11. Tulsi, N. S.; Downey, A. M.; Cairo, C. W., A protected L-bromophosphonomethylphenylalanine amino acid derivative (BrPmp) for synthesis of irreversible protein tyrosine phosphatase inhibitors. *Bioorganic & Medicinal Chemistry* **2010**, 18, (24), 8679-8686.

12. Gao, L.; Sun, H.; Yao, S. Q., Activity-based high-throughput determination of PTPs substrate specificity using a phosphopeptide microarray. *Peptide Science* **2010**.

13. Walchli, S.; Espanel, X.; Harrenga, A.; Rossi, M.; Cesareni, G.; van Huijsduijnen, R. H., Probing protein-tyrosine phosphatase substrate specificity using a phosphotyrosine-containing phage library. *Journal of Biological Chemistry* **2004**, 279, (1), 311-318.

14. Hegedus, Z.; Chitu, V.; Toth, G. K.; Finta, C.; Varadi, G.; Ando, I.; Monostori, E., Contribution of kinases and the CD45 phosphatase to the generation of tyrosine phosphorylation patterns in the T-cell receptor complex zeta chain. *Immunology Letters* **1999**, 67, (1), 31-39.

15. Barr, A. J.; Ugochukwu, E.; Lee, W. H.; King, O. N. F.; Filippakopoulos, P.; Alfano, I.; Savitsky, P.; Burgess-Brown, N. A.; Muller, S.; Knapp, S., Large-scale structural analysis of the classical human protein tyrosine phosphatome. *Cell* **2009**, 136, (2), 352-363.

16. Desmarais, S.; Jia, Z. C.; Ramachandran, C., Inhibition of protein tyrosine phosphatases PTP1B and CD45 by sulfotyrosyl peptides. *Archives of Biochemistry and Biophysics* **1998**, 354, (2), 225-231.

17. Nam, H. J.; Poy, F.; Saito, H.; Frederick, C. A., Structural basis for the function and regulation of the receptor protein tyrosine phosphatase CD45. *Journal of Experimental Medicine* **2005**, 201, (3), 441-452.

18. McNeill, L.; Salmond, R. J.; Cooper, J. C.; Carret, C. K.; Cassady-Cain, R. L.; Roche-Molina, M.; Tandon, P.; Holmes, N.; Alexander, D. R., The differential

regulation of Lck kinase phosphorylation sites by CD45 is critical for T cell receptor signaling responses. *Immunity* **2007**, 27, (3), 425-437.

19. Siu, R.; Fladd, C.; Rotin, D., *N*-cadherin is an in vivo substrate for protein tyrosine phosphatase sigma (PTP sigma) and participates in PTP sigma-mediated inhibition of axon growth. *Molecular and Cellular Biology* **2007**, 27, (1), 208-219.

20. Furge, K. A.; Zhang, Y. W.; Vande Woude, G. F., Met receptor tyrosine kinase: Enhanced signaling through adapter proteins. *Oncogene* **2000**, 19, (49), 5582-5589.

21. PostelVinay, M. C.; Finidori, J., Growth hormone receptor: Structure and signal transduction. *European Journal of Endocrinology* **1995**, 133, (6), 654-659.

22. Sato, A.; Iwama, A.; Takakura, N.; Nishio, H.; Yancopoulos, G. D.; Suda, T., Characterization of TEK receptor tyrosine kinase and its ligands, angiopoietins, in human hematopoietic progenitor cells. *International Immunology* **1998**, 10, (8), 1217-1227.

23. Larose, L.; Gish, G.; Pawson, T., Construction of an SH2 domain-binding site with mixed specificity. *Journal of Biological Chemistry* **1995**, 270, (8), 3858-3862.

24. Brook, A. G., Some molecular-rearrangements of organosilicon compounds. *Accounts of Chemical Research* **1974**, 7, (3), 77-84.

25. Kitas, E. A.; Wade, J. D.; Johns, R. B.; Perich, J. W.; Tregear, G. W., Preparation and use of *N*-alpha-fluorenylmethoxycarbonyl-*O*-dibenzylphosphono-L-tyrosine in continuous-flow solid-phase peptide-synthesis. *Journal of the Chemical Society-Chemical Communications* **1991**, (5), 338-339.

26. Sanderson, S. D.; Perini, F., The synthesis and compositional analysis of phosphopeptides. *Molecular Biotechnology* **1995**, 4, (2), 139-149.

27. Chao, H. G.; Leiting, B.; Reiss, P. D.; Burkhardt, A. L.; Klimas, C. E.; Bolen, J. B.; Matsueda, G. R., Synthesis and application of fmoc-o-[bis(dimethylamino)phosphono]tyrosine, a versatile protected phosphotyrosine equivalent. *Journal of Organic Chemistry* **1995**, 60, (24), 7710-7711.

28. Froneman, M.; Cheney, D. L.; Modro, T. A., Dialkylamino group transfer from titanium (IV) to phosphoryl center - structure reactivity studies. *Phosphorus Sulfur and Silicon and the Related Elements* **1990**, 47, (3-4), 273-281.